

Organizational Results Research Report

September 2008
OR09.007

Preservation of Missouri Transportation Infrastructures: Validation of FRP Composite Technology

Volume 1 of 5

In-Situ Load Testing of Bridges

P-962, T-530, X-495, X-596 and Y-298

Prepared by Missouri S&T
and Missouri Department of
Transportation



FINAL REPORT

RI02-022

**Preservation of Missouri Transportation Infrastructures:
Validation of FRP Composite Technology**

Volume 1

In-Situ Load Testing of Bridges P-962, T-530, X-495, X-596 and Y-298

Prepared for the
Missouri Department of Transportation
Organizational Results

In Cooperation with the
National University Transportation Center

by
Center for Infrastructure Engineering Studies
Missouri University of Science and Technology

John J. Myers, Ph.D., P.E.

David Holdener E.I.T.

Wesley Merkle P.E.

Eli Hernandez

September 2008

The opinions, findings and conclusions expressed in this report are those of the principal investigator and the Missouri Department of Transportation. They are not necessarily those of the U.S. Department of Transportation or the Federal Highway Administration. This report does not constitute a standard, specification or regulation.

TECHNICAL REPORT DOCUMENTATION PAGE

| | | | |
|--|---|--|--------------------------|
| 1. Report No. OR09-007 | 2. Government Accession No. | 3. Recipient's Catalog No. | |
| 4. Title and Subtitle Preservation of Missouri Transportation Infrastructures: Validation of FRP Composite: Volume 1 - In-situ load testing of Bridges P-962, T-530, X-495, X-596 and Y-298 | | 5. Report Date September, 2008 | |
| | | 6. Performing Organization Code Missouri S&T | |
| 7. Author/s J. J. Myers, D. Holdener, W. Merkle, and E. Hernandez | | 8. Performing Organization Report No. RI02-022 | |
| 9. Performing Organization Name and Address Center for Infrastructure Engineering Studies Missouri University of Science & Technology 223 Engineering Research Lab Rolla, MO 65409 | | 10. Work Unit No. (TRAIS) | |
| | | 11. Contract or Grant No. DTRT06-G-0014 | |
| 12. Sponsoring Organization Name and Address U.S. Department of Transportation Research and Special Programs Administration 400 7 th Street, SW Washington, DC 20590-0001 | | 13. Type of report and period covered Final | |
| | | 14. Sponsoring Agency Code MoDOT | |
| 15. Supplementary Notes | | | |
| 16. Abstract <p>Strengthening structures with Fiber-Reinforced Polymer (FRP) composite systems has been growing in popularity over recent years for the many benefits that the technology offers. The umbrella project, "Preservation of Missouri Infrastructure: Validation of FRP Composite Technology Through Field Testing", also known as the Five Bridges Project, was designed to push forward composite strengthening schemes for use on real structures. Using real structures demanded that the strengthened structures be monitored for performance to prove that the composites were working and that they were not losing strength over time. Monitoring the structures meant scheduling load tests for all five bridges. Difficulties in using traditional monitoring equipment, like Linear Variable Displacement Transducer (LVDT) systems, on these structures ordered the search for a better monitoring system.</p> <p>This report presents high-precision Surveying Equipment as a new serviceability monitoring system for load testing; the materials, procedures, and data analysis techniques are discussed as well as a comparison between serviceability monitoring systems. This report also presents the results of the load testing. All five bridges are compared in terms of serviceability before and after strengthening results to show the overall performance of these strengthening schemes. Normalization of the deflection data due to varying truck weights and thermal effects was conducted to help compare the individual tests to one another. Bridge deficiencies and deteriorations are also discussed and noted to help establish a reference for future testing and inspections.</p> | | | |
| 17. Key Words Bridge monitoring, FRP, in-situ load test, static load test, structural evaluation, thermal effect, total station. | | 18. Distribution Statement No restrictions. This document is available to the public through the National Technical Information Service, Springfield, Virginia 22161 | |
| 19. Security Classification (of this report) Unclassified | 20. Security Classification (of this page) Unclassified | 21. No. of Pages 144 | 22. Price Free |

In-Situ Load Testing and Monitoring of Bridges P-962, T-530, X-495, X-596 and Y-298

EXECUTIVE SUMMARY

Strengthening structures with Fiber-Reinforced Polymer (FRP) composite systems has been growing in popularity over recent years for the many benefits that the technology offers. The umbrella project, “Preservation of Missouri Infrastructure: Validation of FRP Composite Technology Through Field Testing,” also known as the Five Bridges Project, was designed to push forward composite strengthening schemes for use on real structures.

Using real structures demanded that the strengthened structures be monitored for performance to prove that the composites were working and that they were not losing strength over time. Monitoring the structures meant scheduling load tests for all five bridges. Difficulties in using traditional monitoring equipment, like Linear Variable Displacement Transducer (LVDT) systems, on these structures ordered the search for a better monitoring system.

This report presents high-precision Surveying Equipment as a new serviceability monitoring system for load testing; the materials, procedures, and data analysis techniques are discussed as well as a comparison between serviceability monitoring systems. This report also presents the results of the load testing. All five bridges are compared in terms of serviceability before and after strengthening results to show the overall performance of these strengthening schemes. Normalization of the deflection data due to varying truck weights and thermal effects was conducted to help compare the individual tests to one another. Bridge deficiencies and deteriorations are also discussed and noted to help establish a reference for future testing and inspections.

ACKNOWLEDGMENTS

The authors would like to acknowledge the funding support provided by the Missouri Department of Transportation and the National University Transportation Center at Missouri University of Science and Technology. The authors are also very appreciative of the help received from the MoDOT maintenance crews in procuring trucks and proper signage during the load testing.

TABLE OF CONTENTS

| | Page |
|--|------|
| LIST OF ILLUSTRATIONS | vii |
| LIST OF TABLES | xi |
| 1. INTRODUCTION | 1 |
| 1.1. BACKGROUND | 1 |
| 1.2. SCOPE AND OBJECTIVES | 3 |
| 1.3. REPORT LAYOUT | 4 |
| 2. COMPOSITE BACKGROUND INFORMATION | 5 |
| 2.1. MANUAL FRP LAY-UP | 5 |
| 2.2. PRE-CURED LAMINATE PLATES | 6 |
| 2.3. NEAR SURFACE MOUNTED BARS | 6 |
| 2.4. STEEL REINFORCED POLYMER | 7 |
| 2.5. MECHANICALLY FASTENED FRP | 8 |
| 3. EXPERIMENTAL PROGRAM | 10 |
| 3.1. PROJECT DESCRIPTION AND BRIDGE OVERVIEW | 10 |
| 3.2. BRIDGE DETAILS AND STRENGTHENING | 15 |
| 3.2.1. Bridge X-596 | 15 |
| 3.2.2. Bridge T-530 | 19 |
| 3.2.3. Bridge X-495 | 22 |
| 3.2.4. Bridge P-962 | 25 |
| 3.2.5. Bridge Y-298 | 28 |
| 3.2.6. Summary of Strengthening and Analytical Capacity Increase | 31 |
| 4. LOAD TESTING AND SURVEYING EQUIPMENT | 32 |
| 4.1. LOAD TESTING | 32 |
| 4.1.1. Static and Dynamic Testing | 32 |
| 4.1.2. Timing and Testing Duration | 33 |
| 4.1.3. Measurements and Instrumentation | 34 |
| 4.1.4. Testing Protocol | 35 |

| | |
|--|----|
| 4.2. USING SURVEYING EQUIPMENT | 35 |
| 4.2.1. Understanding Surveying Equipment | 36 |
| 4.2.2. Limitations of Surveying Equipment | 40 |
| 4.2.3. Comparison Studies..... | 41 |
| 4.2.3.1 Case Study 1: Field Test | 41 |
| 4.2.3.2 Case Study 2: Laboratory Test..... | 44 |
| 4.2.4. Verifying Surveying Equipment for Load Testing..... | 47 |
| 5. FIELD TEST PROGRAM | 49 |
| 5.1. TRUCKS FOR TEST WEIGHT..... | 49 |
| 5.2. TEST SETUP..... | 50 |
| 6. DATA PROCESSING | 55 |
| 6.1. DEFLECTION CALCULATIONS | 55 |
| 6.2. ACCOUNTING FOR THERMAL EFFECTS | 55 |
| 6.3. NORMALIZING DEFLECTION READINGS | 59 |
| 7. RESULTS..... | 66 |
| 7.1. LONGITUDINAL DEFLECTIONS | 66 |
| 7.2. TRANSVERSE DEFLECTION | 68 |
| 7.3. LOAD DISTRIBUTION | 70 |
| 7.4. PRE-STRENGTHENED LOAD TEST MODELING | 72 |
| 7.4.1. Individual Tee-Beam Modeling | 73 |
| 7.4.2. Mass-Section Tee-Beam Modeling | 76 |
| 7.4.3. Finite Element Modeling..... | 77 |
| 7.5. PRE-STRENGTHENED THEORETICAL AND EXPERIMENTAL DEFLECTIONS..... | 78 |
| 7.5.1. Comparison Methods | 78 |
| 7.5.2. Results of Analysis..... | 79 |
| 7.6. VISUAL BRIDGE INSPECTION..... | 84 |
| 7.6.1. Bridge T-530 | 85 |
| 7.6.2. Bridge X-596..... | 86 |
| 7.6.3. Bridge X-495..... | 87 |
| 7.6.4. Bridge P-962..... | 88 |

| | |
|---|-----|
| 7.6.5. Bridge Y-298..... | 89 |
| 8. CONCLUSIONS | 90 |
| APPENDICES | |
| A. 5 BRIDGES NORMALIZED DEFLECTION PROFILES | 92 |
| B. LOAD TESTING DIAGRAMS..... | 105 |
| C. LOAD TESTING FIELD PROCEDURES..... | 115 |
| REFERENCES | 132 |

LIST OF ILLUSTRATIONS

| Figure | Page |
|---|------|
| 1.1. 2007 Age and Deficiency of USA Bridges..... | 2 |
| 2.1. Sheets of FRP for Manual Lay-Up | 5 |
| 2.2. Pre-cured Laminate FRP Installation..... | 6 |
| 2.3. NSM Bar Installation | 7 |
| 2.4. SRP Installation Bridge P-962 | 8 |
| 2.5. MF FRP Installation..... | 9 |
| 3.1. Cross Section Dimension Illustration | 12 |
| 3.2. Bridge X-596 | 16 |
| 3.3. Bridge X-596 Substructure | 16 |
| 3.4. Bridge X-596 Plan View Strengthening Detail | 18 |
| 3.5. Bridge X-596 Cross - Section View Strengthening Detail | 19 |
| 3.6. Bridge X-596 Cross - Side View Strengthening Detail | 19 |
| 3.7. Bridge T-530..... | 20 |
| 3.8. Bridge T-530 Substructure..... | 21 |
| 3.9. Bridge X-495 | 23 |
| 3.10. Bridge X-495 Substructure | 23 |
| 3.11. Bridge P-962 | 26 |
| 3.12. Bridge P-962 Substructure..... | 26 |
| 3.13. Bridge Y-298 | 29 |
| 3.14. Bridge Y-298 Substructure | 29 |
| 3.15. Bridge Y-298 Slab Reinforcement Detail..... | 30 |
| 4.1. Loaded Trucks Used to Test a Bridge..... | 33 |
| 4.2. Two LVDT's Measuring Deflection..... | 34 |
| 4.3. Leica TCA 2003..... | 37 |
| 4.4. Reference Point..... | 37 |
| 4.5. Target Prism..... | 38 |
| 4.6. LVDT's and Target Prisms | 42 |
| 4.7. Total Station Setup..... | 42 |

| | |
|---|----|
| 4.8. Stop 2 – West Span Deflection | 43 |
| 4.9. Stop 3 – West Span Deflection | 44 |
| 4.10. Laboratory Test Setup..... | 45 |
| 4.11. String Transducer and Mounted Target Prism..... | 46 |
| 4.12. Laboratory Test Results | 46 |
| 5.1. MoDOT Provided H20 Truck..... | 50 |
| 5.2. Total Station Test Setup..... | 51 |
| 5.3. Attaching Target Prisms with Range Pole..... | 52 |
| 5.4. Bridge X-596 Truck Stops | 54 |
| 6.1. Bridge X-596 Temperature Over time of Midspan Interior Girder | 56 |
| 6.2. Bridge X-596 Thermal Camber | 57 |
| 6.3. Bridge X-596 Adjustment of Baseline Due to Thermal Effects | 58 |
| 6.4. Bridge X-495 Shading of Deck During Testing | 59 |
| 6.5. Percent Difference of Total Truck Weight over Time..... | 60 |
| 6.6. Stop 4 Transverse Load Distribution | 61 |
| 6.7. Stop 4 Lateral Load Distribution | 62 |
| 6.8. Stop 2 Sketch for Theoretical Deflection Terms | 63 |
| 6.9. Recorded Deflection Bridge P-962 - Stop 2, Exterior Girder..... | 64 |
| 6.10. Normalized Deflection Bridge P-962 - Stop 2, Exterior Girder | 65 |
| 7.1. Average Deflection Percent Difference Bridge P-962..... | 67 |
| 7.2. Average Deflection Percent Difference Bridge T-530 | 67 |
| 7.3. Bridge P-962 Span 1, Stop 2 Midspan Transverse Normalized Deflection | 68 |
| 7.4. Bridge P-962 Span 2, Stop 2 Midspan Transverse Normalized Deflection | 69 |
| 7.5. Bridge P-962 Span 3, Stop 2 Midspan Transverse Normalized Deflection | 70 |
| 7.6. Bridge P-962 Stops 2, 6 and 7 Distribution Fraction..... | 72 |
| 7.7. Transverse Load Distribution | 74 |
| 7.8. Longitudinal Load Distribution | 75 |
| 7.9. Example Deformation Contour Plot | 78 |
| 7.10. Bridge Y-298 West Span | 83 |
| 7.11. Bridge Y-298 East Span..... | 84 |
| 7.12. Bridge T-530 Corrosion of Bents and Cracked Transverse Beam | 85 |

| | |
|--|----|
| 7.13. Bridge X-596 Corrosion of Bents | 86 |
| 7.14. Bridge X-495 Disturbed Region Crack and Peeling of Protective Coating..... | 87 |
| 7.15. Bridge P-962 Corrosion of Transverse Girder and SRP Reinforcement | 88 |

LIST OF TABLES

| Table | Page |
|--|------|
| 3.1. Five Bridges Information Prior to Strengthening | 11 |
| 3.2. Bridge Cross Section Dimensions | 12 |
| 3.3. Existing Steel Reinforcement | 13 |
| 3.4. Bridge Concrete Compressive Strength (ksi) | 14 |
| 3.5. Composite Strengthening Utilized..... | 14 |
| 3.6. Composite Material Properties | 15 |
| 3.7. Bridge X-596 Slab Flexural Strengthening..... | 17 |
| 3.8. Bridge X-596 Girder Flexural Strengthening | 17 |
| 3.9. Bridge X-596 Girder Shear Strengthening | 17 |
| 3.10. Bridge T-530 Slab Flexural Strengthening | 21 |
| 3.11. Bridge T-530 Girder Flexural Strengthening..... | 22 |
| 3.12. Bridge X-495 Slab Flexural Strengthening..... | 24 |
| 3.13. Bridge X-495 Girder Flexural Strengthening | 24 |
| 3.14. Bridge X-495 Girder Shear Strengthening | 25 |
| 3.15. Bridge P-962 Slab Flexural Strengthening | 27 |
| 3.16. Bridge P-962 Girder Flexural Strengthening..... | 27 |
| 3.17. Bridge P-962 Girder Shear Strengthening | 28 |
| 3.18. Bridge Y-298 Slab Flexural Strengthening..... | 30 |
| 3.19. Composite Strengthening on Tested Spans..... | 31 |
| 4.1. Instrumentation Used in Load Testing..... | 35 |
| 6.1. Truck Weights for P-962 (kips) | 60 |
| 7.1. Bridge P-962 Load Distribution Fractions..... | 71 |
| 7.2. Before Strengthening Truck Axle Loads | 73 |
| 7.3. Effective Tee-Beam Widths..... | 75 |
| 7.4. Theoretical and Experimental Deflections for Bridge X-596..... | 80 |
| 7.5. Theoretical and Experimental Deflections for Bridge T-530 | 80 |
| 7.6. Theoretical and Experimental Deflections for Bridge X-495..... | 81 |

1. INTRODUCTION

1.1. BACKGROUND

The infrastructure of the United States of America plays a vital role in the economic and social well being of Americans today. A major expansion of the interstate system took place under the Federal Aid Highway Act of 1956. Under this act, the interstate system was greatly expanded, shaping America for present day. Bridges represent a key component of this infrastructure and need to be maintained. According to the National Bridge Inventory (2007) 25 percent of America's bridges are either structurally deficient or structurally obsolete.

The number of deficient bridges appears to be on the rise, creating concern for future years. Figure 1.1 shows the number of bridges of certain ages and the number of deficient bridges associated with each age. Additionally, the percentage of deficient bridges at each age level has been plotted. According to the trend of Figure 1.1 (National Bridge Inventory 2007) as the bridges built under the Federal Highway Act of 1956 become older, the number of deficient bridges will dramatically increase.

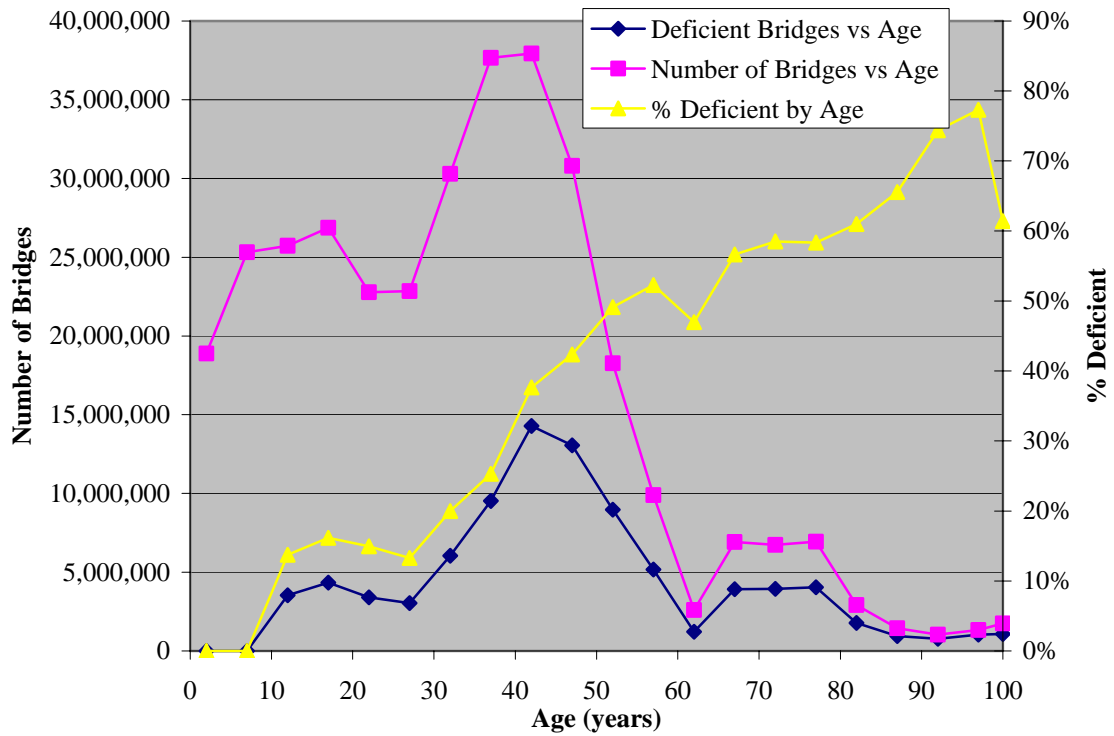


Figure 1.1. 2007 Age and Deficiency of USA Bridges (National Bridge Inventory, 2007)

Bridges become deficient or obsolete for a variety of reasons. Bridge decks typically require major repair or replacement every 15 to 20 years, while the substructure and superstructure tend to last 40 years or more (Koenigsfeld 2003). Deicing salt applications eat away concrete while water seeping through cracks in the concrete corrode unprotected reinforcing steel. Over the past decades, standard truck design weights have increased; as a result, older bridges that are still in good condition do not have the load carrying capacity required for today’s traffic needs. Traffic volumes have increased dramatically in recent years. Safety considerations have changed as well as most roadways today are designed to have 12-foot wide lanes. Both changing traffic demands and an already decaying infrastructure require engineers to find alternative solutions on a slim budget.

Recently, Fiber Reinforced Polymer (FRP) has emerged as a means of repairing structurally deficient bridges. The advantages associated with such a system over conventional strengthening techniques are: expected long term durability, short construction times, and negligible traffic disturbances. In addition the durability and lightweight attributes of FRP materials have led to their implementation in new bridge construction.

Due to the relatively recent application of FRP to bridges, the long-term validation of FRP materials has yet to be fully realized. Load testing of bridges strengthened and constructed with FRP technologies serves as a means of validating the service performance of these materials over time.

1.2. SCOPE AND OBJECTIVES

The primary goal of the Five Bridges Project was to validate bridge strengthening using FRP technologies on a large scale. The project proposed strengthening five bridges in central Missouri with FRP composites and monitoring the bridges with instrumentation biennially for five years thereafter. Both laboratory and field testing was conducted to validate guidelines and specifications. The work focused on Non-Destructive Testing (NDT) techniques, an essential element of successfully monitoring strengthened bridges.

The primary focus of this report is the Load Testing of all five bridges. Over the life of the project, load testing was expected to verify that the strengthening systems were performing as expected. This work was fundamental in verifying the long-term performance of FRP strengthening technologies.

Because of existing site conditions at four of the five bridges, traditional serviceability monitoring techniques, such as Linear Variable Displacement Transducer (LVDT) systems, would be extremely difficult; the search for a better system was initiated. High-precision

Surveying Equipment was employed as an alternative means to monitor serviceability of the project bridges. As the problems with the new system were solved, the protocol for load testing and using the Surveying Equipment was defined and discussed in detail. The Surveying Equipment was also directly compared to the traditional serviceability monitoring techniques in an effort to validate its accuracy for use in load testing of bridges.

1.3. REPORT LAYOUT

This thesis is divided into eight sections and three appendices. Section 1 covers the background of the project, including the scope and objectives. Section 2 describes the strengthening systems utilized on the Five Bridge Project. Section 2 describes load testing, FRP systems, thermal effects on bridges, surveying equipment, and bridge inspection ratings. Section 3 describes the umbrella project. Details for each project bridge include a description of the existing structure and a description of the strengthening systems applied. Section 4 describes load testing and presents surveying equipment as a valid alternative to conventional test setups. Section 5 details the structural monitoring program, load testing equipment and procedures utilized to test the bridges. Section 6 discusses the data processing and analysis procedures. Section 7 presents the results and discussions for all load tests performed. Load test modeling is discussed; theoretical and experimental results are compared. The effects of the FRP strengthening on the structures are discussed in detail through analysis of the load tests. Finally, Section 8 presents a summarized list of conclusions from the conducted research. The Appendices provide graphs of the lateral bridge deflections from each test, details of the test setup for each bridge and a detailed procedure for load testing bridges with the surveying equipment.

2. COMPOSITE BACKGROUND INFORMATION

There are a number of current composite application techniques available for implementation on bridges. Each technique has its own merits and can be project specific in nature; therefore, it is important to understanding each individual technique.

2.1. MANUAL FRP LAY-UP

Manual FRP lay-up is the process of adhering rolled sheets (see Figure 2.1) of FRP to concrete with two-part resin. The types of FRP include Glass (GFRP), Aramid (AFRP) and, the most common for structural applications, Carbon (CFRP). To ensure a good bond the existing concrete surface must be roughened with sandblasting and then smoothed and leveled with putty. Corners must be rounded in the case of shear strengthening with U-wraps to prevent localized stresses in the FRP (ACI Committee 440).



Figure 2.1. Sheets of FRP for Manual Lay-Up

2.2. PRE-CURED LAMINATE PLATES

Pre-cured laminates are plates of the resin and fiber matrix that have been cured prior to application. These plates are applied to the prepared concrete surface with a two-part epoxy similarly to the FRP sheets, as illustrated in Figure 2.2. However, pre-cured laminates need to be properly supported to a soffit during installation to ensure there is a solid bond.



Figure 2.2. Pre-cured Laminate FRP Installation

2.3. NEAR SURFACE MOUNTED BARS

Near surface mounted (NSM) bars are rectangular or circular bars applied by cutting grooves into the existing concrete surface where an increase in moment capacity is required. The grooves are filled with epoxy and the bars are pushed into the grooves, causing excess epoxy to seep out. Additional epoxy is then applied over the bars where needed and the surface is finished. See Figure 2.3 for a picture of the installation of NSM bars.



Figure 2.3. NSM Bar Installation

2.4. STEEL REINFORCED POLYMER

Steel reinforced polymer (SRP) is very similar to FRP; the primary difference being that SRP contains high strength steel wires instead of carbon, glass or aramid fibers. SRP is applied in the same way as FRP sheets; it is impregnated with resin and applied to the prepared concrete surface. See Figure 2.4 depicts the installation of SRP shear strengthening on Bridge P-962.



Figure 2.4. SRP Installation Bridge P-962

2.5. MECHANICALLY FASTENED FRP

The final technology associated with bridge strengthening is mechanically fastened fiber reinforced polymer (MF FRP). MF FRP is essentially pre-cured laminate plates with predrilled holes which are fastened to the concrete surface with mechanical bolts (see Figure 2.5). Because the concrete surface does not need to be prepared, this technique offers a faster installation process.



Figure 2.5. MF FRP Installation

The described strengthening techniques each have merits and shortcomings and should be evaluated on a per project basis before being selected for use. Each technology was implemented on the Five Bridges Project.

3. EXPERIMENTAL PROGRAM

3.1. PROJECT DESCRIPTION AND BRIDGE OVERVIEW

The Five Bridges Project is a research project at Missouri University of Science and Technology (formerly University of Missouri-Rolla) focusing on FRP strengthening validation and is jointly funded by the Missouri Department of Transportation (MoDOT), the Missouri University of Science & Technology University Transportation Center, and private sector funding. The purpose of the project was to aid in making FRP strengthening technologies available to bridge owners and engineering professionals. The project duration spanned five years, from April 3, 2003 to July 31, 2008, to allow for long-term field validation through load testing.

The project was not competitively bid on by the University due to its nature of integrated research. Therefore the repair, strengthening, and long-term monitoring costs of the project were not representative of a typical commercial project.

The individual bridge strengthening was completed utilizing five different composite strengthening techniques on five different structurally deficient bridges throughout the state of Missouri. Each of these structurally deficient bridges was load posted and visually rated prior to strengthening. The construction dates, daily traffic, load posting information and inspection ratings are all summarized in Table 3.1.

Table 3.1. Five Bridges Information Prior to Strengthening

| Bridge Code | Year Built | Average Daily Traffic | Load Posting | | Visual Inspection Rating | | |
|-------------|------------|-----------------------|---------------------|-------------|--------------------------|----------------|--------------|
| | | | Truck Weight (Tons) | Speed (mph) | Deck Rating | Superstructure | Substructure |
| T-0530 | 1937 | 200 | 21 | 15 | 5 | 5 | 5 |
| X-0495 | 1948 | 300 | 19 | 15 | 6 | 6 | 7 |
| X-0596 | 1946 | 2000 | 18 | 15 | 6 | 5 | 5 |
| P-0962 | 1956 | 350 | 18 | 15 | 7 | 6 | 6 |
| Y-0298 | 1937 | 1100 | 18 | 15 | 5 | 5 | 5 |

Four of the five bridges studied for the Five Bridge Project had similar cross section dimensions. The overall cross section dimensions for these bridges are provided in Table 3.2 and illustrated in Figure 3.1 for both the central and end spans. The dimensions and layout of Bridge Y-298 will be provided in section 3.2.5.

The existing steel reinforcement in the girders and deck for each of the bridges is provided in Table 3.3. The yield strength of all steel was assumed to be 40,000 psi. The compressive strength of the concrete in each bridge is also noted in Table 3.4.

Table 3.2. Bridge Cross Section Dimensions

| | | w (in.) | h (in.) | h_f (in.) | b_w (in.) | b (in.) |
|-------|--------------|------------|------------|----------------|----------------|------------|
| X-596 | Central Span | 283 | 39 | 6 | 21 | 107 |
| | End Spans | 283 | 33 | 6 | 17 | 109 |
| T-530 | All Spans | 276 | 37 | 6 | 17 | 78 |
| X-495 | Central Span | 283 | 39 | 6 | 21 | 107 |
| | End Spans | 283 | 33 | 6 | 17 | 109 |
| P-962 | All Spans | 283 | 39 | 6 | 21 | 107 |

Conversion Units: 1-in. = 25.4mm

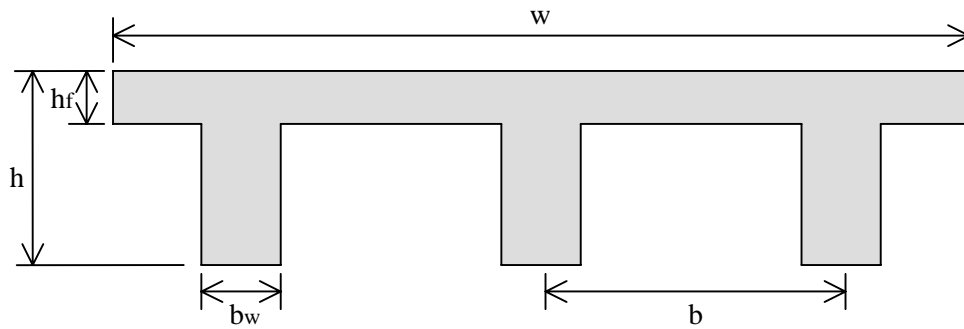


Figure 3.1. Cross Section Dimension Illustration

Table 3.3. Existing Steel Reinforcement

| | | Top Steel | | Bottom Steel | |
|-------|------------------------------|-------------|---------------------------|--------------|--------------------------|
| | | d' (in.) | A's (in ²) | d (in.) | As (in ²) |
| X-596 | Deck - All Spans | 1.75 | 0.24 | 4.75 | 0.48 |
| | Central Span - Interior Beam | 1.75 | 2.10 | 34.63 | 15.63 |
| | Central Span - Exterior Beam | 1.75 | 1.56 | 33.69 | 18.75 |
| | End Span - Interior Beam | 1.75 | 2.01 | 28.63 | 12.50 |
| | End Span - Exterior Beam | 1.75 | 1.47 | 28.63 | 12.50 |
| T-530 | Deck - All Spans | 1.00 | 0.27 | 5.00 | 0.27 |
| | Exterior Girder - All Spans | 1.50 | 1.41 | 33.00 | 12.50 |
| | Interior Girder - All Spans | 1.50 | 2.10 | 33.00 | 12.50 |
| X-495 | Deck - All Spans | 1.75 | 0.24 | 4.75 | 0.48 |
| | Central Span - Interior Beam | 1.75 | 2.10 | 34.63 | 15.63 |
| | Central Span - Exterior Beam | 1.75 | 1.56 | 33.69 | 18.75 |
| | End Span - Interior Beam | 1.75 | 2.01 | 28.63 | 12.50 |
| | End Span - Exterior Beam | 1.75 | 1.47 | 28.63 | 12.50 |
| P-962 | Deck - All Spans | 1.75 | 0.48 | 4.75 | 0.48 |
| | Exterior Girder - All Spans | 1.75 | 2.12 | 25.63 | 12.48 |
| | Interior Girder - All Spans | 1.75 | 3.56 | 25.63 | 12.48 |
| Y-298 | Deck - All Spans | 1.75 | 0.88 | 5.75 | 1.58 |

Conversion Units: 1-in. = 25.4mm; 1 in² = 645.16 mm²

Table 3.4. Bridge Concrete Compressive Strength (ksi)

| | |
|-------|-----------------|
| X-596 | 6.000 |
| T-530 | 6.250 |
| X-495 | 5.450 |
| P-962 | 6.845 |
| Y-298 | 4.000 (assumed) |

Conversion Units: 1 ksi = 6.90 MPa

The bridges were scattered around the state of Missouri with no two bridges lying on the same route. The types of composite strengthening techniques utilized on the bridges are provided in Table 3.5. Notice that FRP manual lay-up strengthening was used on every bridge. The material properties of each individual composite strengthening application are provided in Table 3.6. The following sections provide specific details for each bridge and the strengthening applications used.

Table 3.5. Composite Strengthening Utilized

| Bridge Code | CFRP Sheets by Manual Lay-Up | Pre-cured CFRP Laminates | CFRP NSM Bars | SRP by Manual Lay-Up | MF FRP Laminates |
|-------------|------------------------------|--------------------------|---------------|----------------------|------------------|
| T-0530 | YES | YES | | | |
| X-0495 | YES | | YES | | |
| X-0596 | YES | | YES | | |
| P-0962 | YES | | YES | YES | |
| Y-0298 | YES | | | | YES |

Table 3.6. Composite Material Properties

| FRP System | Dimensions | f_u (ksi) | E_f (ksi) |
|---------------------------|-----------------------|-------------|-------------|
| Manual Lay-up | 0.0065-in. thick | 550 | 33000 |
| Pre-Cured Laminate Plates | 0.0787-in. thick | 350 | 20000 |
| NSM Tape | 0.63-in. x 0.0079-in. | 300 | 19000 |
| NSM Bars | 0.5-in. Diameter | 300 | 19000 |
| SRP 3X2 | 0.0173-in. Thick | 460 | 30000 |
| SRP 3SX | 0.0104-in. Thick | 345 | 30000 |

Conversion Units: 1-in. = 25.4mm

3.2. BRIDGE DETAILS AND STRENGTHENING

3.2.1. Bridge X-596. Bridge X-596 is located on Highway C and spans Lander's Fork Creek in Morgan County, Missouri. This bridge was originally constructed in 1946 and consists of three simply supported reinforced concrete spans of lengths 42-ft 6-in. (13.0m), 52-ft 6-in. (16.0m), and 42-ft 6-in. (13.0m) with a roadway width of 20-ft (6.1m). The 6-in. (152mm) deck is supported by three tee beams spaced on 9-ft (2.7m) centers. Load testing was conducted on the center span.

The condition of X-596 prior to strengthening was such that there were cracks in the exterior girders with exposed reinforcement. Figure 3.2 depicts the bridge and Figure 3.3 shows the condition of the superstructure. In addition, there were cracks at the connections between girders and the intermediate diaphragms and bents. The end bents were in overall good condition aside from rusty steel bearing plates.



Figure 3.2. Bridge X-596



Figure 3.3. Bridge X-596 Superstructure

X-596 was strengthened using NSM bars for flexure and FRP manual layup for flexure and shear. Tables 3.7, 3.8 and 3.9 show the amount of composite flexural and shear strengthening utilized on the slab and girders.

Table 3.7. Bridge X-596 Slab Flexural Strengthening

| Span | Type | Amount | Capacity Increase |
|---------|---------------|--------------------------------|-------------------|
| Central | NSM Tape | 2 per Groove at 12-in. O/C | 78% |
| End | Manual Lay-up | 1 ply 6-in. Wide at 15-in. O/C | 61% |

Conversion Units: 1-in. = 25.4mm

Table 3.8. Bridge X-596 Girder Flexural Strengthening

| Span | Girder | Description | Capacity Increase |
|---------|----------|---|-------------------|
| Central | Interior | Manual Lay-up: 4 Plies 20-in. Wide; NSM Bars: 4 total | 42% |
| Central | Exterior | None | N/A |
| End | Interior | Manual Lay-up: 4 Plies 20-in. Wide; NSM Bars: 4 total | 44% |
| End | Exterior | Manual Lay-up: 2 Plies 16-in. Wide | 16% |

Conversion Units: 1-in. = 25.4mm

Table 3.9. Bridge X-596 Girder Shear Strengthening

| Span | Girder | Description | Capacity Increase |
|---------|----------|--|-------------------|
| Central | Interior | Manual Lay-up: 1 Ply Continuous U-Wrap | 26% |
| Central | Exterior | None | N/A |
| End | Interior | Manual Lay-up: 2 Ply Continuous U-Wrap | 52% |
| End | Exterior | None | N/A |

In order to install these composites, 116-ft³ (3.285m³) of deteriorating concrete was removed and the new surface was cleaned. The surface was then prepared for the placement of FRP via manual lay-up by rounding corners and roughening with sandblasting. The installation

details for Bridge X-596 are provided in Figures 3.4, 3.5 and 3.6. These strengthening details were typical for Bridges T-530, X-495 and P-962.

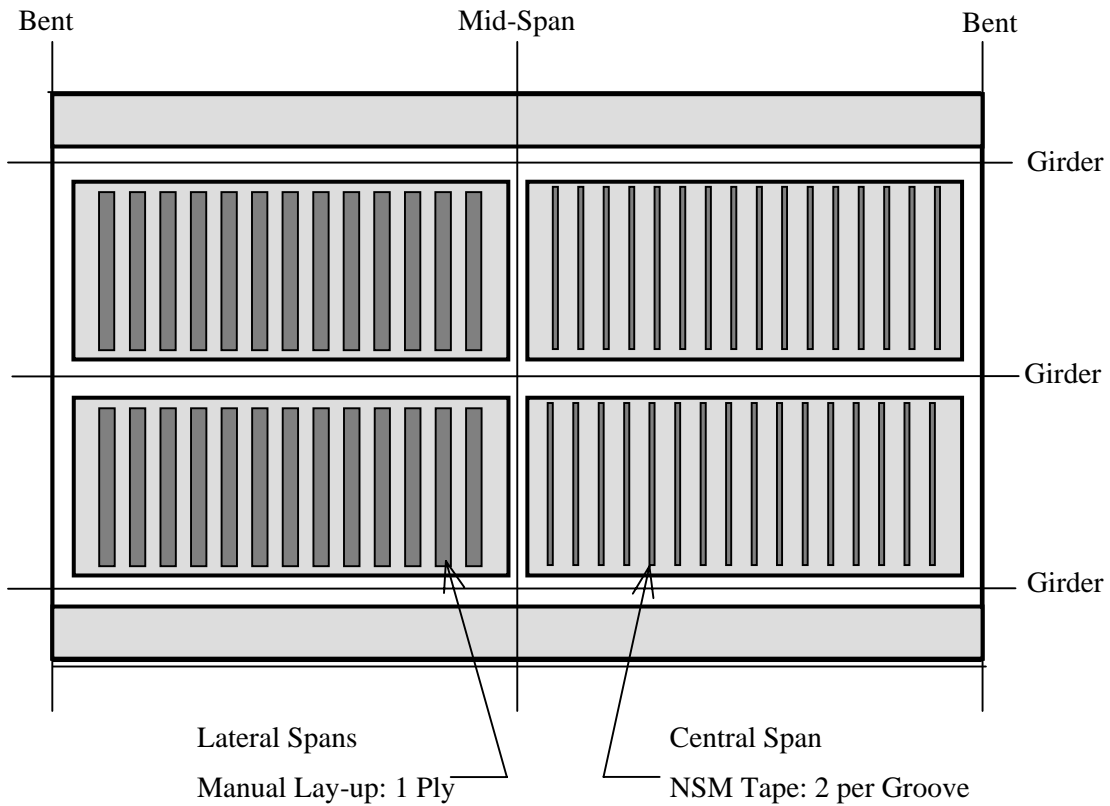


Figure 3.4. Bridge X-596 Plan View Strengthening Detail

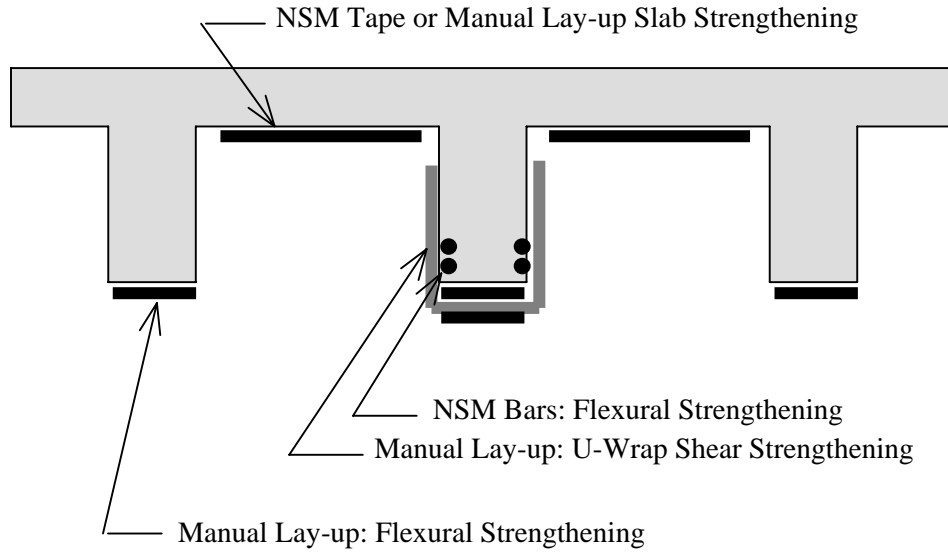


Figure 3.5. Bridge X-596 Cross - Section View Strengthening Detail

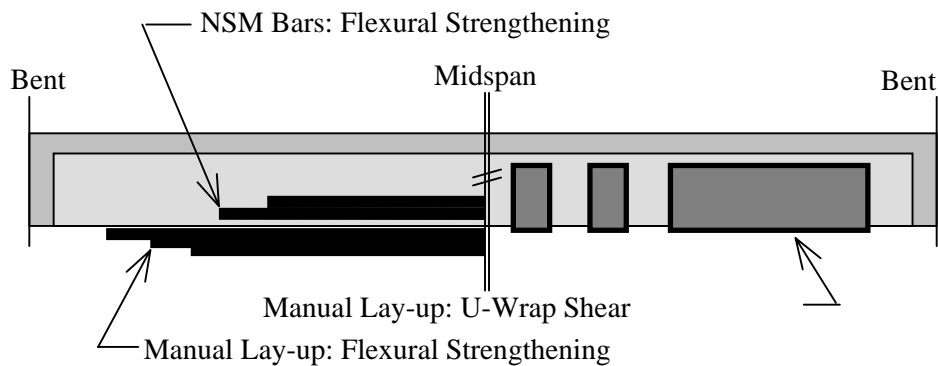


Figure 3.6. Bridge X-596 Cross - Side View Strengthening Detail

3.2.2. Bridge T-530. Bridge T-530 is located on Highway M and spans Crooked Creek in Crawford County, Missouri. This bridge was originally constructed in 1937 and consists of five simply supported spans, all 47-ft (14.3m) long with a roadway width of 23-ft (7.0m). The 6-in. (152mm) deck is supported by four tee beams spaced 6-ft 6-in. (2.0m) on center. Load testing was conducted on the second span from the North abutment.

Bridge T-530 before strengthening is shown in Figures 3.7 and 3.8. Prior to strengthening, the concrete exhibited some spalling along the bridge edges. The concrete in the deck and beams was noted to be in good condition, with only minor cracks that required no injection. The piers and abutments were in good condition also, but the bents showed some deterioration due to steel corrosion.



Figure 3.7. Bridge T-530



Figure 3.8. Bridge T-530 Substructure

T-530 was strengthened in flexure using both manual lay-up and precured laminates on the deck and girders. Ten-ft³ (0.283m³) of concrete was removed from deteriorated areas and the surfaces were prepared before the reinforcement was placed. Tables 3.10 and 3.11 list the quantities, types and flexural capacity increase achieved on the slab and girders.

Table 3.10. Bridge T-530 Slab Flexural Strengthening

| Span | Type | Amount | Capacity Increase |
|---------|-----------------|----------------------------------|-------------------|
| 1, 3, 5 | Manual Lay-up | 1 Ply 9-in. Wide at 15-in. O/C | 141% |
| 2, 4 | Laminate Plates | 1 Plate 3-in. Wide at 15-in. O/C | 143% |

Conversion Units: 1-in. = 25.4mm

Table 3.11. Bridge T-530 Girder Flexural Strengthening

| Span | Girder | Description | Capacity Increase |
|---------|----------|------------------------------------|-------------------|
| 1, 3, 5 | Interior | Manual Lay-up: 4 Plies 16-in. Wide | 29% |
| 1, 3, 5 | Exterior | Manual Lay-up: 2 Plies 16-in. Wide | 15% |
| 2, 4 | Interior | 1 Laminate Plate: 12-in. Wide | 29% |
| 2, 4 | Exterior | 1 Laminate Plate: 12-in. Wide | 15% |

Conversion Units: 1-in. = 25.4mm

3.2.3. Bridge X-495. X-495 is located on Highway C and spans Crane Pond Creek in Iron County, Missouri. This bridge was originally constructed in 1948 and consists of three simply supported spans of lengths 42-ft 6-in. (13.0m), 52-ft 6-in. (16.0m), and 42-ft 6-in. (13.0m) with a deck width of 24-ft (7.3m). The 6-in. (152mm) deck is supported by three tee beams spaced 9-ft on center. Load testing was conducted on the center 52-ft 6-in. (16.0m) span.

Prior to strengthening, the condition of the beams, abutments and piers were noted to be in good condition. Of the bridges tested in this project, bridge X-495 was in the best condition considering its overall age and average rating. See Figures 3.9 and 3.10 for visual details of the bridge prior to strengthening.



Figure 3.9. Bridge X-495



Figure 3.10. Bridge X-495 Substructure

X-495 was strengthened in flexure using NSM bars and manual FRP lay-up. Due to the good condition of this bridge, repair work did not require the removal of deteriorated concrete.

The surface was prepared in accordance with accepted practices for installation of FRP via manual lay-up and NSM bars. Tables 3.12, 3.13 and 3.14 show the amount of composite flexural and shear strengthening utilized for Bridge X-495 on the slab and girders.

Table 3.12. Bridge X-495 Slab Flexural Strengthening

| Span | Type | Amount | Capacity Increase |
|------|---------------|--------------------------------|-------------------|
| All | Manual Lay-up | 1 ply 6-in. Wide at 14-in. O/C | 65% |

Conversion Units: 1-in. = 25.4mm

Table 3.13. Bridge X-495 Girder Flexural Strengthening

| Span | Girder | Description | Capacity Increase |
|---------|----------|---|-------------------|
| Central | Interior | Manual Lay-up: 5 Plies 20-in. Wide | 40% |
| Central | Exterior | None | N/A |
| End | Interior | Manual Lay-up: 5 Plies 16-in. Wide; NSM Bars: 2 total | 44% |
| End | Exterior | Manual Lay-up: 2 Plies 16-in. Wide | 16% |

Conversion Units: 1-in. = 25.4mm

Table 3.14. Bridge X-495 Girder Shear Strengthening

| Span | Girder | Description | Capacity Increase |
|---------|----------|---|-------------------|
| Central | Interior | Manual Lay-up: 1 Ply Continuous U-Wrap | 30% |
| Central | Exterior | None | N/A |
| End | Interior | Manual Layup: 2 Plies Continuous U-Wrap | 51% |
| End | Exterior | Manual Lay-up: 1 Ply 12-in. Wide; U-Wrap 24-in. O/C | 18% |

Conversion Units: 1-in. = 25.4mm

3.2.4. Bridge P-962. Bridge P-962 is located on Highway B and spans Dousinbury Creek in Dallas County, Missouri. This bridge was originally constructed in 1956 and consists of three simply supported spans, all 42-ft 6-in. (13.0m) long, with a 23-ft (7.0m) wide deck. The 6-in. (152mm) deck is supported by three tee beams spaced 9-ft (2.7m) on center. Load testing was conducted on all three spans with primary monitoring focused on span 1.

Prior to strengthening, the bridge beams and piers were noted to be in good condition; see Figures 3.11 and 3.12. The abutments were not in good condition and the deck required some repairs.



Figure 3.11. Bridge P-962



Figure 3.12. Bridge P-962 Substructure

P-962 was strengthened in flexure using NSM bars, manual FRP lay-up and SRP. In order to place the SRP and FRP on the bottom of the bents, 20-ft³ (0.566m³) of concrete was removed. In addition, cleaning and substrate preparation was required for the SRP and FRP sheets.

Table 3.15. Bridge P-962 Slab Flexural Strengthening

| Span | Type | Amount | Capacity Increase |
|------|--------------|-----------------------------|-------------------|
| 1, 2 | Manual Layup | 1 Ply 6" Wide at 14-in. O/C | 64% |
| 3 | SRP 3X2 | 1 Ply 4" Wide at 20-in. O/C | 62% |

Conversion Units: 1-in. = 25.4mm

Table 3.16. Bridge P-962 Girder Flexural Strengthening

| Span | Girder | Description | Capacity Increase |
|------|----------|---|-------------------|
| 1, 2 | Interior | Manual Layup: 5 Plies 16-in. Wide plus 4 NSM Bars | 56% |
| 1, 2 | Exterior | Manual Layup: 3 Plies 16-in. Wide | 25% |
| 3 | Interior | SRP 3X2: 3 Plies 16-in. Wide | 54% |
| 3 | Exterior | SRP 3X2: 2 Plies 16-in. Wide | 49% |

Conversion Units: 1-in. = 25.4mm

Table 3.17. Bridge P-962 Girder Shear Strengthening

| Span | Girder | Description | Capacity Increase |
|------|----------|---|-------------------|
| 1, 2 | Interior | Manual Layup: 4 Plies Continuous U-Wrap | 64% |
| 1, 2 | Exterior | Manual Layup: 1 Ply Continuous U-Wrap | 24% |
| 3 | Interior | SRP 3SX: 3 Plies Continuous U-Wrap | 63% |
| 3 | Exterior | SRP 3SX: 1 Ply Continuous U-Wrap | 36% |

3.2.5. Bridge Y-298. Bridge Y-298 is located on Highway U and spans Crews Branch Creek in Pulaski County, Missouri. This bridge was originally constructed in 1937 and consists of two continuous spans, each 15-ft (4.6m) long, 7-in. (178mm) deep and 27-ft (8.2m) wide. The load testing was conducted on both spans.

Prior to strengthening, it was noted that the east span was in poor condition due to poor drainage, especially close to the edge of the bridge. Also, upon visual inspection the east span showed permanent deflection. The west span concrete was sound, but, due to improper concrete cover, had some exposed reinforcement. See Figures 3.13 and 3.14 for the visual appearance of Y-298 before strengthening.



Figure 3.13. Bridge Y-298



Figure 3.14. Bridge Y-298 Substructure

Y-298 required the use of two strengthening techniques for flexure. The first was FRP lay-up, which was difficult to install due to the poor condition of the concrete substrate. The second strengthening procedure involved placing MF FRP laminates in the areas with severe

corrosion. The laminates were bolted to the substrate and provided a quick means of strengthening the bridge where proper surface preparation would have been difficult; however, the long-term performance of this strengthening technique is questionable. Table 3.18 shows the type of flexural reinforcement utilized on Bridge Y-298 and Figure 3.15 shows a plan view of bridge Y-298 with a detail for the composite reinforcement installation.

Table 3.18. Bridge Y-298 Slab Flexural Strengthening

| Span | Type | Amount | Capacity Increase |
|------|--------------|-------------------------------|-------------------|
| Both | Manual Layup | 2 Plies 8" Wide at 12-in. O/C | 23% |

Conversion Units: 1-in. = 25.4mm

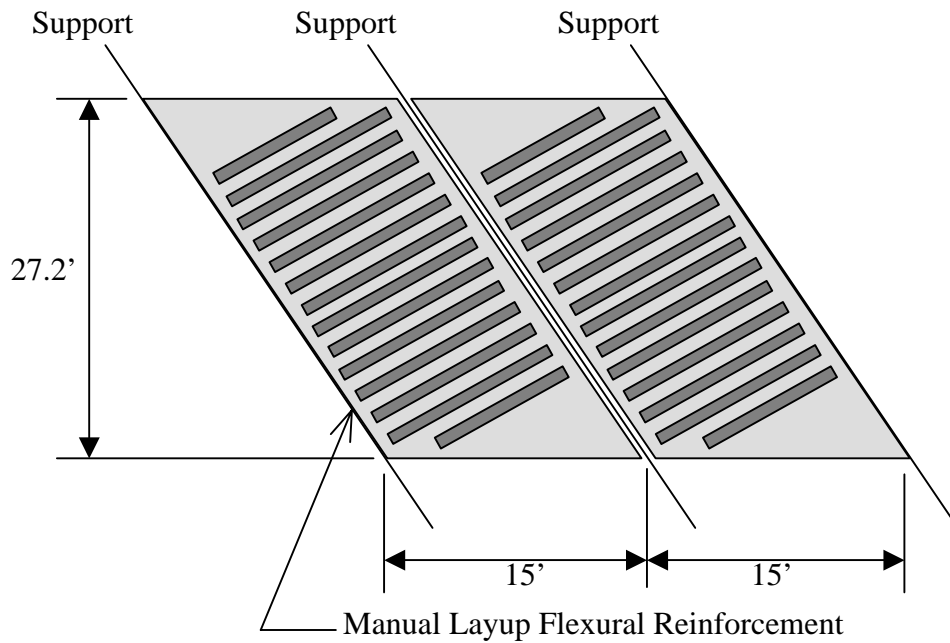


Figure 3.15. Bridge Y-298 Slab Reinforcement Detail

3.2.6. Summary of Strengthening and Analytical Capacity Increase. For strengthening purposes, placement location and quantity of the FRP reinforcement were important when considering long-term field validation with load testing. Table 3.19 shows the type, amount, placement location and flexural capacity gained by adding the reinforcement to the girders of the load tested spans. An important distinction is that the exterior girders of bridges X-495 and X-596 have not been strengthened.

Table 3.19. Composite Strengthening on Tested Spans

| Bridge & Tested Span | Girder | Flexural Reinforcement Description | Analytical Capacity Increase |
|----------------------|----------|--|------------------------------|
| X-596 Span 2 | Interior | Manual Lay-up: 4 Plies 20-in. Wide; (4) NSM Bars | 42% |
| | Exterior | None | N/A |
| T-530 Span 2 | Interior | 1 Laminate Plate: 12-in. Wide | 29% |
| | Exterior | 1 Laminate Plate: 12-in. Wide | 15% |
| X-495 Span 2 | Interior | Manual Lay-up: 5 Plies 20-in. Wide | 40% |
| | Exterior | None | N/A |
| P-962 Span 1 & 2 | Interior | Manual Lay-up: 5 Plies 16-in. Wide; (4) NSM Bars | 56% |
| | Exterior | Manual Layup: 3 Plies 16-in. Wide | 25% |
| P-962 Span 3 | Interior | SRP 3X2: 3 Plies 16-in. Wide | 54% |
| | Exterior | SRP 3X2: 3 Plies 16-in. Wide | 49% |

Conversion Units: 1-in. = 25.4mm

4. LOAD TESTING AND SURVEYING EQUIPMENT

4.1. LOAD TESTING

Load testing is observing and measuring the response of a structure subjected to controlled loads in the elastic range (AASHTO 2003). Load testing has many purposes and benefits to match; it allows engineers to determine unknown factors, such as composite action and unintended fixity levels, continuity, and participation of other members. Load testing is proven to be an effective way for structural engineers to evaluate the structural performance of a bridge (AASHTO 2002). Several researchers have investigated in-situ load testing of bridges (Vurpillot et al., 1998, Oh et al., 2002, Pfeil, 1981, Benmokrane et al., 1999, Stallings et al., 2000).

There are two main types of load testing: diagnostic testing and proof testing. A diagnostic load test is chosen to find the response characteristics of a structure, including load response, load distribution, validating analytical models, and evaluating the effectiveness of structural repairs and upgrades where the structure may not be accurately load rated (AASHTO 2003). The Five-Bridges Project utilized diagnostic load testing to prove that the FRP strengthening is working effectively. Alternatively, the proof load test is designed to establish the safe load carrying capacity of the structure while loading the structure within the elastic range (AASHTO 2003). Determining the load rating for a bridge would be evaluated from a proof load test.

4.1.1. Static and Dynamic Testing. The load testing procedure for the Five Bridges diagnostic and proof load tests could be performed using static or dynamic loads, or both. Static loads are stationary loads; they induce no vibrations. The location and magnitude of the loads may change during testing. Parking a standard loaded truck on the structure tends to be easiest

method of testing real structures (Figure 4.1). Dynamic load tests use moving loads to induce vibrations and find the very rapid loading response of the structure. These tests allow for the analysis of dynamic load allowance, frequency, vibration, and a stress range for fatigue evaluation (AASHTO 2003). Driving loaded trucks over pre-determined locations at given speeds is the easiest method of testing dynamic loading.



Figure 4.1. Loaded Trucks Used to Test a Bridge

4.1.2. Timing and Testing Duration. Timing of the load testing is also a variable. In load testing buildings, ACI Committee 318 recommends applying a load for 24 hours before taking loaded measurements, and then removing the load for 24 hours before taking the final measurements (ACI Committee 318). Rapid load testing has been gaining in popularity as an

alternative to the 24-hour load testing scheme. Rapid load testing applies the load in multiple steps; the structure is also loaded and unloaded in multiple cycles (ACI Committee 437).

4.1.3. Measurements and Instrumentation. A variety of measurements can be made during the load test. Strain gauges are commonly applied to structural components at critical locations. Measuring strain allows engineers to evaluate stress distribution and contribution of members. Typically, electrical resistance gauges are used; however, other methods of measuring strain are also used. Displacement is another common measurement. Linear Variable Displacement Transducers (LVDT's – see Figure 4.2) are popular tools because they can measure both static and dynamic loads. LVDT and dial gauges both require stable support assemblies and recommended accuracies of 0.0001 and 0.001 inches respectively (ACI Committee 437). Without stable support the accuracy is greatly reduced. Other measurements include rotation and acceleration; rotation is critical for torsional effects and finding fixity levels in a structure. Table 4.1 lists a summary of the measurements made and devices used for load testing.



Figure 4.2. Two LVDT's Measuring Deflection

Table 4.1. Instrumentation Used in Load Testing (ACI Committee 437)

| Measurement | Device | Precision | Range |
|-------------|---------------------|------------------|----------------------|
| Deflection | LVDT | 0.0001 in | 2 in |
| | Dial Gage | 0.001 in | 3 in |
| Strain | Strain Gage | 1 $\mu\epsilon$ | 3,000 $\mu\epsilon$ |
| | Extensometer | 50 $\mu\epsilon$ | 10,000 $\mu\epsilon$ |
| | LVDT | 50 $\mu\epsilon$ | 10,000 $\mu\epsilon$ |
| Crack Width | Extensometer | 0.0001 in | 0.2 in |
| Load | Load Cell | 10 lb | 200,000 lb |
| | Pressure Transducer | 100 lb | 200,000 lb |

Conversion Units: 1 in = 25.4 mm; 1 lb = 4.45 N

4.1.4. Testing Protocol. Protocols for a load test on a building are generally decided by the organization running the test (ACI Committee 437). While researchers have attempted to refine testing procedures, the fundamental protocol remains unchanged (ACI Committee 437). When load testing is proposed, the details of load application, instrumentation, and personnel should be carefully planned (AASHTO 2002). Load testing is only warranted when economics, safety, site conditions, and structural evaluation considerations are determined to be acceptable.

4.2. USING SURVEYING EQUIPMENT

Because of existing site conditions at four of the five bridges, traditional serviceability monitoring techniques, like using Linear Variable Displacement Transducer (LVDT) systems, would have been extremely difficult; the search for a better system ended with the decision to use Surveying Equipment in place of LVDTs. The purpose of the following sections is to authenticate use of Surveying Equipment in structural monitoring applications. The details herein include: introducing the surveying equipment, discussing development of the necessary

procedures for using the equipment, directly comparing the two systems in structural monitoring applications, and reviewing three comparison studies to verify the accuracy of the surveying equipment.

4.2.1. Understanding Surveying Equipment. Traditional land surveying techniques use many components, with the total station as the principal device. The total station (Figure 4.3) was set atop a secure tripod in a location with an unobstructed view of the field targets. Reference points (Figure 4.4), or backsites, were set in place to transfer a horizontal angle or an elevation from the reference point to the total station, and then from the total station to the target prisms (Figure 4.5). The reference points also served to check that the total station had not moved. The reference point was a prism mounted atop a secure tripod and the targets were prisms fixed atop a metal rod (range pole). In the case of load testing, the prisms were fixed to points on the tested structure.



Figure 4.3. Leica TCA 2003



Figure 4.4. Reference Point



Figure 4.5. Target Prism

The total station obtained three-dimensional coordinates of every target by measuring a horizontal angle, vertical angle, and the distance between points. The instrument was automatically set to take four angle readings per recorded shot (measurement); this was done internally by four diodes optically reading a fine bar code set on a glass ring inside the instrument. During operation, the instrument continuously read the bar codes on the horizontal and vertical planes. This “electronic protractor” inside the Leica TCA 2003 (Leica 2003) was accurately read to 0.5 arc-seconds ($1/7200$ degrees).

The total station measured distance by using an EDM (Electronic Distance Meter); the EDM sent a laser signal to the glass prism target, which reflected the signal back to the total station. The time taken for the signal to return to its origin was multiplied by the signal speed to obtain the target distance. The total station adjusted the signal speed based on field conditions (temperature, pressure, etc.), so that the instrument could measure a distance accurate to 1 mm plus 1 ppm (1-in. = 25.4mm). The EDM could be set to measure distance using one of several measuring programs. The programs took multiple distance readings and recorded the average distance for each recorded shot (measurement); some programs took less time but were also less

accurate. With a horizontal angle, vertical angle, and distance measurement, coordinate geometry was used to transfer three-dimensional coordinates to a target. The total station automatically recorded the coordinates with a point number, point description, date, time, and atmospheric conditions.

The targets were glass prisms in enclosed cases. The glass prism was designed to reflect the laser signal back to the total station without interference from other nearby objects. Moisture, dirt, and surface scratches on the prisms could obstruct the signal, so the prisms must be well kept.

While past load testing showed that traditional Surveying Equipment was not accurate enough to measure small deformations (Yang and Myers 2003), recent advances in technology have made it possible to use surveying equipment to monitor deformation in structural monitoring applications. The new and more accurate Leica TCA 2003 Total Station could measure deformation accurate to 0.005 inches or better at close range (less than 200 feet), making it comparable to traditional systems that use LVDT's. The Leica Total Station became even more accurate through the use of robotics; the instrument rotated on the horizontal and vertical axes independently, recognizing and locking onto targets automatically. The user manually located the targets at the start of testing, and the Total Station automatically relocated the target and measured deformation. Because the instrument was extremely sensitive to vibration and movement, automation helped to eliminate human error, requiring less user interaction with instrument during operation.

4.2.2. Limitations of Surveying Equipment. Before implementation, many advantages and disadvantages were known about using the Surveying Equipment in place of LVDTs for load testing project bridges. After completing the three case studies and comparing the two systems, additional issues became apparent.

Setup time of the LVDT system at the bridge site had long been a problem. For spans clearing less than fifteen feet above stable soil, setup time easily took several hours. Soil under the tripods must be compacted, the tripods and LVDTs must be assembled and wired, and the LVDT's must be checked. For a bridge span over deep water or average span height above fifteen feet, scaffolding was mandatory for the LVDTs, adding much more time and effort. In the worst case, the surveying equipment was set up in about forty-five minutes. Every component (soil, scaffolding, and tripods) supporting the LVDT introduces error into the system. Target height and site conditions were practically irrelevant with the Total Station.

The LVDT system was designed for laboratory use and adapted for field use. Using this system in the field required much more time, effort, and manpower for both preparation and testing. While two people or more set up the surveying equipment, one person can set up and operate the Total Station without much additional effort. Site conditions were critical when using the LVDT system. The electronic equipment required significant wiring and a generator as well. The electrical components were very sensitive to the weather, mainly water, which created obvious problems for load testing bridges. The surveying equipment was designed for outdoor use; all components were rugged and waterproof, including the Total Station. The Total Station measured accurately regardless of weather conditions.

With testing time the LVDT system regained popularity. If twenty points were monitored on the structure, the Total Station took over twenty minutes to measure those points while the

LVDT system measured continuously. If the bridge was heavily traveled, then the road could feasibly be closed for long periods of time. If a twenty-four hour sustained load test was chosen, which is recommended for in-situ testing by ACI, then the issue of additional measuring time needed with the Total Station was eliminated (ACI Committee 318). For rapid load testing, the structure would be loaded and unloaded cyclically multiple times (ACI Committee 437). Rapid load testing was not feasible with the Total Station because of the time required to measure every point.

The continuous monitoring of LVDT system allowed for real-time output. Any equipment problems were noticed during testing and corrected. Real-time monitoring was not possible with the Total Station; any problems during testing were well documented and later corrected during data analysis. Continuous monitoring also allowed for dynamic load testing with LVDTs; again this was not possible with the Total Station.

The Total Station used in testing has an internal error directly associated with how accurately it can measure angles and distances. For load testing instrumentation monitoring deformation, it was recommended that LVDT systems have an accuracy of 0.0001 inches, or 0.001 inches if dial gauges were used instead of LVDTs (ACI Committee 437).

4.2.3. Comparison Studies. Three comparison studies were performed to verify the accuracy of the surveying equipment. Two tests were performed in the field while one was performed in the laboratory.

4.2.3.1 Case Study 1: Field Test. The first test took place at Bridge Y-298 in Pulaski County, Missouri. This bridge was chosen for a comparison study because the area underneath the structure is easily accessible, making setup of the LVDT system relatively easy. Figure 4.6 and Figure 4.7 show the low clearance of the substructure, as well as the setup of the LVDT and

surveying systems. Setup time for the surveying equipment took about fifteen minutes; setup time for the LVDT system took over sixty minutes.



Figure 4.6. LVDTs and Target Prisms



Figure 4.7. Total Station Setup

The load test of Bridge Y-298 consisted of four truck stops. During each stop, overloaded MoDOT H20 dump trucks were parked on the bridge in specified locations. Deflection was measured with both systems in six locations per span, or twelve total locations. The Total Station took over ten minutes to measure while the LVDT system took only a few minutes. The amount of time needed by the Total Station is a function of how many points are being monitored. The LVDT system measures instantaneously; however, several minutes are allowed initially for the bridge to stabilize under loading. This factor was ignored with the Total Station because it spent the first minutes measuring reference points. Figure 4.8 and Figure 4.9 show the results of two stops over the west span of the bridge.

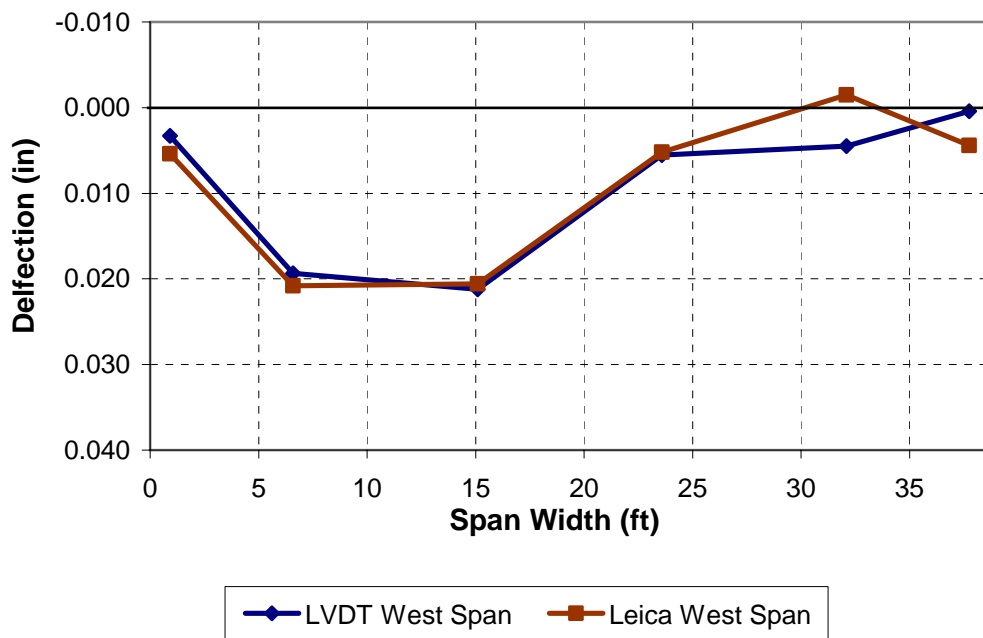


Figure 4.8. Stop 2 – West Span Deflection

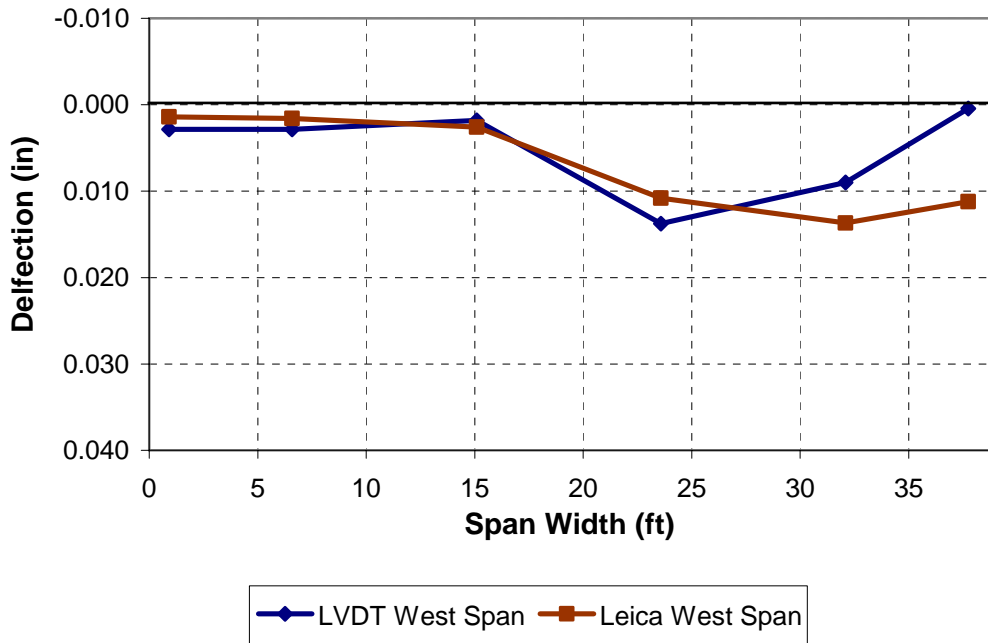


Figure 4.9. Stop 3 – West Span Deflection

Forty samples were taken for comparison between the LVDT and surveying systems. The (absolute) variance between the two systems was as follows: average: 0.003 inches, median: 0.002 inches, maximum: 0.012 inches. The internal accuracy of the Total Station was 0.002 inches for this test. Discrepancy between systems may be due to the setup of the LVDT supporting tripods (shown in Figure 4.6), as a stable tripod base is fundamental to acceptable readings. In this case, where the tripods sat on rock, slipping was possible but unlikely.

4.2.3.2 Case Study 2: Laboratory Test. The laboratory test utilized three deformation monitoring systems: string transducers, LVDTs and surveying equipment. The goal of a laboratory comparison was to minimize error by testing under ideal conditions. While the surveying equipment was primarily designed for field use, the string transducer and LVDT systems were not. Stable footings low to a concrete floor (i.e. no tall tripods, no scaffolding), organized equipment (Figure 4.10), and climate control helped eliminate potential error

associated with using equipment outside the laboratory. The surveying equipment was adapted to laboratory use without incident (Figure 4.11).

The specimen tested was a thirty-four foot prestressed concrete I-beam. The I-beam was loaded with two hydraulic jacks, shown in Figure 4.10. While the string transducer and LVDT systems were set to monitor deflection continuously, the Total Station could only measure when the load was constant. The Total Station was set to measure three times throughout the test; the results of one measurement are shown in Figure 4.12. Some LVDTs and string transducers were not functioning properly, so they were removed from this analysis.

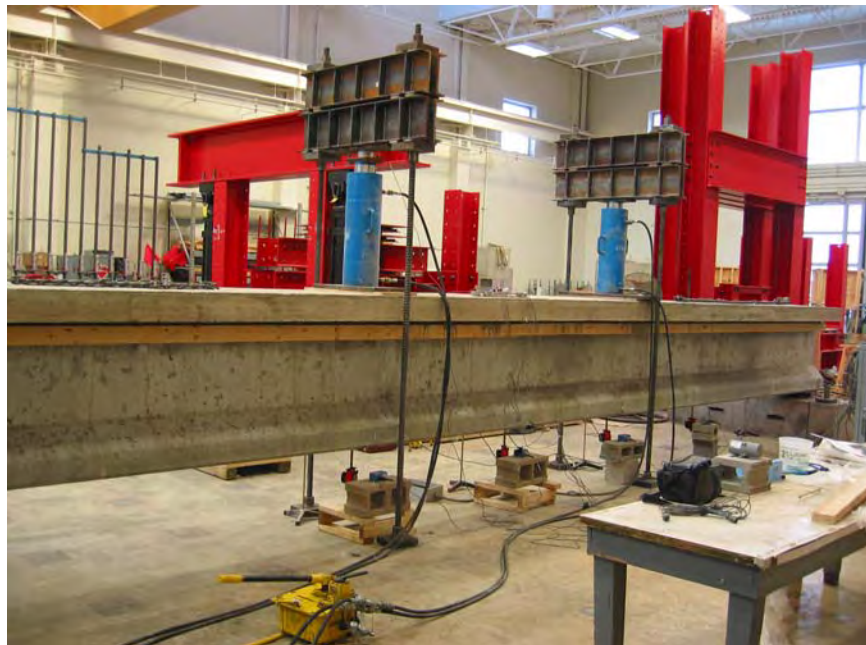


Figure 4.10. Laboratory Test Setup

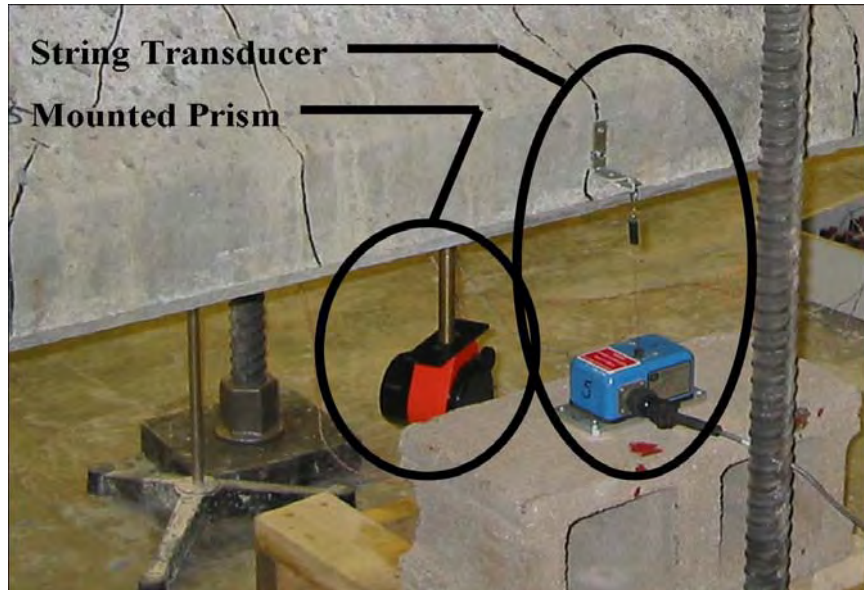


Figure 4.11. String Transducer and Mounted Target Prism

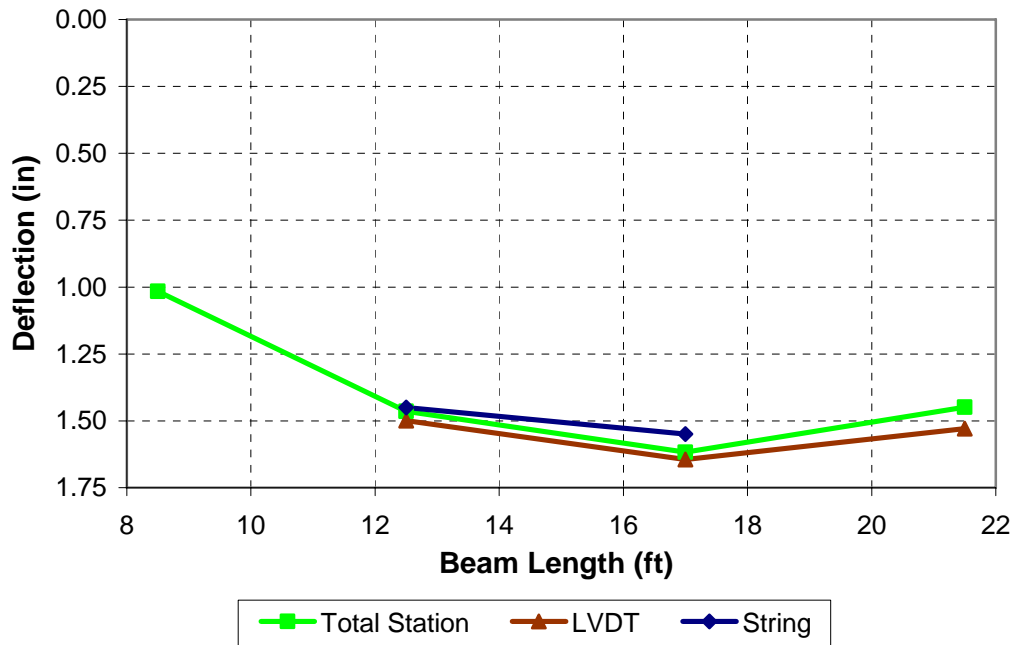


Figure 4.12. Laboratory Test Results

For system comparison during the sampled measurements, the surveying equipment was compared to the LVDT system at three locations (nine total samples); the string transducer

system was compared at two locations (six total samples). The mean variance between the surveying equipment and LVDT system was 0.04 inches; the mean variance between the surveying equipment and string transducer system was 0.02 inches; the mean variance between the LVDT and string transducer systems was 0.06 inches. At every instance, the measured deflection by the surveying equipment fell between the two laboratory systems. Variance between all three measuring systems was consistent, regardless of deformation magnitude.

Error could most likely be due to several sources. First, the string transducers, LVDTs, and prisms were not mounted as close to each other as possible, at a given location. If the instrumentation was not located in the same proximity, torsion/rotation effects could influence the readings. Second, during testing when the load was held constant, it was noted that the hydraulic jacks do not actually hold a constant load. This was plotted (Load versus Deformation via LVDTs and String Transducers) after testing, which automatically sets the surveying equipment at a disadvantage. However, this does not account for the difference between string transducer and LVDT readings. Compared to the variances between these two systems, internal error of the Total Station was negligible.

4.2.4. Verifying Surveying Equipment for Load Testing. The prior sections presented surveying equipment as an alternative means to monitor serviceability of structures during static load testing. With the appropriate equipment, setup procedure and operation during testing, as well as an appropriate data analysis procedure, the accuracy of surveying equipment challenges that of traditional deformation monitoring systems using LVDTs.

A major setback in using surveying equipment was that real-time monitoring was not possible. Additionally, surveying equipment cannot be used to monitor serviceability during a

dynamic load test. However, for the Five Bridges project, the benefits of using surveying equipment for Structural Deformation Monitoring far outweighed the drawbacks, therefore only the surveying equipment was used in load testing.

5. FIELD TEST PROGRAM

Load testing represented an imperative step in validating the effectiveness of FRP composites in the field. The first series of load tests began in July of 2003 and have been conducted semi annually since, once each fall and once each spring with the final series of testing taking place during the spring of 2008. The first series of tests was conducted on the pre-strengthened bridge. This initial testing was very important because the results would later be compared to subsequent testing of the strengthened bridge. The following sections provide a brief explanation of load testing procedures for the 5 Bridge Project. For in depth instructions and procedures for test setup and Total Station operation see Appendix C.

5.1. TRUCKS FOR TEST WEIGHT

The load testing procedure for the Five Bridges Project involved the static placement of two loaded H20 dump trucks provided by MoDOT (Figure 5.1). Load tests utilizing loaded dump trucks have been conducted in the past and are an effective and simple means to evaluate bridges (Stone, 2002). The weight of the trucks was recorded to account for any large variances in weight between load tests and the potential of a considerable difference in deflection. The weights of both the front and rear tandem axles were recorded. For modeling purposes and to assist in the normalization of the load test deflection data, the dimensions of the truck axles and distances to the centerline of each tire were recorded as well.



Figure 5.1. MoDOT Provided H20 Truck

5.2. TEST SETUP

As indicated, testing utilized a Leica TCA 2003 Total Station and optical surveying prisms for targets located on the bridge and reference points; see Figure 5.2 for a load test setup example.

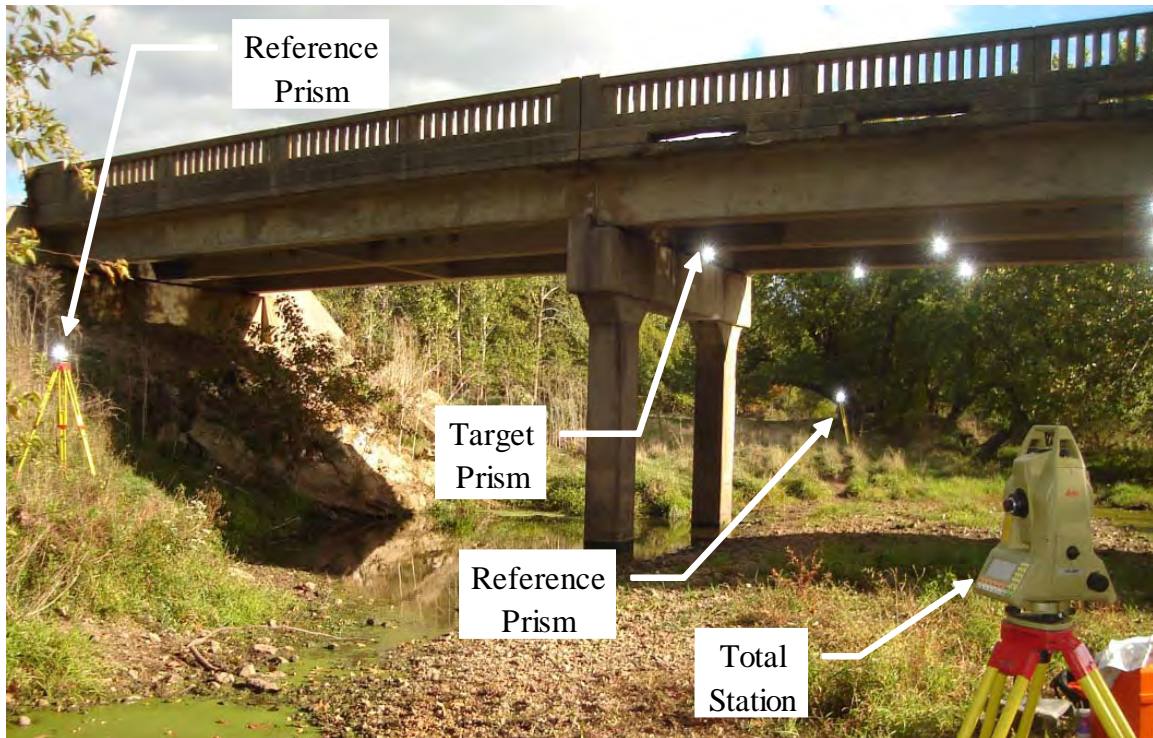


Figure 5.2. Total Station Test Setup

Iron plates were epoxied to the underside of the bridges at predetermined locations along the span and given time to cure prior to load testing. The plates remained for future load tests. Magnetized target prisms were then attached to the plates using a range pole. Figure 5.3 shows the attachment of the magnetized target prisms to the soffit of the bridge girders.



Figure 5.3. Attaching Target Prisms with Range Pole

During this time, an ideal location for the Total Station was selected. The Total Station was set atop a well-founded tripod and then leveled. The Total Station operator ensured the target prisms were visible through the sight. Next, three reference prisms were positioned at contrasting elevation points as far apart as possible and directed at the Total Station. The reference prisms served as guides in determining if the Total Station exhibited any movement between readings.

After the described process was completed, the Total Station was ready to automatically record the locations of all prisms. All targets were located and named in a sequential order, which was well documented in a field book. The Total Station was set to record each data point three times. Bridge traffic was stopped and the elevation of each point before loading was determined to establish a baseline. Next, the loaded dump trucks were placed on the bridge deck in configurations that would induce the largest stresses and deflections in the structure. Five stops each were conducted on bridges X-596, T-530, X-495 and P-962. Figure 5.4 shows the

stops used on bridge X-59; similar stops were used on the other bridges, though that additional presence of a skew angle should be noted. The stops and exact locations of the target prisms have been provided in Appendix B.

The first three stops were conducted with both trucks side-by-side driving down the length of the bridge. Stop 1 was conducted with both rear axles near the edge of the span to induce a maximum shear case. Stop 2 was conducted with both trucks side by side at midspan; this was a maximum moment configuration. Stop 3 was similar to stop 1 in that it produced a large shear case, only on the opposite side of the bridge. Stop 4 and 5 were overload conditions intended to produce maximum moments and, therefore, deflections on the exterior girder (Stop 4) and interior girder (Stop 5).

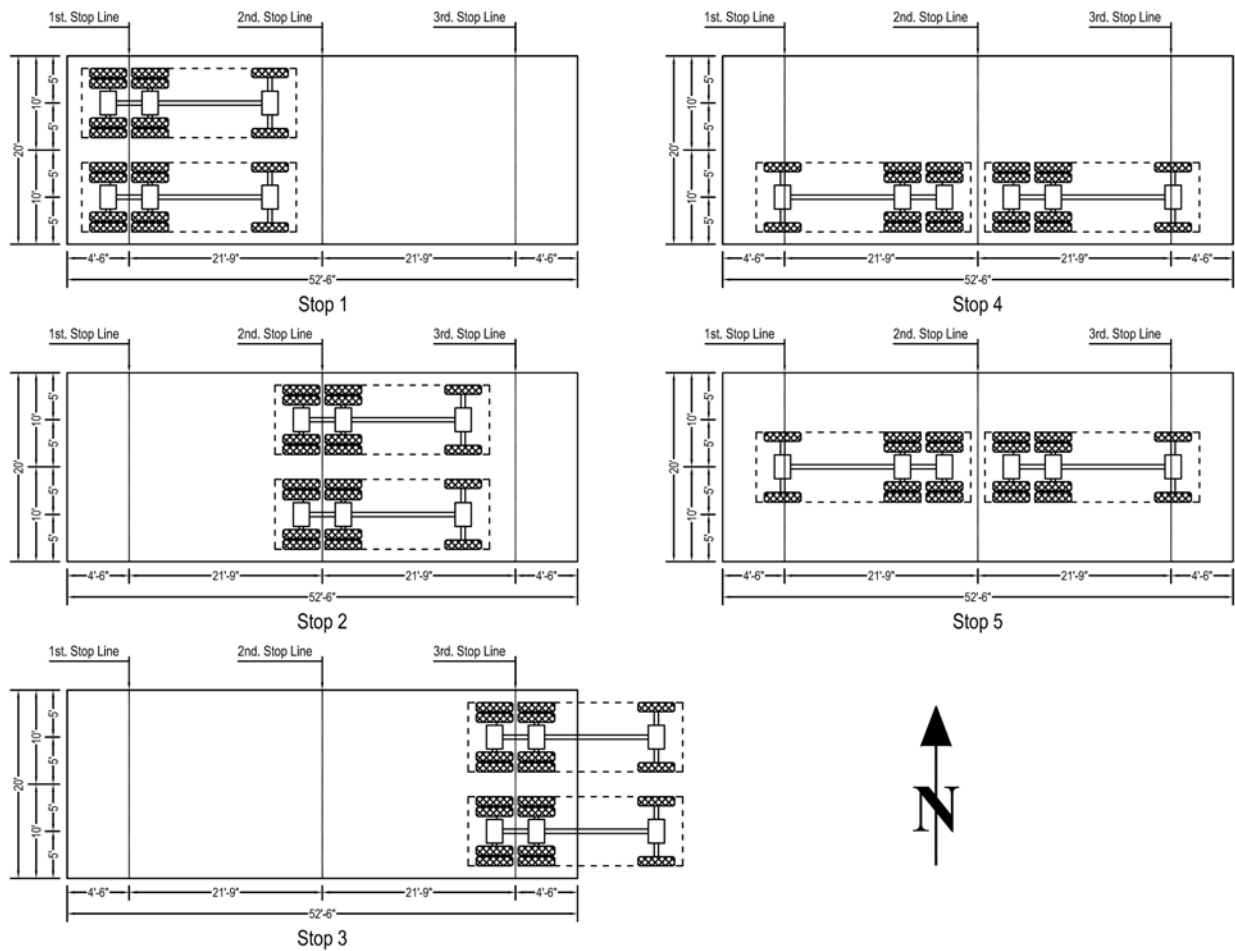


Figure 5.4. Bridge X-596 Truck Stops

Only two stops were conducted on bridge Y-298 due to the small size of the bridge. After the trucks had been placed, the bridge was given five minutes to settle under the load and the Total Station recorded the new elevations. The trucks were then moved off of the bridge and traffic was allowed to pass. After the final stop, the bridge was given five minutes to rebound and a final no load run was conducted to determine if the bridge elevation had changed from the first reading. This concluded the load test and the Total Station, reference prisms and target prisms could be removed and the data processed.

6. DATA PROCESSING

6.1. DEFLECTION CALCULATIONS

The deflection of the girders from each pass was determined by taking the difference between the baseline and the recorded stop elevations. The three readings taken for each point elevation were first analyzed. If any of the readings varied from the other two by more than 0.005in. (0.127mm), it was removed from consideration. The remaining points were then averaged to determine the point elevation. The baseline was subtracted from the calculated elevation to determine the deflection at the prism.

6.2. ACCOUNTING FOR THERMAL EFFECTS

Temperature readings were recorded with a temperature gun on the top deck and at the bottom of the girders three times during testing in order to quantify thermal effects. Figure 6.1 shows the temperature variance over time for Bridge X-596 at midspan of the interior girder. This test was conducted in the morning and an increasing temperature gradient was observed. A similar temperature rise was common for most conducted tests. The temperature variance shown in Figure 6.2 is one of the more extreme cases in temperature fluctuation observed during testing. During overcast days, the temperature variance was observed to be much lower.

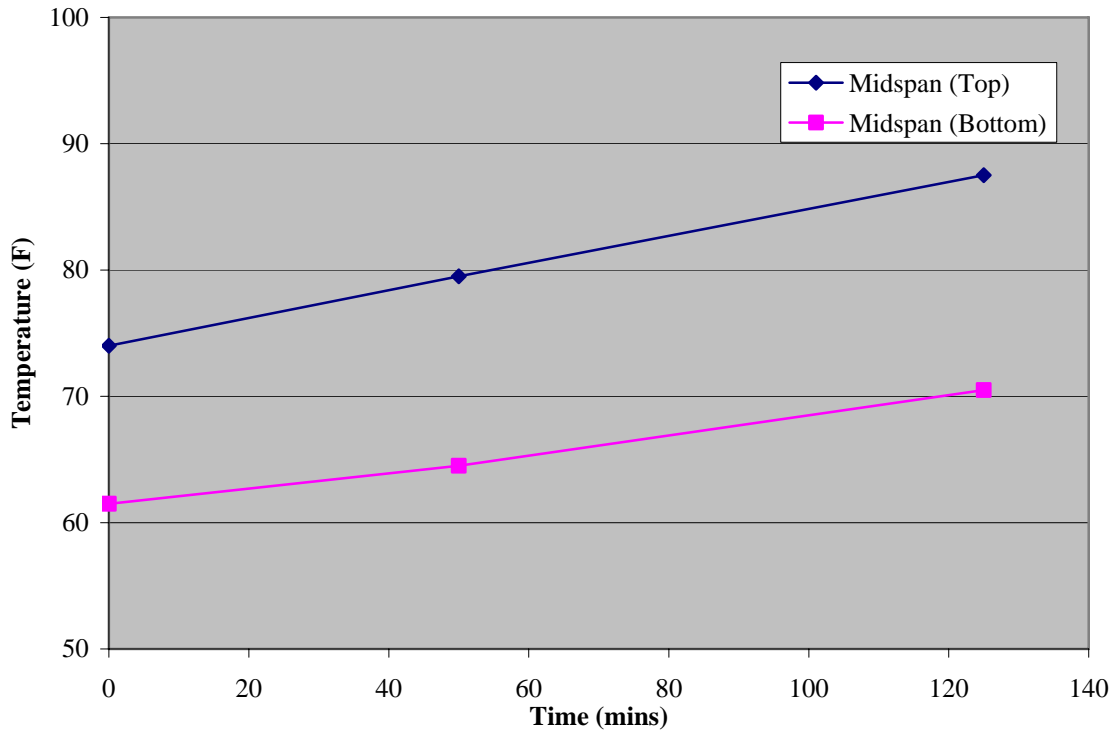


Figure 6.1. Bridge X-596 Temperature Over time of Midspan Interior Girder

The temperature increase resulted in a thermal camber of the bridge, which was apparent in subtracting the elevation of the final no load test from the initial no load test. For the temperature increase shown in Figure 6.1, the camber was calculated and is graphically represented in Figure 6.2. Figure 6.2 also has the weather conditions and air temperatures at both the test start and end.

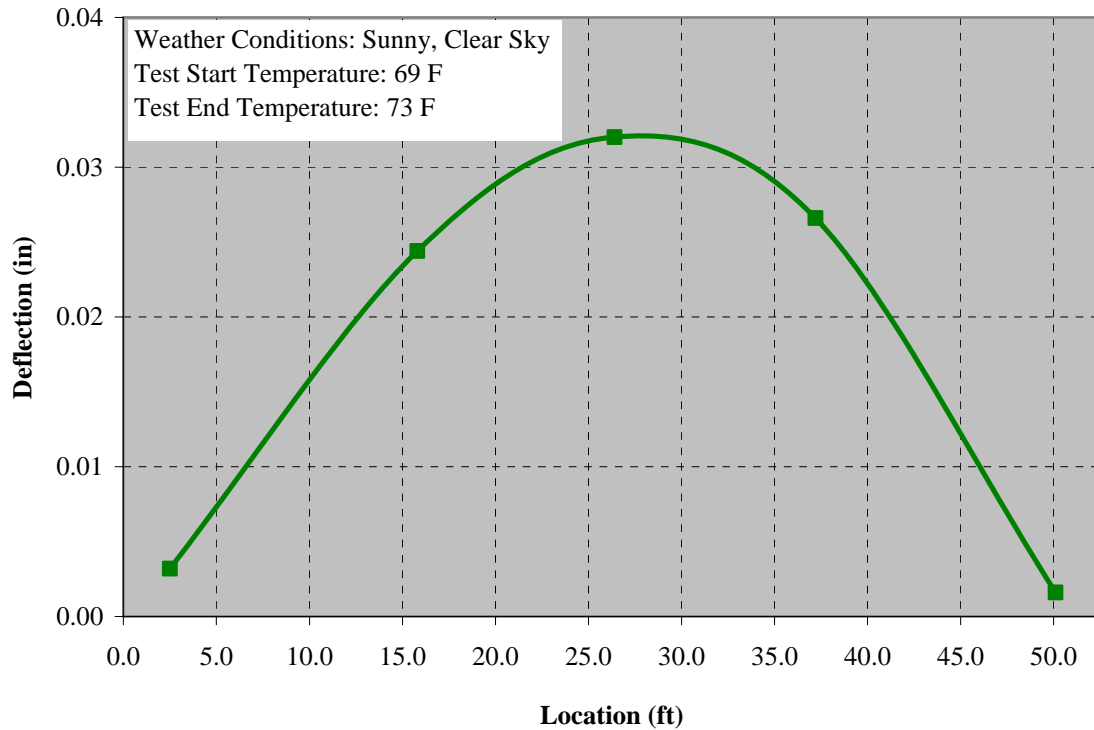


Figure 6.2. Bridge X-596 Thermal Camber

In order to appropriately account for the camber of the bridge due to thermal effects during testing, an appropriate baseline was established for each stop during testing. For most of the bridges (excluding Y-298) 5 truck positions, or stops, were conducted during testing. The thermal effects were accounted for by taking a weighted average of the first no load stop and the final no load stop based upon when the stop occurred. Figure 6.3 shows the linearly adjusted baselines for the camber effects.

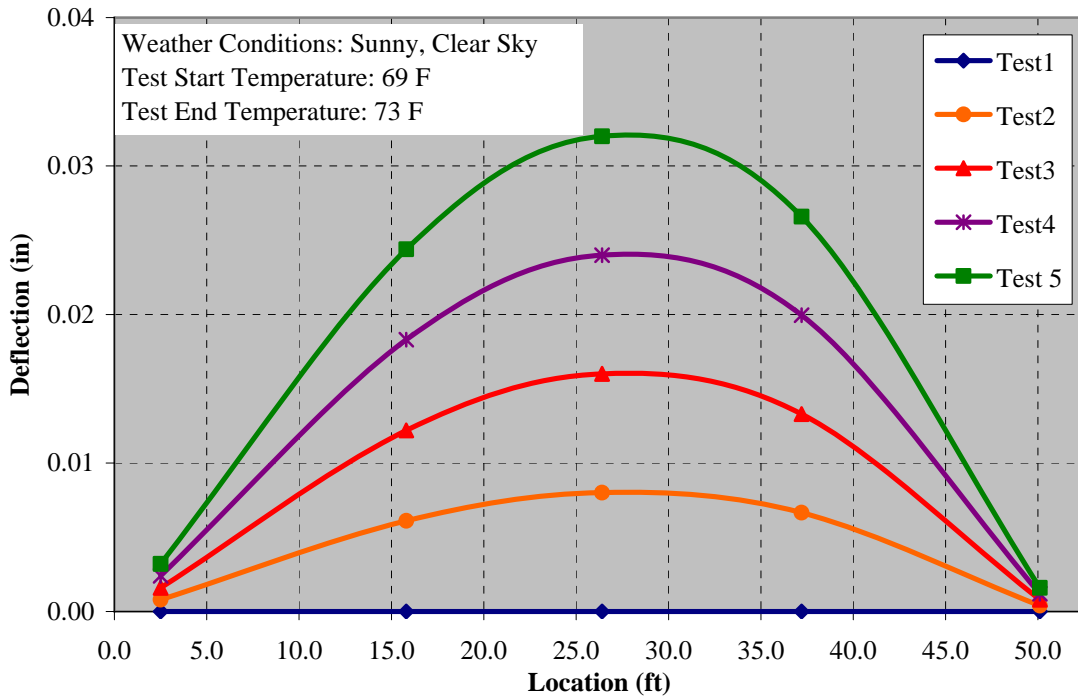


Figure 6.3. Bridge X-596 Adjustment of Baseline Due to Thermal Effects

Test 1 occurred closest to the first no load test and therefore used the first no load as a baseline. Test 2 utilized a weighted average of 75 percent camber from the first no load and 25 percent from the second no load and so forth. A linear relationship was the most appropriate way to account for thermal deflections because quantifying the exact temperature throughout the cross section would have been very difficult. In addition, for some bridges portions of the deck could be shaded during the test whereas other spots remained in the sunlight and recorded much larger temperature values. This meant the temperature was not only varying throughout the depth of the bridge section, but over the entire deck surface. Figure 6.4 shows the shading of Bridge X-495 during Stop 3, which was the halfway point of testing. Testing of the bridge began in the early morning with the entire deck shaded; when testing was completed, the entire deck surface was sunlit.



Figure 6.4. Bridge X-495 Shading of Deck During Testing

6.3. NORMALIZING DEFLECTION READINGS

The individual truck weights varied from test to test and this variance needed to be accounted for when comparing the deflection readings obtained from the total station. Table 6.1 shows the tabulated truck weights for each test of bridge P-962 and Figure 6.5 shows graphically the percent difference from the original total truck weights over time for each bridge. Notice that all of the total truck weights for bridge P-962 are greater to or equal to the original Test 1 total truck weights.

Table 6.1. Truck Weights for P-962 (kips)

| | | Test1 | Test2 | Test3 | Test4 | Test5 | Test6 | Test7 | Test8 | Test9 | Test10 | Test11 |
|-------------------|------------|--------|--------|--------|--------|--------|--------|--------|--------|--------|--------|--------|
| Truck 1 (Kips) | Rear Axle | 38.72 | 40.72 | 38.72 | 40.56 | 44.84 | 46.95 | 44.70 | 48.08 | 45.62 | 45.38 | 46.1 |
| | Front Axle | 13.36 | 17.16 | 13.36 | 18.98 | 13.98 | 19.17 | 14.78 | 15.06 | 14.24 | 18.54 | 13.92 |
| | Total | 52.08 | 57.88 | 52.08 | 59.54 | 58.82 | 66.12 | 59.48 | 63.14 | 59.88 | 63.92 | 60.02 |
| Truck 2 (Kips) | Rear Axle | 43.04 | 41.72 | 43.04 | 44.20 | 44.96 | 46.95 | 45.32 | 45.70 | 46.24 | 45.33 | 42.64 |
| | Front Axle | 17.22 | 12.72 | 17.22 | 16.76 | 13.70 | 19.17 | 14.42 | 15.22 | 14.84 | 18.51 | 13.92 |
| | Total | 60.26 | 54.44 | 60.26 | 60.96 | 58.66 | 66.12 | 59.74 | 60.92 | 61.06 | 63.84 | 56.56 |
| Total Weight | | 112.34 | 112.32 | 112.34 | 120.50 | 117.48 | 132.24 | 119.22 | 124.06 | 120.94 | 127.76 | 116.58 |
| % Difference | | 0% | -0.02% | 0.00% | 7.26% | 4.58% | 17.71% | 6.12% | 10.43% | 7.66% | 13.73% | 3.77% |

Conversion Units: 1 kip = 4.448 kN

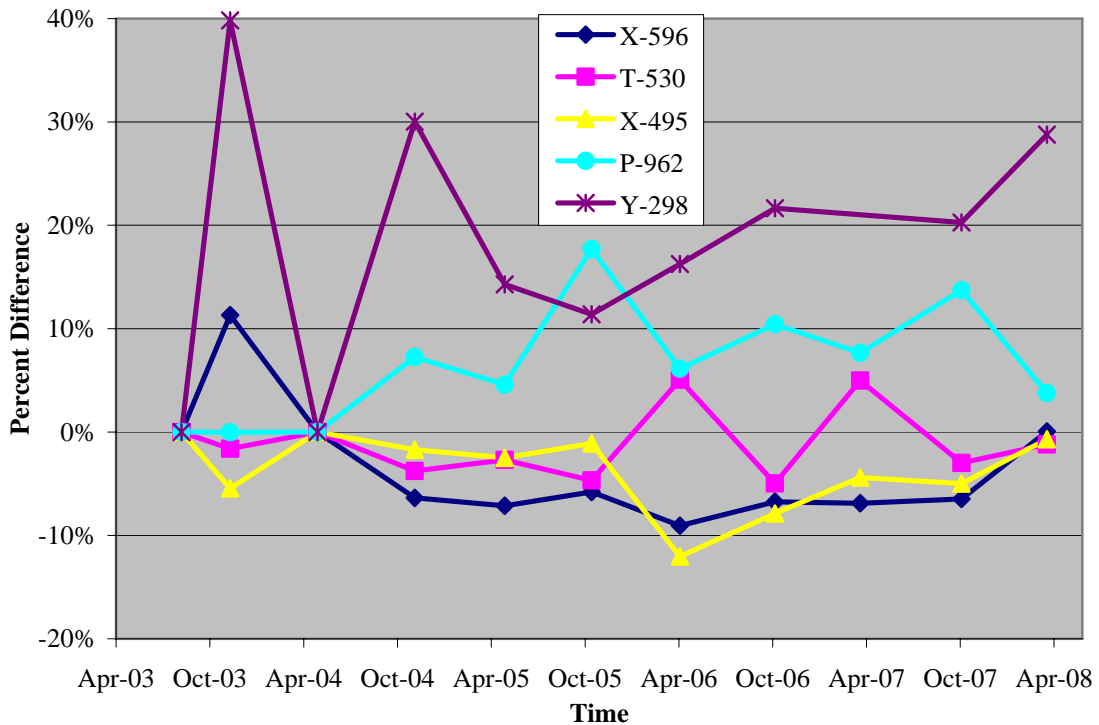


Figure 6.5. Percent Difference of Total Truck Weight over Time

Normalization of the truck weights was obtained by taking the ratio of the theoretical deflection of the first test to the theoretical deflection of the test after strengthening and multiplying this ratio by the experimental deflection recorded during the test after strengthening. The normalized deflection is shown in the following equation:

$$\text{Normalized } \Delta_{\text{Test } i} = \left(\frac{\text{Theoretical } \Delta_{\text{Test } 1}}{\text{Theoretical } \Delta_{\text{Test } i}} \right) \text{Experimental } \Delta_{\text{Test } i} \quad (1)$$

The ratio of theoretical girder deflections was determined by neglecting shear deformations and assuming an elastic, uncracked section subjected to point loads from the truck wheel loads. The transverse distribution factors for each girder were determined by assuming a truck wheel load of 0.5 at each truck wheel location. Figure 6.6 shows the layout of the wheel loads for Stop 4, which can also be used for Stop 2 by employing the principle of superposition. The reactions or individual distribution factors were then determined through structural analysis.

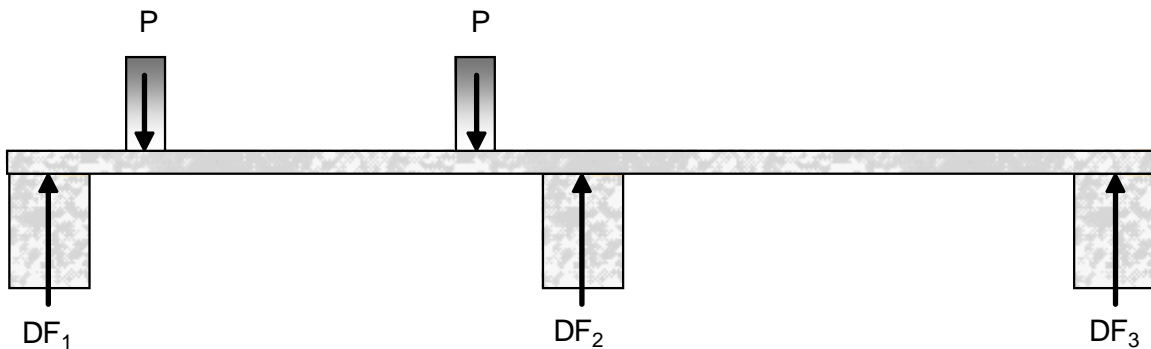


Figure 6.6. Stop 4 Transverse Load Distribution

Once the amount of load transferred to each girder was determined, a longitudinal load distribution could be modeled for each girder from loads at each axle location. Figure 6.7 shows a schematic of such a loading scheme for Stop 4. Because the trucks used for testing were known to change from test to test and the truck dimensions varied, recording the axle widths and dimensions for each axle during each test was important.

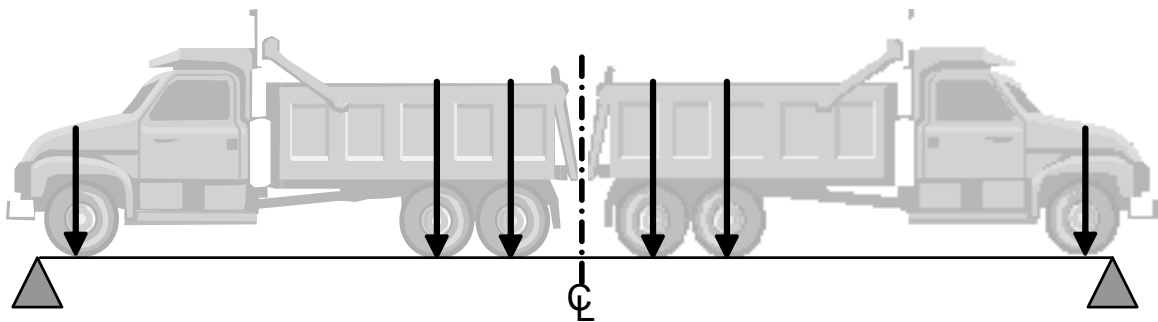


Figure 6.7. Stop 4 Lateral Load Distribution

Equation 2 shows the expanded equation for determining the ratio of theoretical deflections; Equation 3 is a simplified version of Equation 2. Figure 6.8 helps to illustrate the different terms in Equation 3 for Stop 2. The term j is the number of point loads from the axles, x is the distance to the target prism from the end of the span, a is the shorter of the distances from the end of the span to the point load being considered and b is the longer distance from the end of the span to the point load under consideration.

$$\frac{\text{Theoretical } \Delta_{\text{Test 1}}}{\text{Theoretical } \Delta_{\text{Test } i}} = \frac{\sum_1^j \frac{P_{1j} b_{1j} x}{6EIL} (L^2 - b_{1j}^2 - x^2)}{\sum_1^j \frac{P_{ij} b_{ij} x}{6EIL} (L^2 - b_{ij}^2 - x^2)} \quad (2)$$

$$\frac{\text{Theoretical } \Delta_{\text{Test 1}}}{\text{Theoretical } \Delta_{\text{Test } i}} = \frac{\sum_1^j P_{1j} b_{1j} (L^2 - b_{1j}^2 - x^2)}{\sum_1^j P_{ij} b_{ij} (L^2 - b_{ij}^2 - x^2)} \quad (3)$$

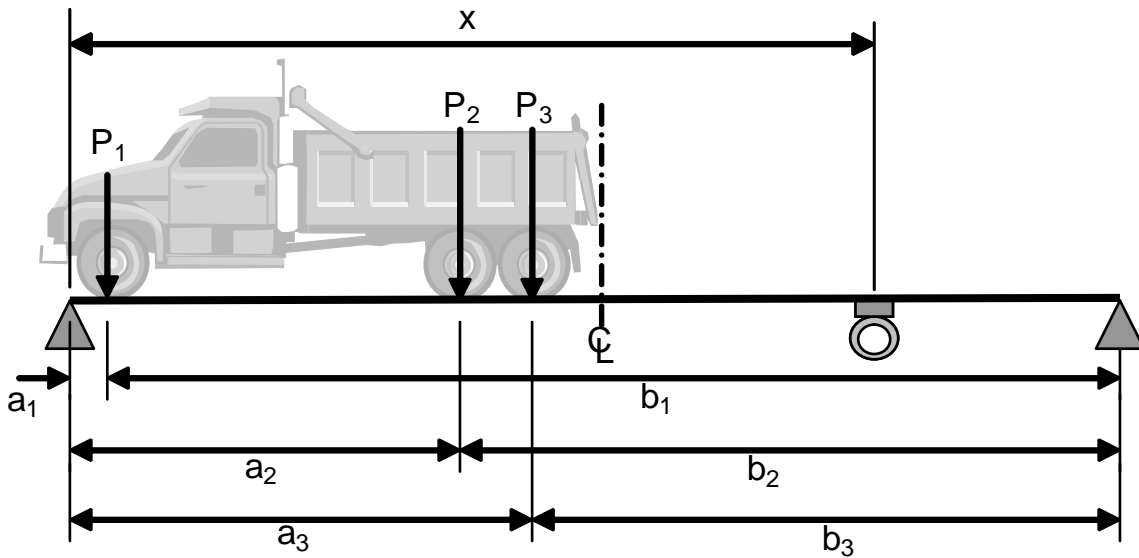


Figure 6.8. Step 2 Sketch for Theoretical Deflection Terms

Once the ratio of the theoretical deflection was determined for each prism location for all tests, multiplying the ratio by the deflection obtained during testing normalized the deflection values. The normalized deflection values from the post-strengthening tests could now be compared to Test 1. Figure 6.9 shows the recorded deflection data before normalization from

Stop 2, the exterior girder of the bridge, for all 11 tests conducted on bridge P-962. Figure 6.10 shows the data after normalization.

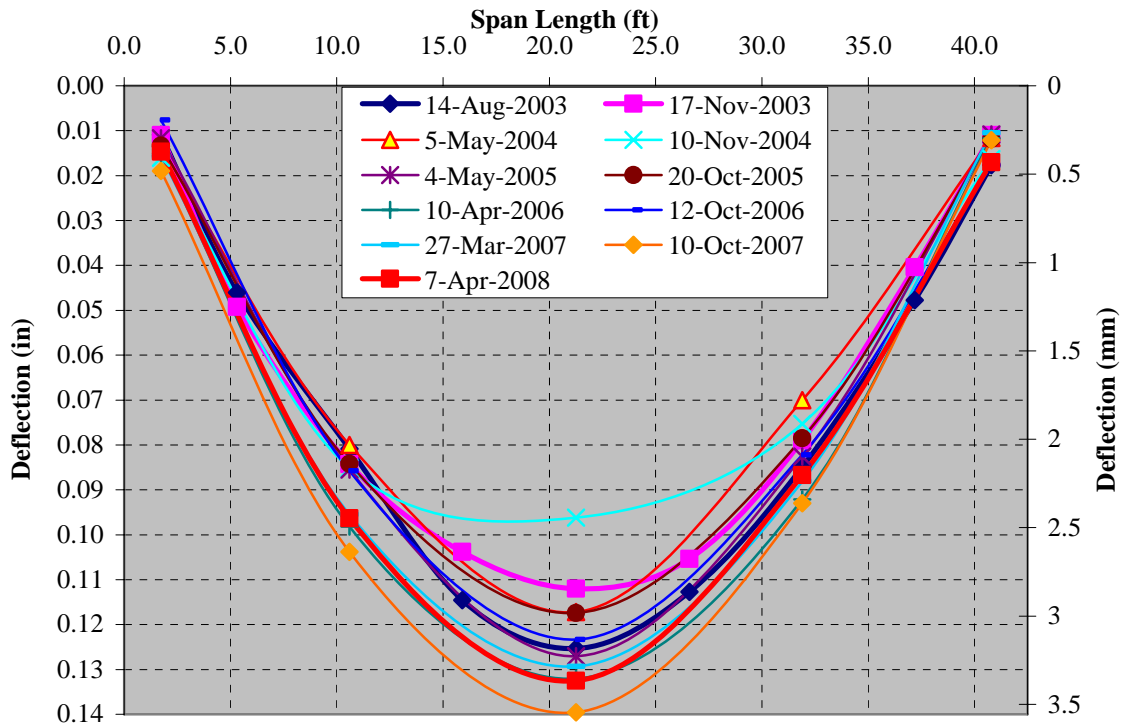


Figure 6.9. Recorded Deflection Bridge P-962 - Stop 2, Exterior Girder

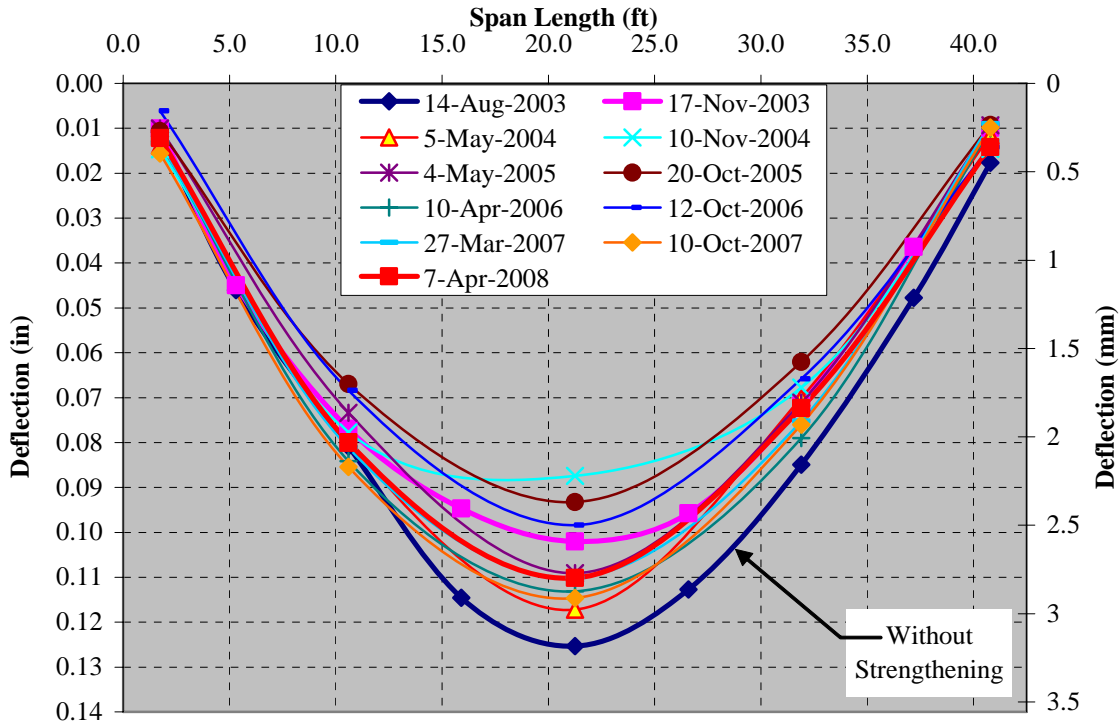


Figure 6.10. Normalized Deflection Bridge P-962 - Stop 2, Exterior Girder

Notice that Test 1 (before strengthened test) shows an apparent increase in deflection after normalization. This is due to increased truck weights after the first test was conducted. Normalizing the data as illustrated helped to account for the variance in truck weights based upon the provided front and rear tandem axle weights. The axle weights were divided evenly between wheels on each axle, thus there was no way to account for differences in individual wheel loads which could be induced by a load shifted to one side. Additionally, the truck axle loads imposed upon the bridge could vary from the actual recorded weight due to the truck's load shifting during transportation.

7. RESULTS

7.1. LONGITUDINAL DEFLECTIONS

The normalized deflections for Bridges X-596, T-530, X-495 and P-962 are presented in Appendix A for truck stops 2, 4 and 5. Stops 1 and 3 were neglected due to the low amount of deflection induced for this case of maximum shear.

For Bridges P-962 and T-530, there was an apparent gain in stiffness and therefore a reduction in member deflection after strengthening. There was also an increase in the normalized deflection for Bridges P-962 and T-530 which approaches the original deflection of these bridges prior to strengthening.

In order to better graphically present this change, the average of all deflected points was calculated for each test and a percent difference was then computed based upon the original Test 1 data. The results are presented in Figure 7.1 and Figure 7.2 for Bridge P-962 and Bridge T-530, respectively. A linearly trend line was plotted and displays a line that approaches the original deflection of the bridge. The apparent increase in deflection could be attributed to a softening of the FRP material utilized during strengthening or to the deterioration of other bridge components as the bridge aged. The varying thermal effects also may have impacted this apparent loss in stiffness, though bond softening at the interface of the FRP composites and the concrete substrate over the observed time could have been a factor as well.

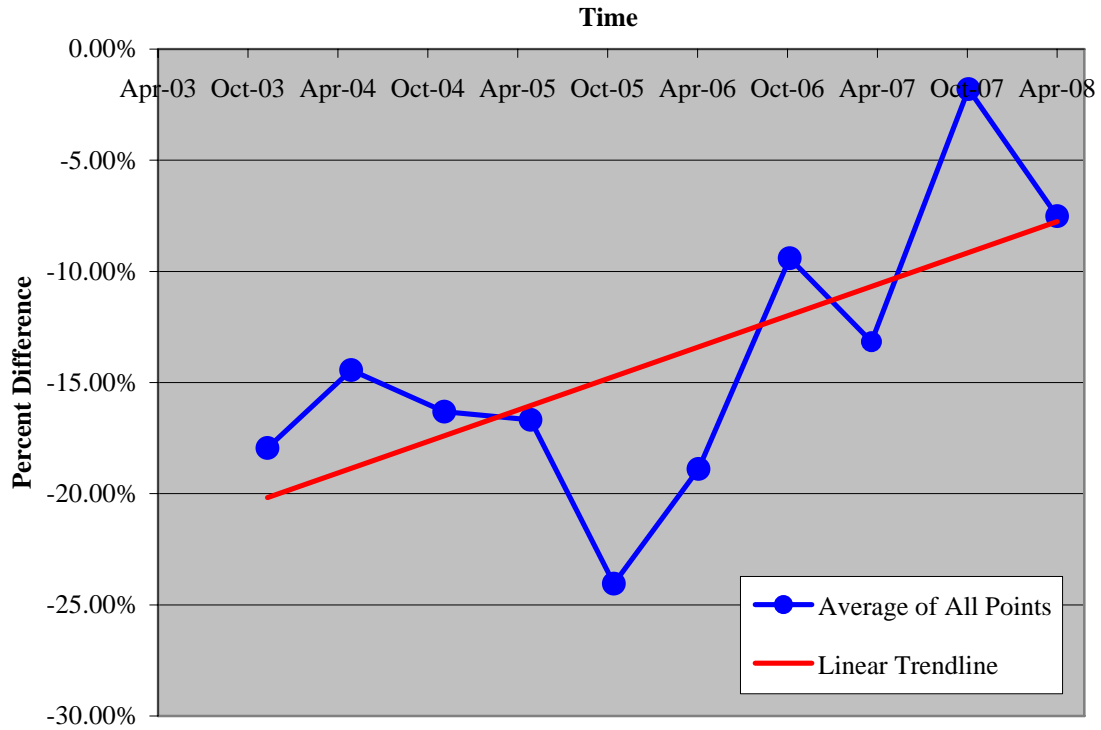


Figure 7.1. Average Deflection Percent Difference Bridge P-962

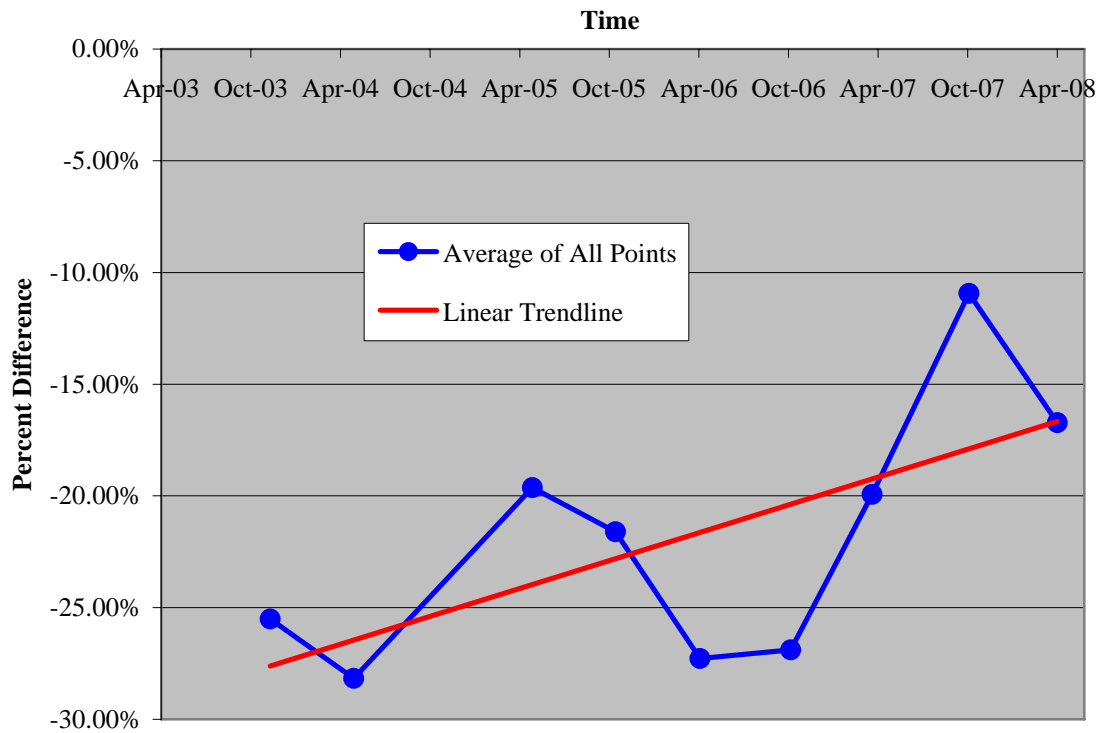


Figure 7.2. Average Deflection Percent Difference Bridge T-530

Bridges X-495 and X-596 utilized no strengthening on the exterior girders of the tested spans. This may account for the lack of variance between the pre and post strengthened deflections.

7.2. TRANSVERSE DEFLECTION

The normalized transverse girder deflection at midspan was plotted to gain an understanding of girder deflections relative to each other. The transverse deflection has been plotted below for span 1 of bridge P-962 in Figure 7.3. The results indicate an increased deflection on the western exterior girder.

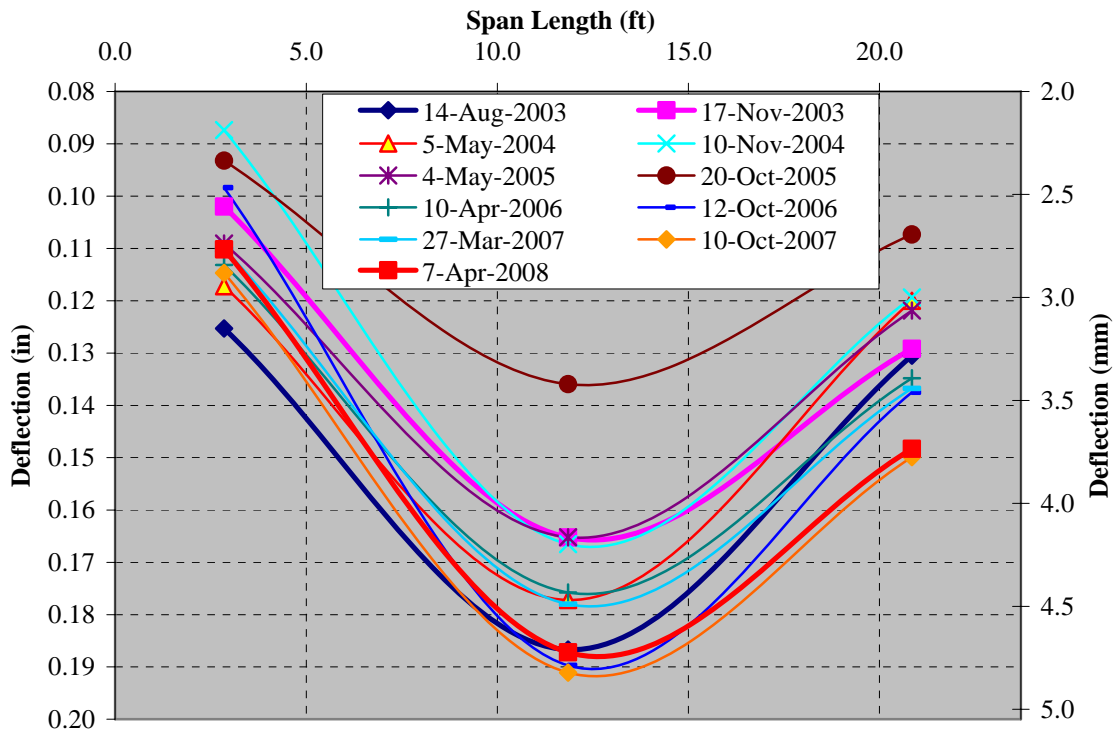


Figure 7.3. Bridge P-962 Span 1, Stop 2 Midspan Transverse Normalized Deflection

Additionally, spans 2 and 3 were monitored for bridge P-962 under Stop 2 loading configuration. The midspan girder deflections (Figures 7.4 and 7.5) display a similar trend of an increased deflection of the western exterior girders. Note that span 3 was strengthened with SRP reinforcement which upon visual inspection exhibited localized signs of rusting. The deflection data for span 3 does not show larger deflections over time or larger deflections than span 1 or 2. The SRP is therefore still performing adequately with no appreciable loss in steel area due to rusting.

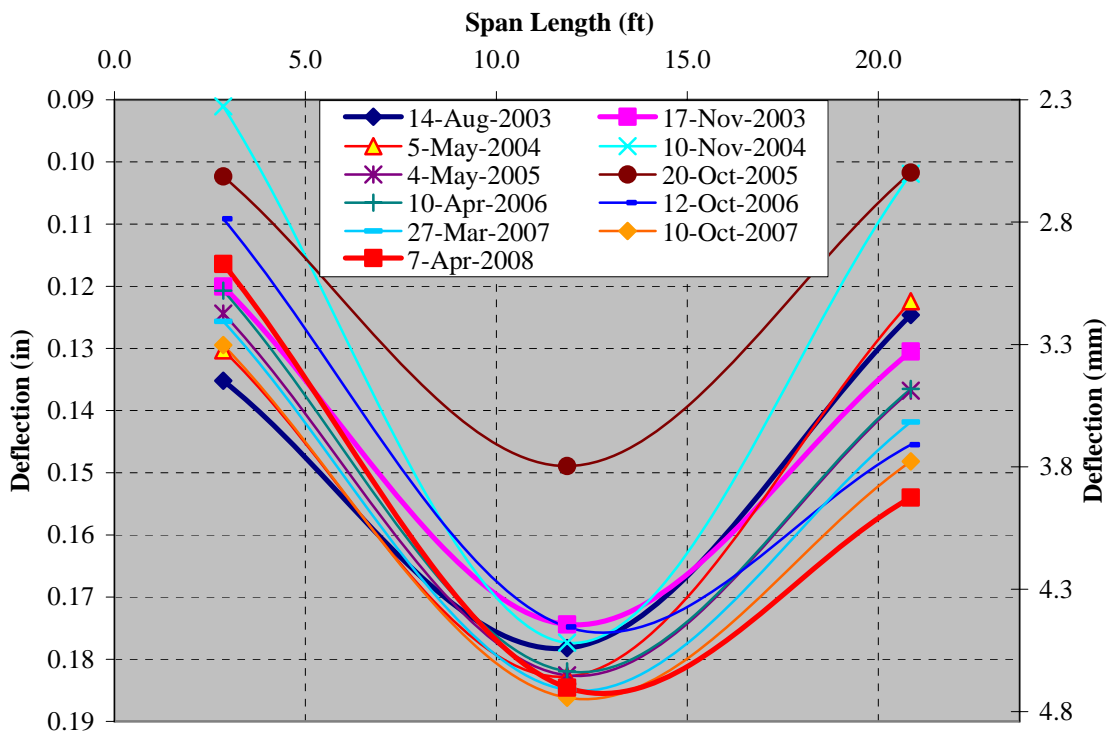


Figure 7.4. Bridge P-962 Span 2, Stop 2 Midspan Transverse Normalized Deflection

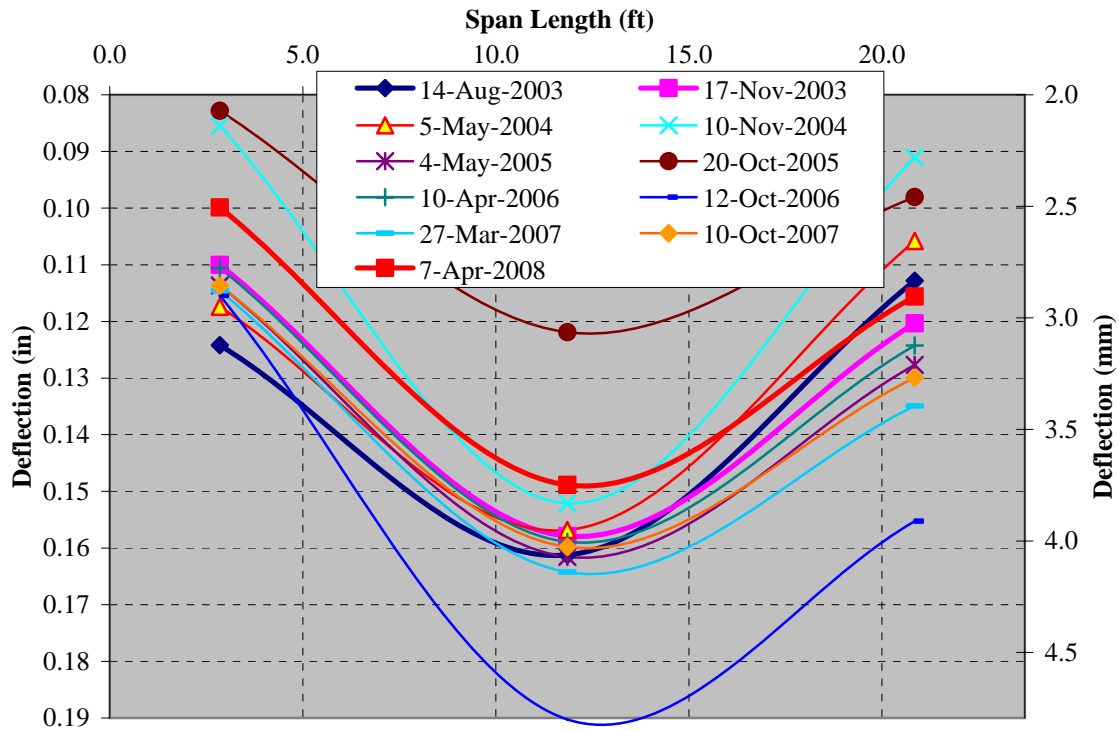


Figure 7.5. Bridge P-962 Span 3, Stop 2 Midspan Transverse Normalized Deflection

7.3. LOAD DISTRIBUTION

The normalized load distribution was also examined in order to determine if strengthening had influenced the amount of load carried by each girder. Again, bridge Y-298 was not examined due to the complex geometry present and the lack of flexural girders. Load distribution fractions were determined by dividing the normalized deflection of each girder at midspan by the sum of the total girder deflections. This fraction would be the apparent percentage of load carried by the girder. The load distribution fractions for Bridge P-962 are displayed in Table 7.1.

Table 7.1. Bridge P-962 Load Distribution Fractions

| | | Bridge P-962 | | | | | | | | | | |
|--------|--------|--------------|-------|-------|-------|-------|-------|-------|-------|-------|--------|--------|
| Stop | Girder | Test1 | Test2 | Test3 | Test4 | Test5 | Test6 | Test7 | Test8 | Test9 | Test10 | Test11 |
| Stop 2 | 1 | 0.28 | 0.26 | 0.28 | 0.23 | 0.28 | 0.28 | 0.27 | 0.23 | 0.26 | 0.25 | 0.25 |
| | 2 | 0.42 | 0.42 | 0.43 | 0.45 | 0.42 | 0.40 | 0.41 | 0.45 | 0.42 | 0.42 | 0.42 |
| | 3 | 0.29 | 0.33 | 0.29 | 0.32 | 0.31 | 0.32 | 0.32 | 0.32 | 0.32 | 0.32 | 0.33 |
| Stop 4 | 1 | 0.41 | 0.43 | 0.42 | 0.44 | 0.42 | 0.40 | 0.44 | 0.40 | 0.42 | 0.40 | 0.42 |
| | 2 | 0.42 | 0.42 | 0.43 | 0.40 | 0.43 | 0.43 | 0.41 | 0.43 | 0.42 | 0.43 | 0.42 |
| | 3 | 0.17 | 0.15 | 0.15 | 0.16 | 0.15 | 0.18 | 0.15 | 0.17 | 0.16 | 0.17 | 0.16 |
| Stop 5 | 1 | 0.26 | 0.25 | 0.23 | 0.23 | 0.26 | 0.30 | 0.26 | 0.25 | 0.25 | 0.26 | 0.30 |
| | 2 | 0.47 | 0.48 | 0.49 | 0.49 | 0.49 | 0.46 | 0.47 | 0.48 | 0.48 | 0.48 | 0.48 |
| | 3 | 0.27 | 0.27 | 0.28 | 0.28 | 0.26 | 0.24 | 0.27 | 0.27 | 0.27 | 0.26 | 0.22 |
| Stop 6 | 1 | 0.31 | 0.28 | 0.30 | 0.25 | 0.28 | 0.29 | 0.27 | 0.25 | 0.28 | 0.28 | 0.26 |
| | 2 | 0.41 | 0.41 | 0.42 | 0.48 | 0.41 | 0.42 | 0.41 | 0.41 | 0.41 | 0.40 | 0.41 |
| | 3 | 0.28 | 0.31 | 0.28 | 0.28 | 0.31 | 0.29 | 0.31 | 0.34 | 0.31 | 0.32 | 0.34 |
| Stop 7 | 1 | 0.31 | 0.28 | 0.31 | 0.26 | 0.28 | 0.27 | 0.28 | 0.25 | 0.28 | 0.28 | 0.27 |
| | 2 | 0.40 | 0.41 | 0.41 | 0.46 | 0.40 | 0.40 | 0.40 | 0.41 | 0.40 | 0.40 | 0.41 |
| | 3 | 0.28 | 0.31 | 0.28 | 0.28 | 0.32 | 0.32 | 0.32 | 0.34 | 0.33 | 0.32 | 0.32 |

These fractions can also be displayed over time to identify any changes that may occur from test to test. The fractions for Stops 2, 6 and 7 have been plotted for bridge P-962 in Figure 7.6. Stops 2, 6 and 7 configured the trucks side by side at midspan for each of the three spans.

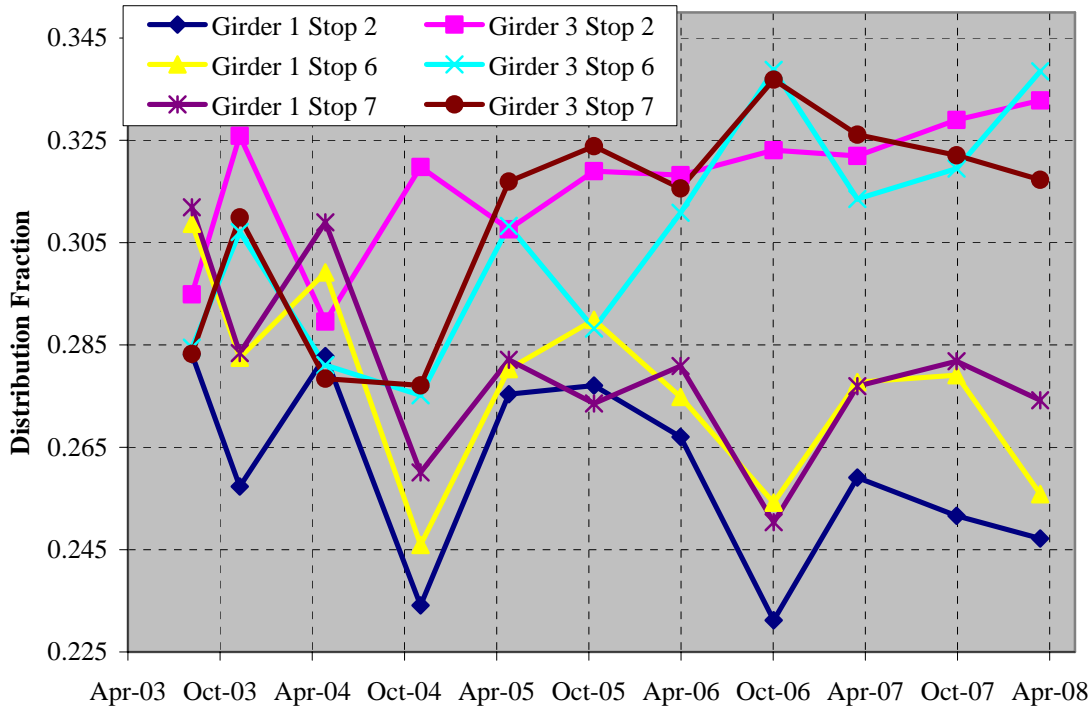


Figure 7.6. Bridge P-962 Stops 2, 6 and 7 Distribution Fraction

Figure 7.6 clearly shows that the western exterior girders (denoted as girder 1 for all stops) took more of the load as testing progressed through time. The strengthening on the exterior girders of each individual span was the same. Therefore, this increase in distribution could have been caused by inconsistencies in the installation of the FRP material. Another possibility is lateral misplacement of the trucks during testing.

7.4. PRE-STRENGTHENED LOAD TEST MODELING

Several theoretical models were created in an effort to accurately predict the deflections produced from load testing. This section discusses the concepts, approaches, assumptions, and procedures for each model. The models used basic calculations to find pre-strengthened deflection measurements. The loads used were taken from the truck weight tickets collected

during testing, the measured truck dimensions and the truck stop diagrams (Appendix B) were used to locate the wheel loads, which were assumed to act as point loads. The axle loads for each truck are shown in Table 7.2.

Table 7.2. Before Strengthening Truck Axle Loads

| Bridge | Truck 1 (kips) | | | Truck 2 (kips) | | |
|--------|----------------|------------|-------|----------------|------------|-------|
| | Rear Axles | Front Axle | Total | Rear Axles | Front Axle | Total |
| X-596 | 41.03 | 17.59 | 58.62 | 40.01 | 17.15 | 57.16 |
| T-530 | 40.90 | 16.80 | 57.70 | 38.32 | 16.40 | 54.72 |
| X-495 | 42.32 | 12.76 | 55.08 | 42.48 | 12.72 | 55.20 |
| P-962 | 38.72 | 13.36 | 52.08 | 43.04 | 17.22 | 60.26 |
| Y-298 | 25.48 | 11.35 | 36.83 | 25.48 | 11.35 | 36.83 |

For every structure except Bridge Y-298, the skew angle was ignored because it was less than thirty degrees (AASHTO 2002). The same material properties and quantities used for design were also used in the bridge modeling.

7.4.1. Individual Tee-Beam Modeling. Individual Tee-Beam analysis was performed for each deck girder/reinforced concrete tee-beam structure (not Bridge Y-298). This analysis broke the cross-section into individual tee-beams and ignored any contribution of the barrier walls. The girders were assumed to provide rigid support to the slab, so the slab strip was analyzed using classical beam theory; this assumption was originally made for analysis and design of the strengthening systems. The truck wheel loads were distributed to the tee-beam girders (Figure 7.7). Using the distributed point loads, a longitudinal loading scheme was then developed for each girder (Figure 7.8).

The effective flange width (b_{eff}) was calculated from AASHTO 8.10.1 (2002). The interior and exterior girder flange widths are given in Equations 4 and 5, respectively; Table 7.3 lists the effective flange widths used for each bridge.

$$b_{eff} = \min\left(\frac{L}{4}, 12h_s + b, S\right) \quad (4)$$

$$b_{eff} = b + \min\left(\frac{L}{12}, 6h_s, \frac{S-b}{2}\right) \quad (5)$$

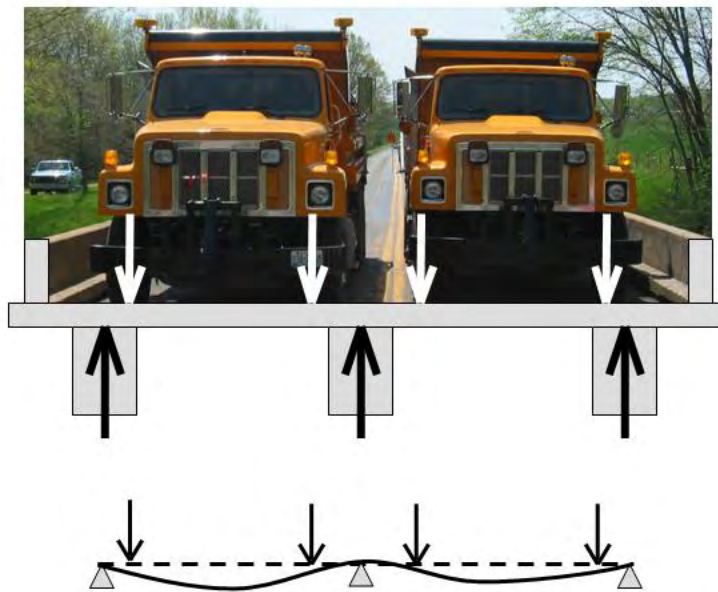


Figure 7.7. Transverse Load Distribution

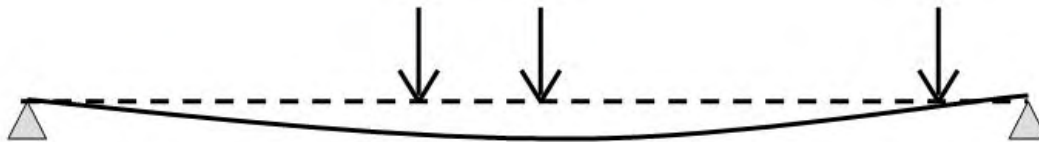


Figure 7.8. Longitudinal Load Distribution

Table 7.3. Effective Tee-Beam Widths

| Bridge | Interior Girder (in) | Exterior Girder (in) |
|--------|----------------------|----------------------|
| X-596 | 57.0 | 93.0 |
| T-530 | 78.0 | 47.5 |
| X-495 | 57.0 | 93.0 |
| P-962 | 89.0 | 53.0 |

The resulting interior and exterior reinforced-concrete tee-beams were analyzed as simply-supported structures. The gross moment of inertia was used in every case to calculate stiffness as each structure was assumed to be uncracked.

7.4.2. Mass-Section Tee-Beam Modeling. This modeling scheme worked similarly to the individual tee-beam modeling discussed in the previous section. This scheme was again only used to model deck girder/reinforced concrete tee-beam structure. The difference was that the entire cross-section of the bridge was taken as one tee-beam; the entire deck was treated as the flange and all three girders were treated as one (sum the widths and reinforcements). The truck loads were therefore not distributed to the individual beams, as shown in Figure 7.8.

While this model could not differentiate between interior and exterior girder deflections, it did set a general value. The model allowed for the concrete barrier walls to contribute to stiffness, though these barrier walls were ignored during design; however, they are known to contribute to the structure's overall stiffness (Galati, Casadei, and Nanni 2003). Using the dimensions shown in the plans for each bridge, a basic contributing shape was developed for each wall. For bridges X-596, T-530, and X-495, the contributing section was simplified to 13 inches tall by 20 inches wide. The remaining portions were ignored as they were very slim in the cross-section and were assumed to be too flimsy to contribute to the overall stiffness. For Bridge P-962, the contributing section was 8 inches tall by 20 inches wide, set atop another 20 inches tall by 8 inches wide block.

The barrier walls were assumed to be built from the same concrete as the rest of the structure; a perfect bond between the wall and deck structure was also assumed. To see the barrier walls' effects, the resulting tee-beam's gross moment of inertia was computed with the barrier walls set to zero, fifty, and one-hundred percent effective. Again, each structure was assumed to be uncracked.

7.4.3. Finite Element Modeling. Finite Element Modeling (FEM) was performed using the Ansys Classic 7.1 software package (ANSYS 2003). While FEM was the most complex way to estimate deflection, using the computer and software package made FEM a desirable method for this analysis.

Several assumptions were made in using FEM. The bridges were assumed to have consistent material properties in all locations. Their elements behaved as a linear, elastic and isotropic material. The modulus of elasticity for concrete (E_c) was defined by Equation 6 (Nawy 2000). Concrete compressive strength (f'_c) was given for each bridge in Table 3.4. Poisson's ratio (ν) was assumed to be 0.20 (ACI Committee 318).

$$E_c = 57,000\sqrt{f'_c} \quad (6)$$

The element SOLID65 was chosen to model three-dimensional reinforced concrete with or without reinforcing steel bars. Flexural reinforcement was added to the tee-beams for all of the bridges except Bridge Y-298 where the deck reinforcement was added. The bridge geometry was taken from Section 3. Two models were developed for each bridge, one with and one without the barrier wall. Each structure was modeled using a cracked and uncracked section. Flexural cracks were simulated in the beams by changing the modulus of elasticity to near zero for a block of elements near midspan at a depth approximated by cracking moment calculations.

To model each bridge with FEM, first the inputs were set. The bridge span was then drawn using the known geometries. Next, the model was meshed into "brick" elements no more than six inches on one side; the structure was broken into approximately 100,000 nodes (elements). The supports were then set to accurately represent the simply supported bridge span.

Loads were next applied according to which truck stop was modeled. With all inputs set, the model was solved and vertical deformation was plotted on a three-dimensional contour map.

Figure 7.9 shows an example of the output from Ansys.

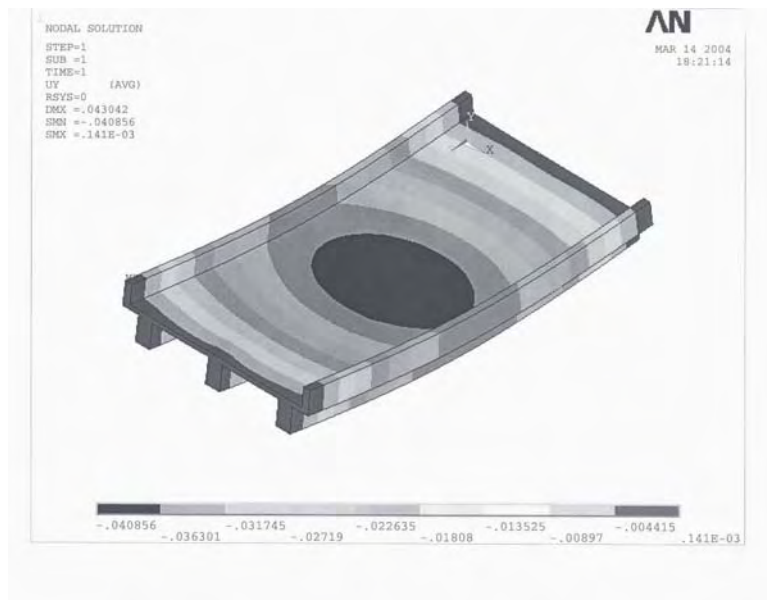


Figure 7.9. Example Deformation Contour Plot

7.5. PRE-STRENGTHENED THEORETICAL AND EXPERIMENTAL DEFLECTIONS

This section compares the theoretical models defined in the previous section with the measurements obtained in the field. Only before-strengthening testing numbers were used as the models were developed considering the original un-strengthened structures. The results are discussed and compared with the visual inspection ratings for each structure.

7.5.1. Comparison Methods. Only the maximum flexural testing (truck stops) data was used because of the assumption that the shear contribution to deflection was insignificant in comparison to the flexural contribution. Also noted in the results was that the two truck stops produced varying results, most likely due to the wheel loads being too close to the abutment (less

than the cross-section depth). The inaccuracy associated with placing such loads would have a significant effect near the ends of the span. Truck stops one and three were therefore ignored.

For comparison, only the midspan deflections of the interior and exterior girders (monitored with nine targets per girder) were used. The calculated deflections for each bridge and each loading scenario were taken from all three models discussed in the previous section. For each theoretical value, a percent error was computed; this was the difference between theoretical and experimental values divided by the experimental value. A positive error value meant that the theory over-estimated the deflection; negative error value meant that the theory under-estimated the deflection. The comparison was made for before-strengthening load testing only.

7.5.2. Results of Analysis. Tables 7.4 through 7.7 show the results of theoretical and experimental (pre-strengthened) deflection comparisons for each bridge except Bridge Y-298. A percent error relative to the measured value is listed for every model.

Table 7.4. Theoretical and Experimental Deflections for Bridge X-596 (in.)

| Truck Stop | 2 | 2 | 4 | 4 | 5 | 5 |
|-----------------------|----------|----------|----------|----------|----------|----------|
| Girder | Exterior | Interior | Exterior | Interior | Exterior | Interior |
| Measured Deflection | 0.125 | 0.147 | 0.151 | 0.125 | 0.108 | 0.147 |
| Tee-Beam Analysis | 0.150 | 0.290 | 0.287 | 0.254 | 0.045 | 0.399 |
| | 20% | 97% | 90% | 103% | -58% | 171% |
| Mass-Section Analysis | 0.201 | | 0.176 | | 0.176 | |
| Barrier Wall 0% | 48% | | 28% | | 38% | |
| Mass-Section Analysis | 0.164 | | 0.143 | | 0.148 | |
| Barrier Wall 50% | 21% | | 4% | | 16% | |
| Mass-Section Analysis | 0.138 | | 0.121 | | 0.129 | |
| Barrier Wall 100% | 1% | | -12% | | 1% | |
| FEM No Barrier Wall | 0.195 | 0.229 | 0.279 | 0.195 | 0.158 | 0.225 |
| | 56% | 56% | 85% | 56% | 46% | 53% |
| FEM with Barrier Wall | 0.095 | 0.102 | 0.109 | 0.084 | 0.08 | 0.092 |
| | -24% | -31% | -28% | -33% | -26% | -37% |

Table 7.5. Theoretical and Experimental Deflections for Bridge T-530 (in.)

| Truck Stop | 2 | 2 | 4 | 4 | 5 | 5 |
|-----------------------|----------|----------|----------|----------|----------|----------|
| Girder | Exterior | Interior | Exterior | Interior | Exterior | Interior |
| Measured Deflection | 0.089 | 0.109 | 0.113 | 0.114 | 0.075 | 0.112 |
| Tee-Beam Analysis | 0.179 | 0.354 | 0.157 | 0.283 | 0.005 | 0.220 |
| | 101% | 225% | 39% | 148% | -93% | 96% |
| Mass-Section Analysis | 0.145 | | 0.124 | | 0.124 | |
| Barrier Wall 0% | 46% | | 9% | | 33% | |
| Mass-Section Analysis | 0.117 | | 0.099 | | 0.099 | |
| Barrier Wall 50% | 18% | | -13% | | 6% | |
| Mass-Section Analysis | 0.097 | | 0.083 | | 0.087 | |
| Barrier Wall 100% | -2% | | -27% | | -7% | |
| FEM No Barrier Wall | 0.145 | 0.165 | 0.218 | 0.19 | 0.11 | 0.161 |
| | 63% | 51% | 93% | 67% | 47% | 44% |
| FEM with Barrier Wall | 0.093 | 0.135 | 0.14 | 0.145 | 0.075 | 0.135 |
| | 4% | 24% | 24% | 27% | 0% | 21% |

Table 7.6. Theoretical and Experimental Deflections for Bridge X-495 (in.)

| Truck Stop | 2 | 2 | 4 | 4 | 5 | 5 |
|-----------------------|----------|----------|----------|----------|----------|----------|
| Girder | Exterior | Interior | Exterior | Interior | Exterior | Interior |
| Measured Deflection | 0.088 | 0.105 | 0.130 | 0.097 | 0.091 | 0.127 |
| Tee-Beam Analysis | 0.146 | 0.288 | 0.284 | 0.252 | 0.045 | 0.395 |
| | 66% | 174% | 118% | 160% | -51% | 211% |
| Mass-Section Analysis | 0.2 | | 0.176 | | 0.171 | |
| Barrier Wall 0% | 107% | | 55% | | 57% | |
| Mass-Section Analysis | 0.164 | | 0.143 | | 0.143 | |
| Barrier Wall 50% | 70% | | 26% | | 31% | |
| Mass-Section Analysis | 0.138 | | 0.121 | | 0.121 | |
| Barrier Wall 100% | 43% | | 7% | | 11% | |
| FEM No Barrier Wall | 0.201 | 0.242 | 0.295 | 0.212 | 0.173 | 0.245 |
| | 128% | 130% | 127% | 119% | 90% | 93% |
| FEM with Barrier Wall | 0.09 | 0.096 | 0.104 | 0.082 | 0.078 | 0.089 |
| | 2% | -9% | -20% | -15% | -14% | -30% |

Table 7.7. Theoretical and Experimental Deflections for Bridge P-962 (in.)

| Truck Stop | 2 | 2 | 4 | 4 | 5 | 5 |
|-----------------------|----------|----------|----------|----------|----------|----------|
| Girder | Exterior | Interior | Exterior | Interior | Exterior | Interior |
| Measured Deflection | 0.125 | 0.187 | 0.154 | 0.156 | 0.109 | 0.197 |
| Tee-Beam Analysis | 0.085 | 0.150 | 0.141 | 0.122 | 0.022 | 0.191 |
| | -32% | -20% | -8% | -22% | -80% | -3% |
| Mass-Section Analysis | 0.354 | | 0.288 | | 0.288 | |
| Barrier Wall 0% | 127% | | 86% | | 88% | |
| Mass-Section Analysis | 0.140 | | 0.114 | | 0.114 | |
| Barrier Wall 50% | -10% | | -26% | | -25% | |
| Mass-Section Analysis | 0.087 | | 0.071 | | 0.071 | |
| Barrier Wall 100% | -44% | | -54% | | -54% | |
| FEM No Barrier Wall | 0.229 | 0.277 | 0.33 | 0.235 | 0.197 | 0.278 |
| | 83% | 48% | 114% | 51% | 81% | 41% |
| FEM with Barrier Wall | 0.134 | 0.206 | 0.17 | 0.18 | 0.095 | 0.203 |
| | 7% | 10% | 10% | 15% | -13% | 3% |

The individual tee-beam analysis was noted to be accurate in some instances, but radically inaccurate and inconsistent in many cases. This was most likely due to the fact that the girders were assumed to provide rigid support to the slab, which was not the case, making the load distribution inaccurate. This analysis was removed from further consideration.

For each given truck stop, consistencies were noticed both between the models and between the bridges. Differences in percent error from one model to another were similar from one bridge to the next. When the barrier wall was considered, the stiffness increased, and as a result the estimated deflection decreased. This was true for the mass-section models and the FEM models. To quantify a health rating of the bridge, the percent errors were averaged into one number for each bridge.

Initially it was noted that for Bridge P-962, the average percent error of the models was significantly different than that of the other three bridges (X-596, T-530, and X-495). In fact, the theoretical deflection was typically much less than the measured deflection, especially with both FEM models. This indicated a higher level of softening (i.e. cracking) had occurred with this structure. Although there were no obvious visual deficiencies in the structure, the FEM models were run again with cracked sections instead of uncracked sections for this bridge. Percent error values were then more consistent with the other three bridges. The results are shown in Table 7.7

Only FEM models were produced for Bridge Y-298. Modeling schemes included both continuous and simply supported span structures with and without the barrier walls. The length-to-width ratio of each span was found to be about three, making each span one-way by definition (ACI Committee 318). As expected, the barrier walls were found to be insignificant. The simply supported model more accurately resembled the field measurements. This was valid because the condition of the structure was relatively poor, so the concrete was most likely cracked, perhaps

due to overloaded conditions, and the actual continuity of the spans would have therefore be small. The resulting FEM models were compared to the load testing results, shown in Figures 7.10 and 7.11. Average theoretical error values were computed similarly to the other four bridges, except only one model (shown in Figures 7.10 and 7.11) was used.

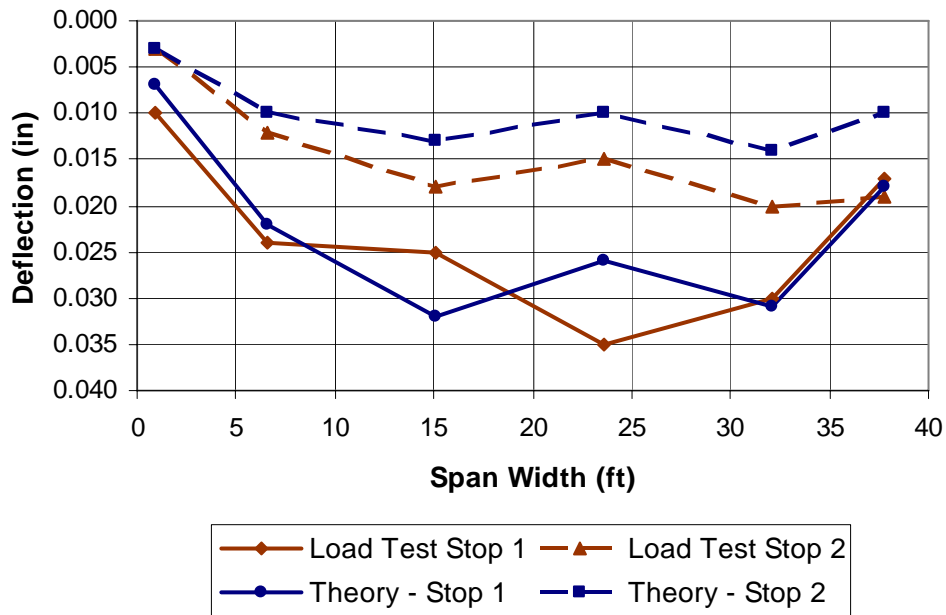


Figure 7.10. Bridge Y-298 West Span

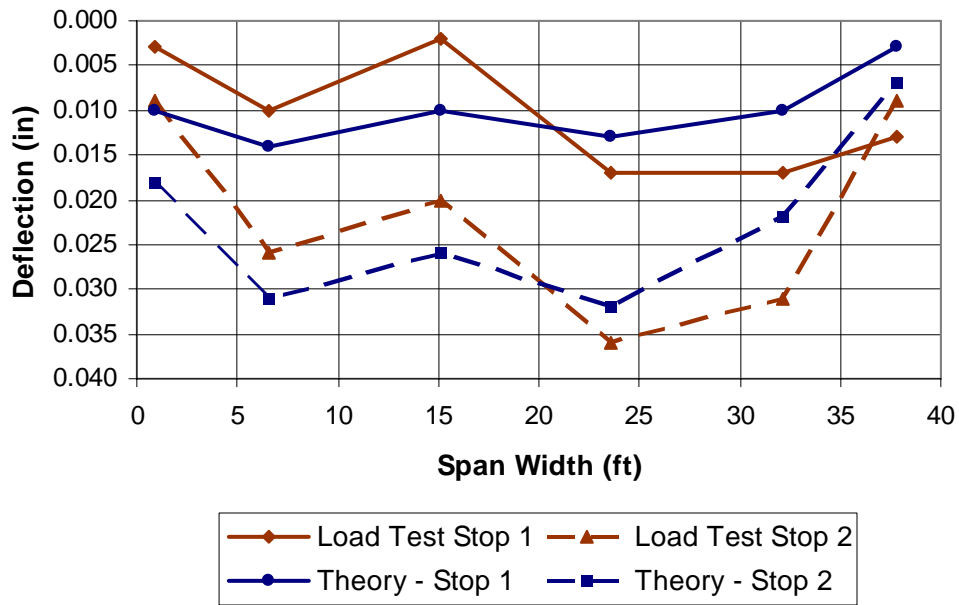


Figure 7.11. Bridge Y-298 East Span

For Bridge Y-298, complex geometry made drawing conclusions from theoretical and experimental results difficult. For both tests on the east span, the predicted deflection was less than the actual deflection from span width 20 to 28 feet, whereas the opposite was observed from span width two to 20 feet. This finding was consistent with an area of damaged concrete found underneath this span of the structure, span width 25-35 feet, which could weaken the structure and reduce its stiffness.

7.6. VISUAL BRIDGE INSPECTION

An effort was made during each of the last four series of bridge tests to visually inspect the bridges for any degradation. The structural defects observed were primarily related to the structural members of the pre-strengthened bridge with very little problems observed with the FRP materials.

7.6.1. Bridge T-530. Bridge T-530 showed signs of severe corrosion of the bents due to the propagation of water from the deck surface. These bents were corroded before the bridge was strengthened and need to be monitored in the future to ensure structural integrity. The presence of a flexural crack was also noted on the midspan transverse beam of the tested span. The size of the crack was noted, and did not noticeably increase in size when testing under truck load. Figure 7.12 shows the location and a depiction of the corrosion of the bents and the flexural crack of the transverse girder.

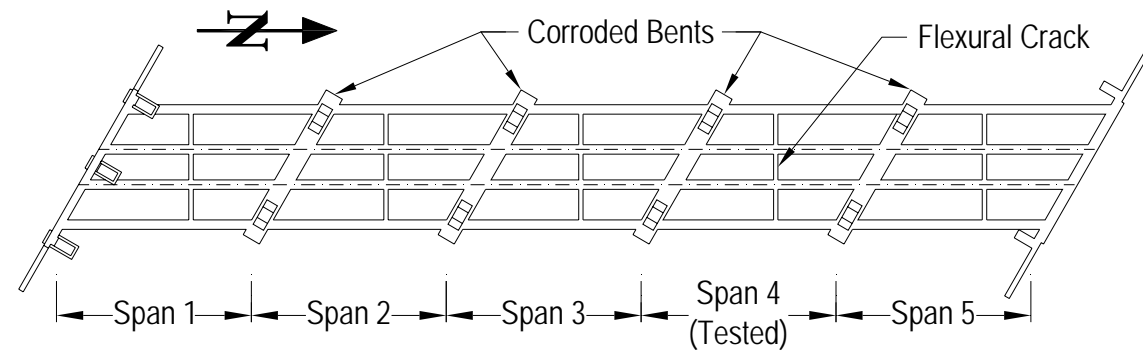


Figure 7.12. Bridge T-530 Corrosion of Bents and Cracked Transverse Beam

7.6.2. Bridge X-596. Bridge X-596 also exhibited bent corrosion. The exterior face of one bent had spalled off, exposing the reinforcement. This occurred between tests 8 and 9 and was not present prior to construction. In addition, another bent exhibited corrosion at the intersection of the transverse beam with the column. The locations and a picture of each decayed bent are shown in Figure 7.13. Additional corrosion was also observed on the barrier walls in the form of exposed reinforcement and deteriorated concrete.

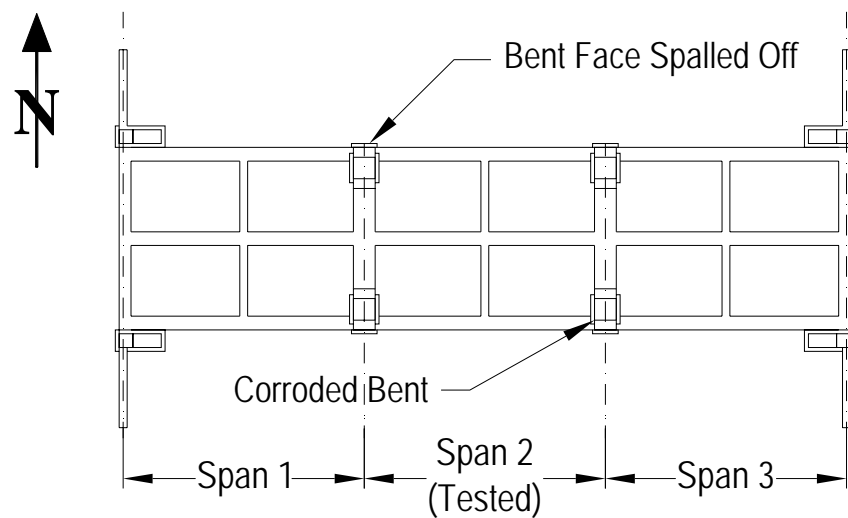


Figure 7.13. Bridge X-596 Corrosion of Bents

7.6.3. Bridge X-495. The presence of an endspan crack in the disturbed region was noted during the 8th series of tests. This crack did not propagate further when observed during later tests. Additionally, the protective coating on the FRP applied to one bent via manual lay-up is peeling from the bent soffit. This may be due to poor installation or water drainage from the deck. This phenomenon was not observed on the other bent, which was in good condition. The disturbed region crack and protective layer peeling is shown in Figure 7.14 along with the locations of the occurrences. Lastly, there is an appreciable amount of scour around the foundations of one of the bents. This is in the deeper part of the creek and was observed during the 8th test when the water visibility was fairly clear.

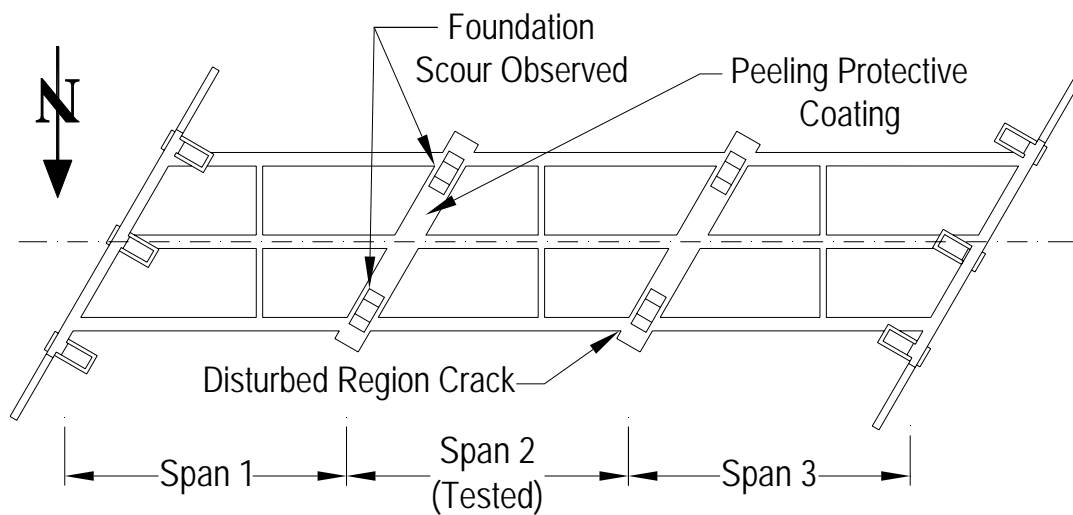


Figure 7.14. Bridge X-495 Disturbed Region Crack and Peeling of Protective Coating

7.6.4. Bridge P-962. The transverse girder at one of the bents showed signs of corrosion in the form of exposed and rusted rebar from spalled concrete. Also, the SRP utilized to strengthen the third span showed signs of rust in many places. This was especially prevalent in locations where water was able to drain from the deck to the girders or bents. The transverse girder corrosion and rusting of SRP can be observed in Figure 7.15 along with the locations of the occurrences.

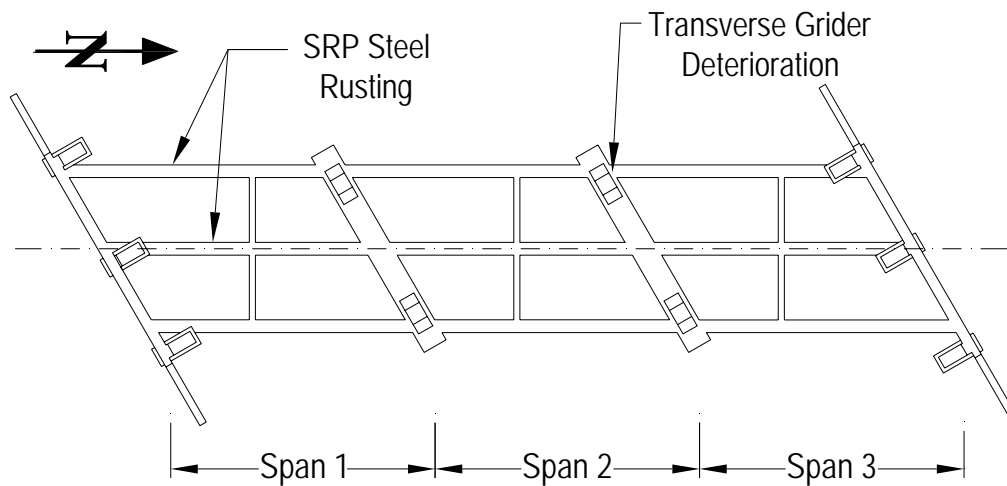


Figure 7.15. Bridge P-962 Corrosion of Transverse Girder and SRP Reinforcement

The rusting of the SRP was the worst strengthening deterioration observed on any of the bridges. If SRP is allowed to rust even slightly, then the entire strengthening system could be compromised due to the overall small area of the wires. Future inspections will be very important in order to ensure the SRP is performing adequately.

7.6.5. Bridge Y-298. The condition of bridge Y-298 was relatively poor prior to the application of the FRP strengthening. For this reason, mechanically fastened FRP was utilized in deteriorated areas for quick strengthening without the tedious surface preparation required for bonded applications. The condition of Y-298 has not substantially changed since strengthening. A permanent deflection at the northern side of the eastern span still exists. Additionally, there is some scour at the eastern abutment.

8. CONCLUSIONS

The objective of this research was to evaluate the long-term service performance of the concrete bridges strengthened with FRP technologies and to inspect and observe any deterioration of those bridges. The following conclusions can be drawn from this research work:

- Where site problems make LVDT and dial gauge systems very difficult to set up and operate successfully, surveying equipment is an ideal alternative.
- Surveying equipment can compete with traditional systems when monitoring the serviceability of structures during static load testing
- Surveying equipment cannot be used to monitor serviceability of structures during dynamic load testing.
- Thermal effects were significant in load testing for the Five Bridges Project.
- The apparent increase in stiffness achieved by adding FRP strengthening is primarily attributed to the restraint of concrete cracks from opening.
- There was a decrease in deflection and a subsequent apparent increase in stiffness for bridges T-530 and P-962 due to strengthening.
- For Bridges X-495 and X-596, it is difficult to quantify the apparent increase in stiffness due to strengthening with load testing. This is due to a lack of flexural strengthening of the exterior girders.
- The apparent increase in stiffness for Bridges T-530 and P-962 due to strengthening is decreasing according to an average percent difference trend line.
- The distribution fractions, or coefficients, for the western exterior girders of Bridge P-962 have been increasing over time.
- Overall, there has been no dramatic increase in the deflection of the tested bridges.

- The visual inspections conducted during testing have yielded some important information that will be helpful in tracking future degradations of bridge components or FRP strengthening.

The following commentary is presented based on the retrofit systems implemented and general observations to date:

- For strengthening of RC bridges with FRP in the field where limited manpower exists for installation, mechanically or adhesively fastened pre-cured plates appear to be a promising technology. For short span structures as few as two individuals can install the strengthening system and this technique appears ideal for county level agency installation. Other techniques such as Manual Lay-Up, NSM Bar, and SRP are generally more field intensive installation techniques and therefore require greater manpower.
- Based on the visual inspections to date, the SRP system exhibited signs of steel corrosion and was the worst observed strengthening deterioration for any system used. Corrosion of the high strength wire in the SRP system is particularly concerning due to its thin cross-section. The authors believe that a much more durable polymer system is required that will better protect the steel wire for this type system to hold promise in an aggressive external environment. This technique is not recommended for further field demonstration until a more durable protective polymer is used in combination with the steel wire.

APPENDIX A.
5 BRIDGES NORMALIZED DEFLECTION PROFILES

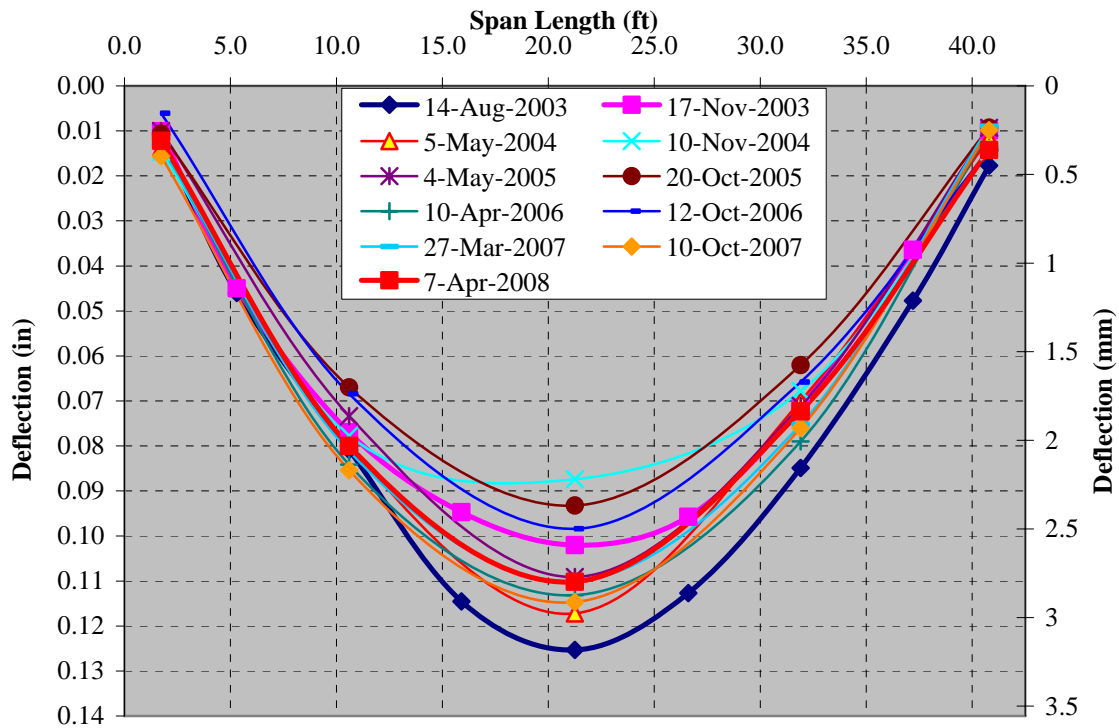


Figure A.1. Normalized Deflection Bridge P-962 - Stop 2, Exterior Girder

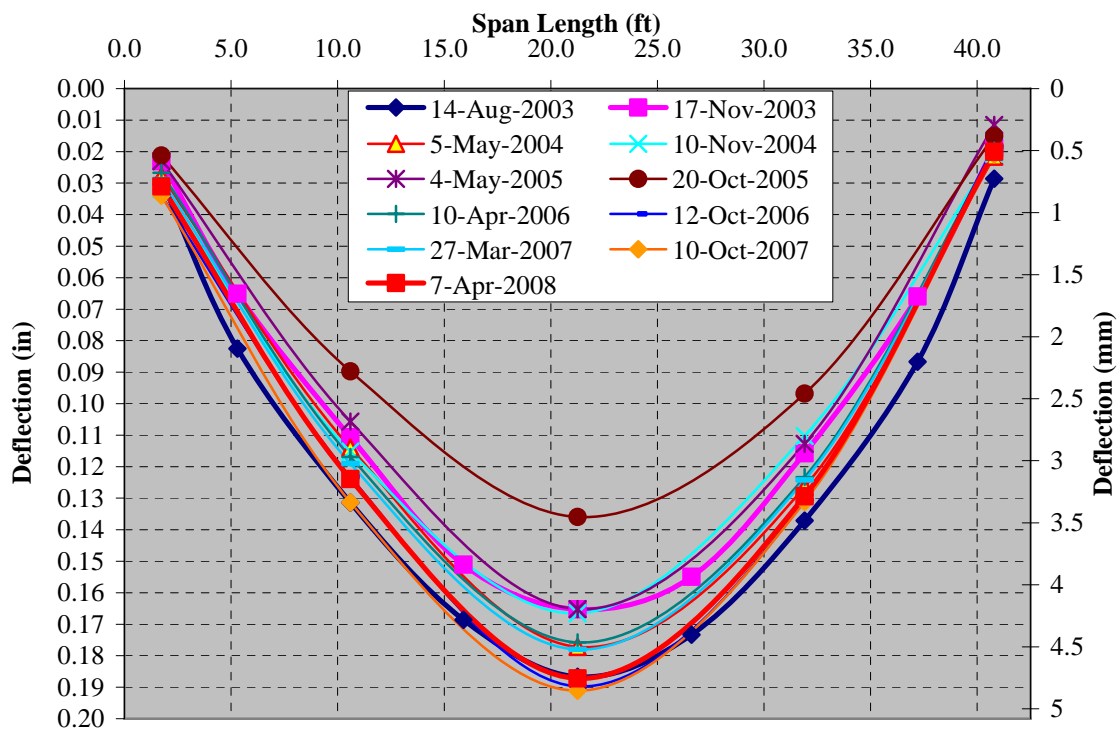


Figure A.2. Normalized Deflection Bridge P-962 - Stop 2, Interior Girder

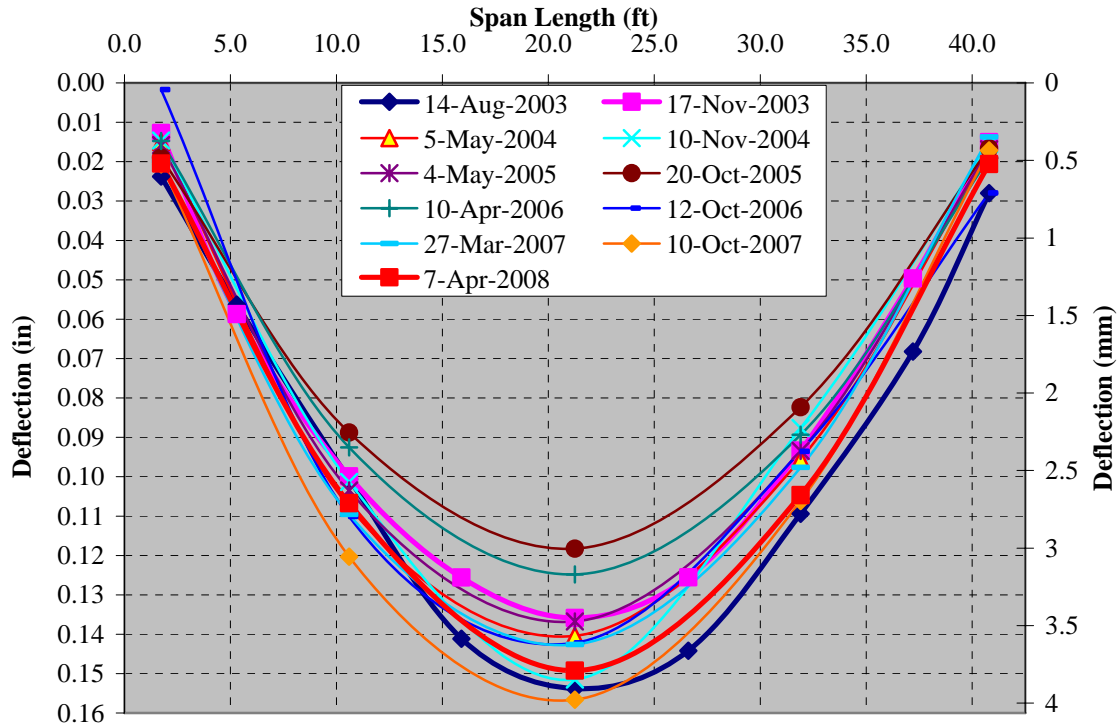


Figure A.3. Normalized Deflection Bridge P-962 - Stop 4, Exterior Girder

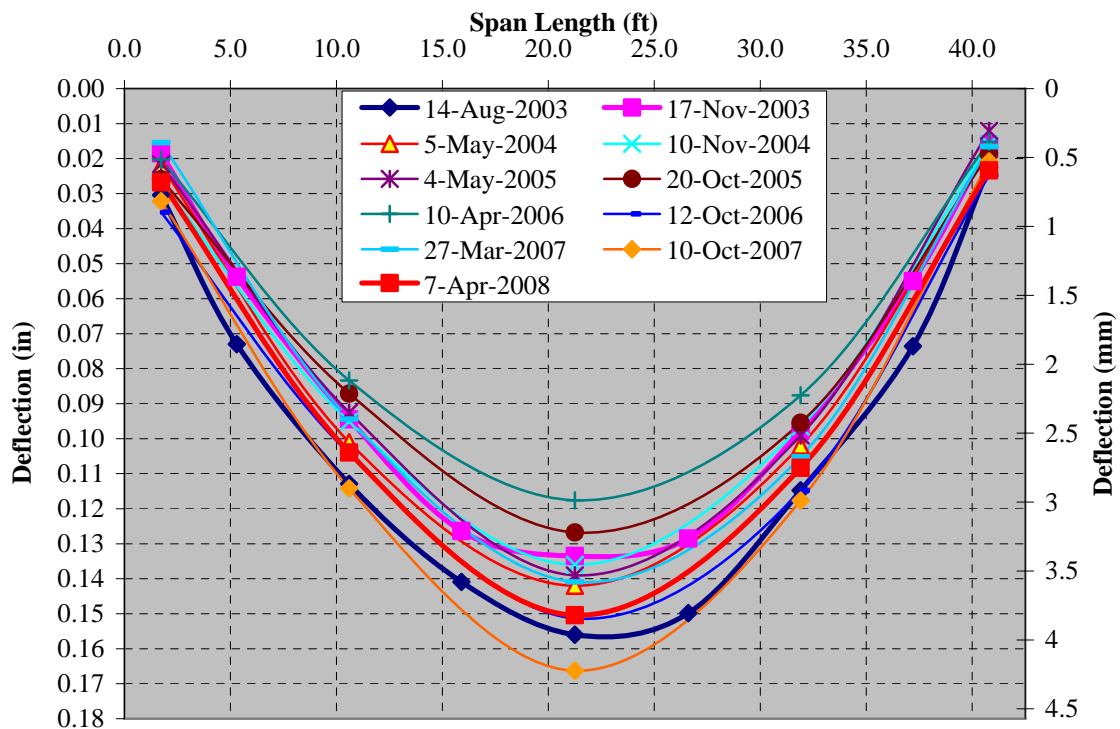


Figure A.4. Normalized Deflection Bridge P-962 - Stop 4, Interior Girder

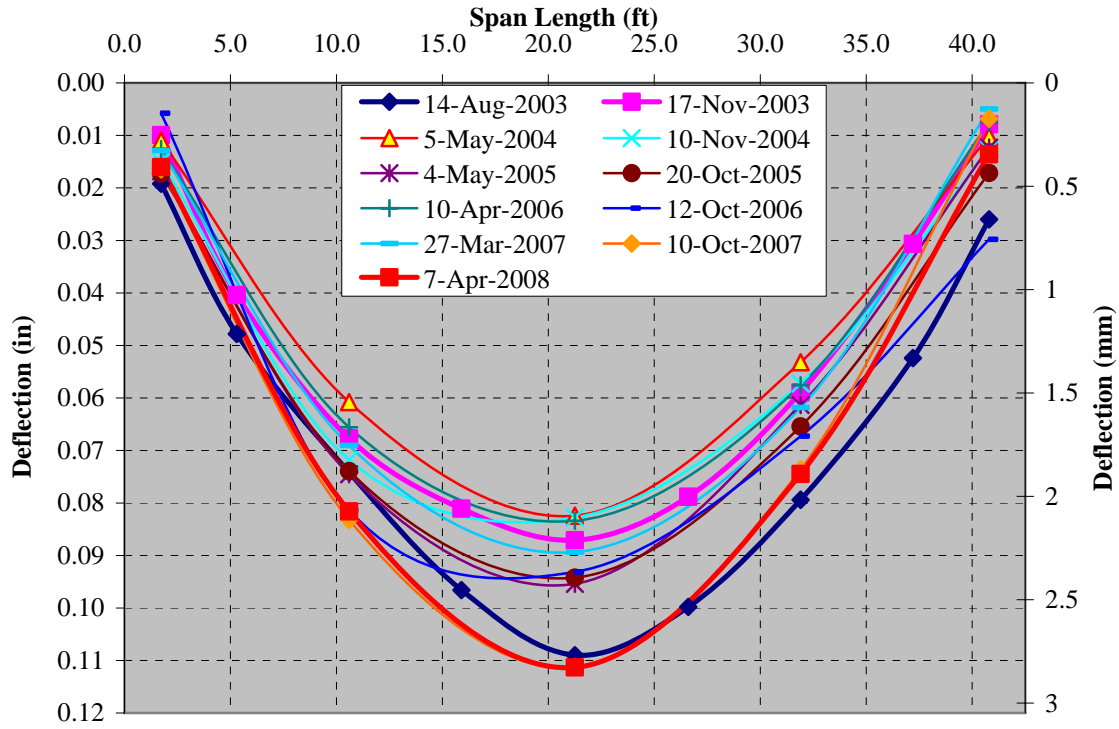


Figure A.5. Normalized Deflection Bridge P-962 - Stop 5, Exterior Girder

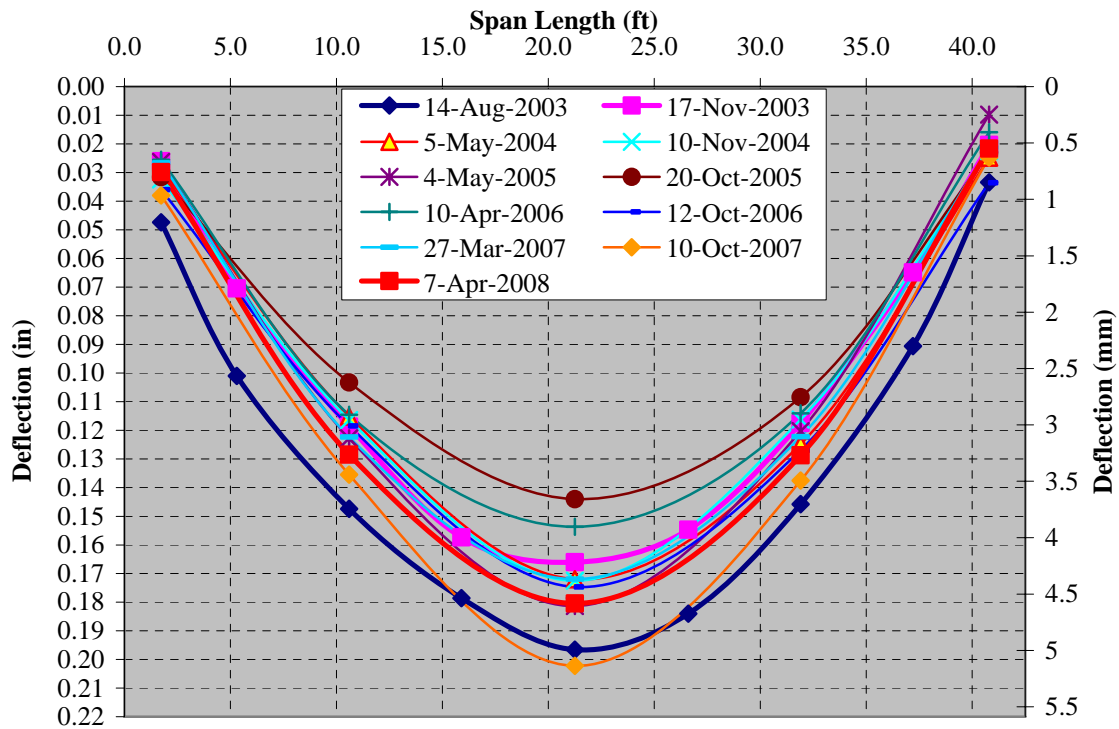


Figure A.6. Normalized Deflection Bridge P-962 - Stop 5, Interior Girder

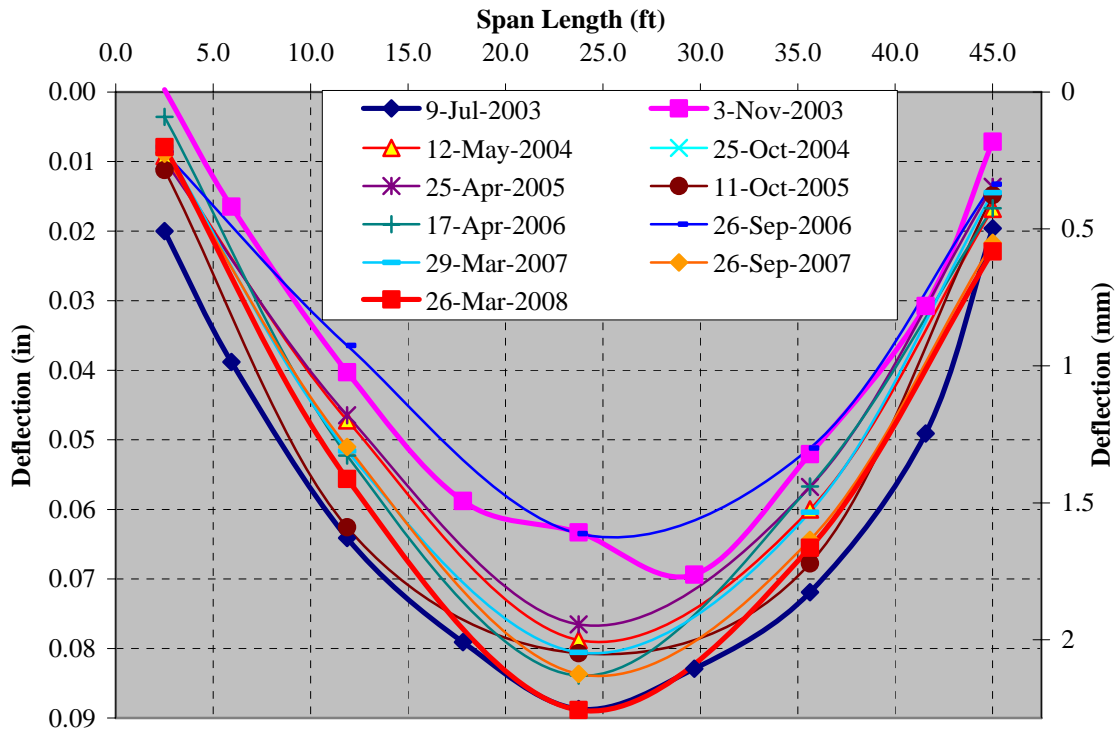


Figure A.7. Normalized Deflection Bridge T-530 - Stop 2, Exterior Girder

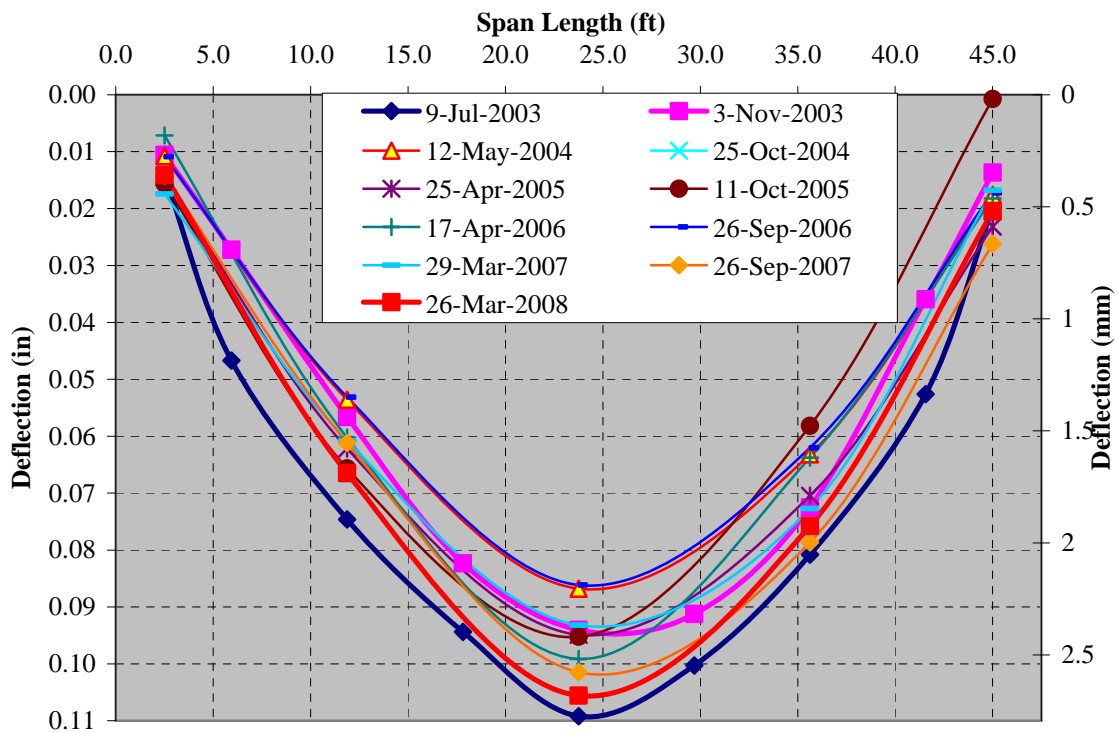


Figure A.8. Normalized Deflection Bridge T-530 - Stop 2, Interior Girder

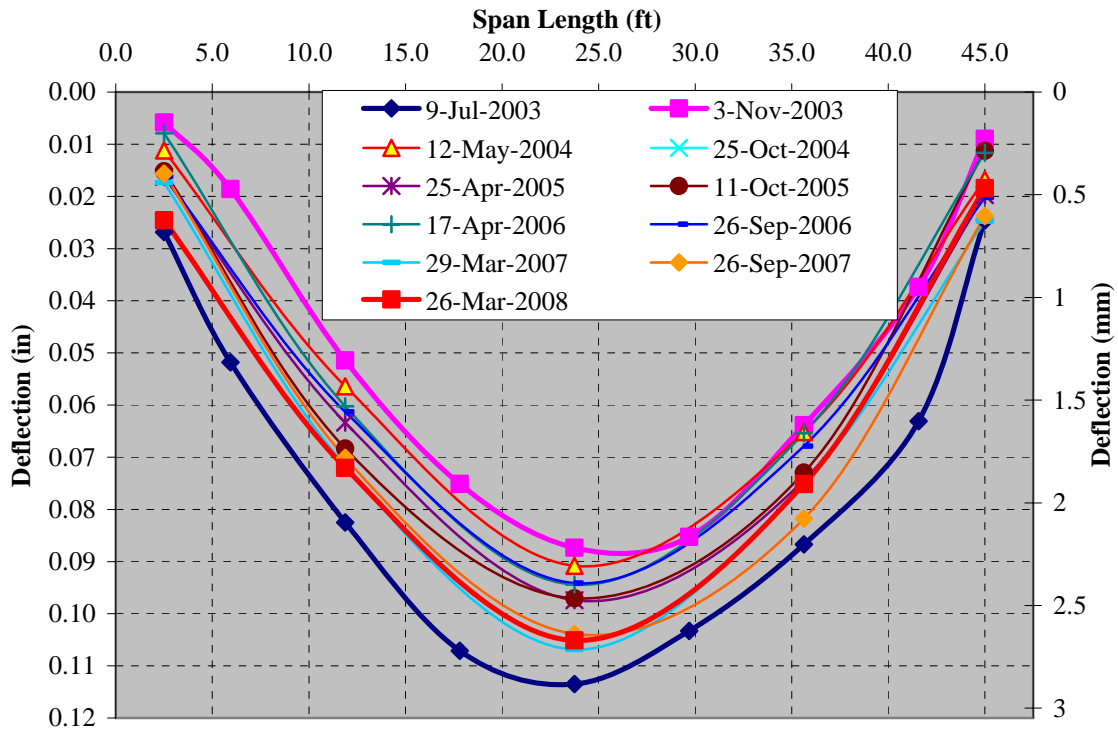


Figure A.9. Normalized Deflection Bridge T-530 - Stop 4, Exterior Girder

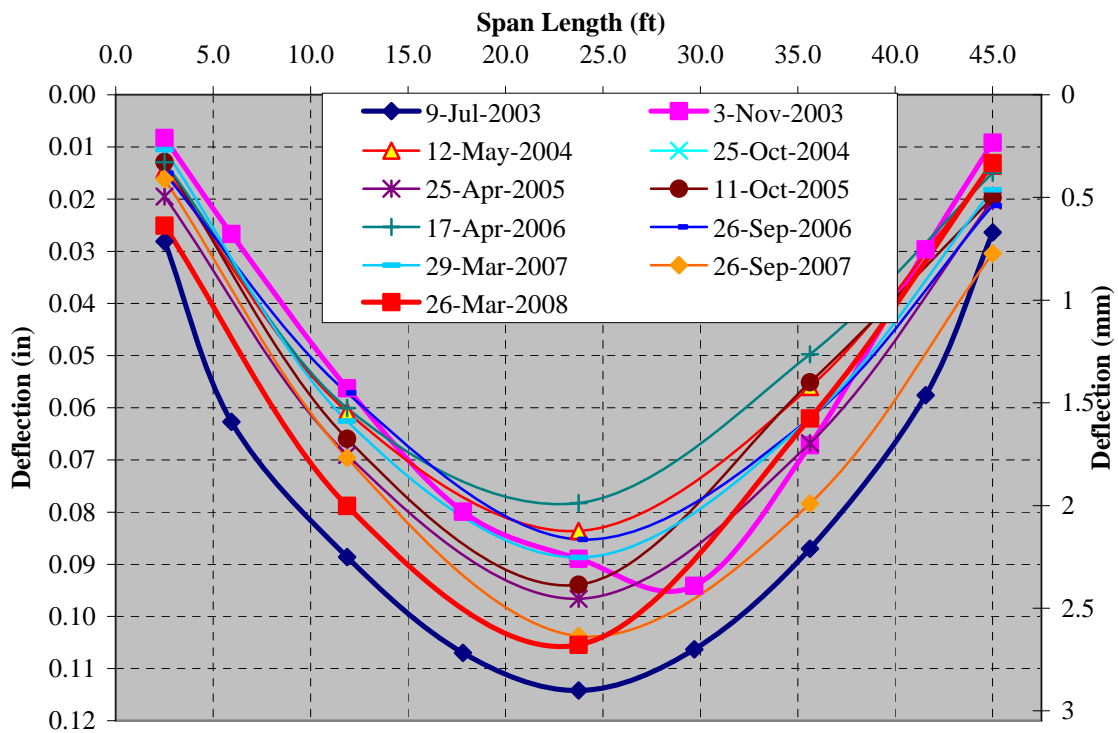


Figure A.10. Normalized Deflection Bridge T-530 - Stop 4, Interior Girder

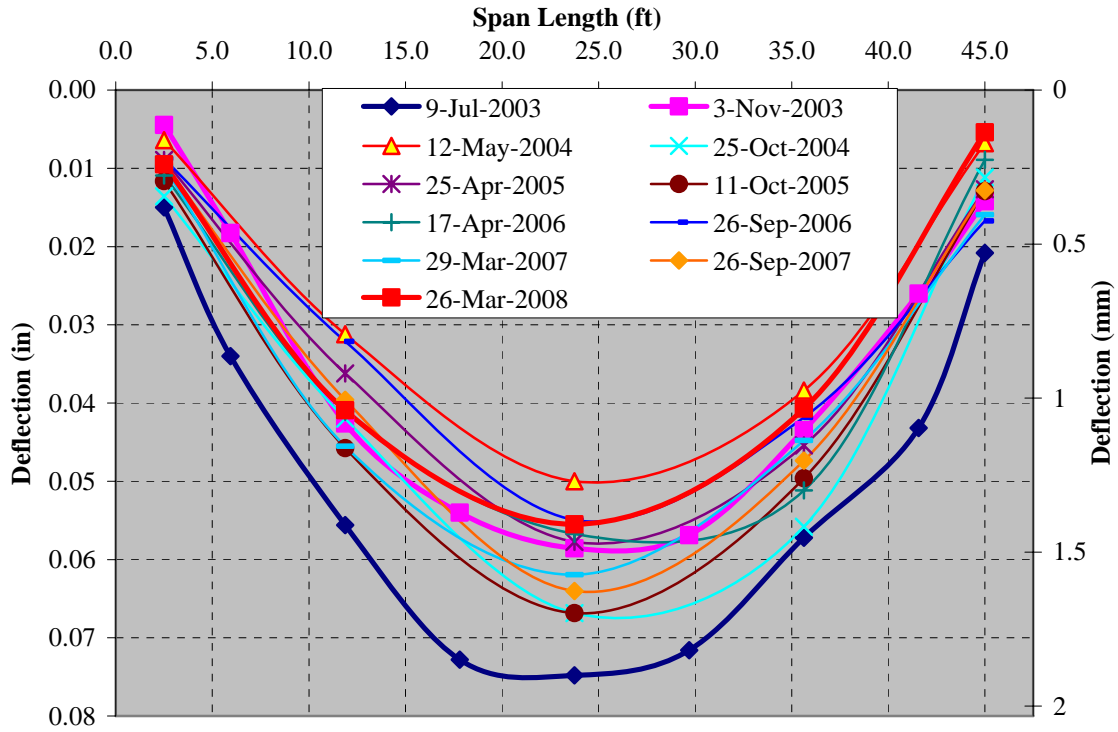


Figure A.11. Normalized Deflection Bridge T-530 - Stop 5, Exterior Girder

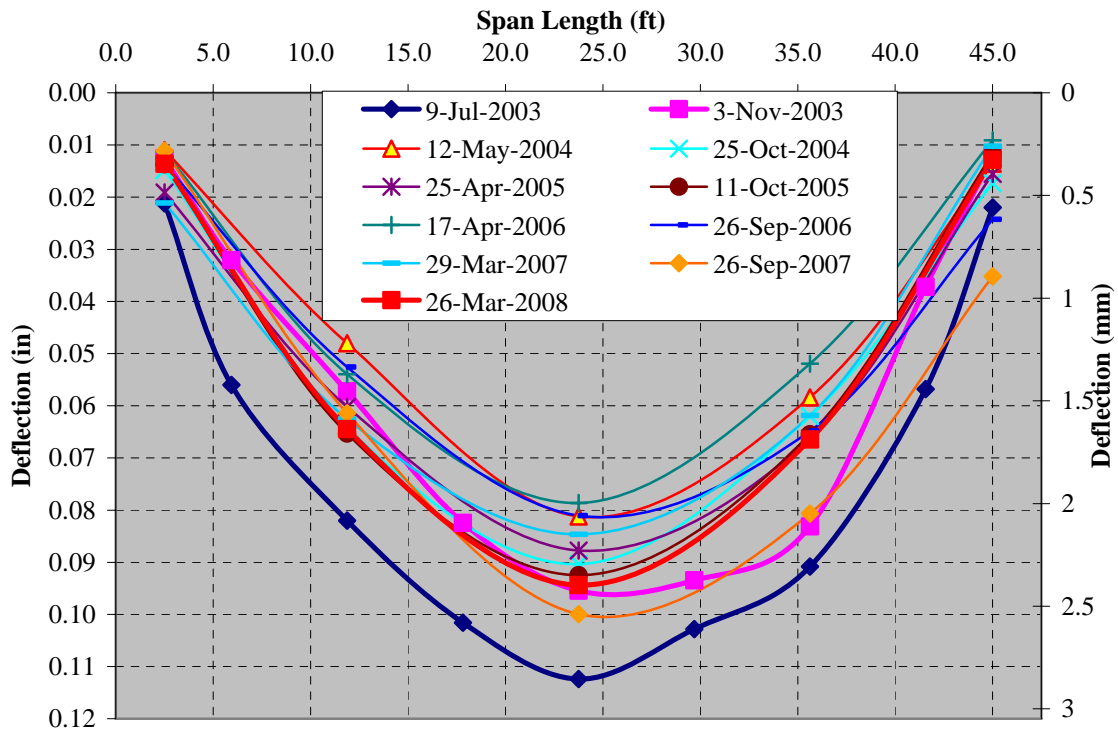


Figure A.12. Normalized Deflection Bridge T-530 - Stop 5, Interior Girder

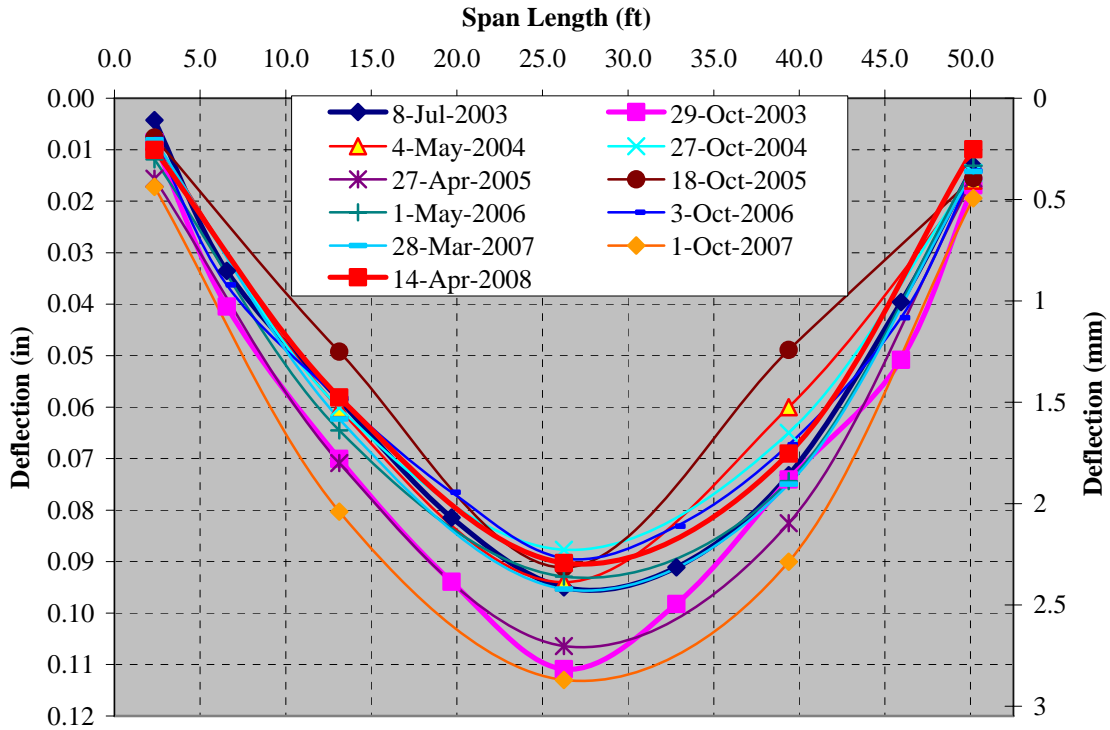


Figure A.13. Normalized Deflection Bridge X-495 - Stop 2, Exterior Girder

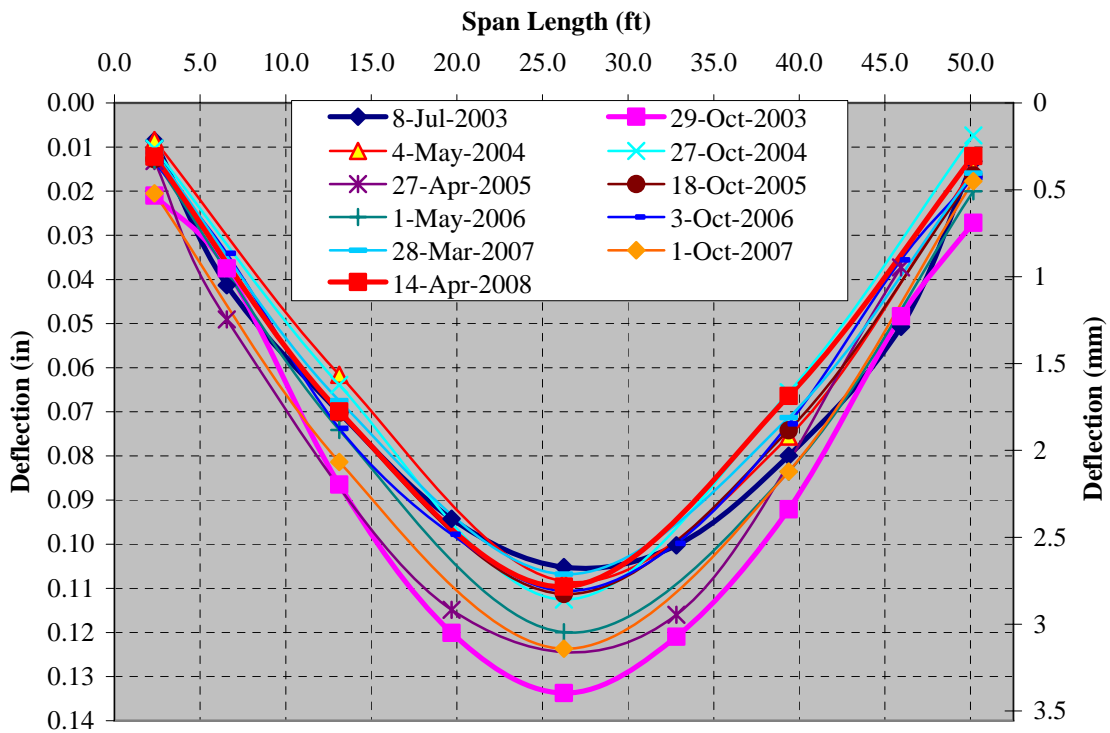


Figure A.14. Normalized Deflection Bridge X-495 - Stop 2, Interior Girder

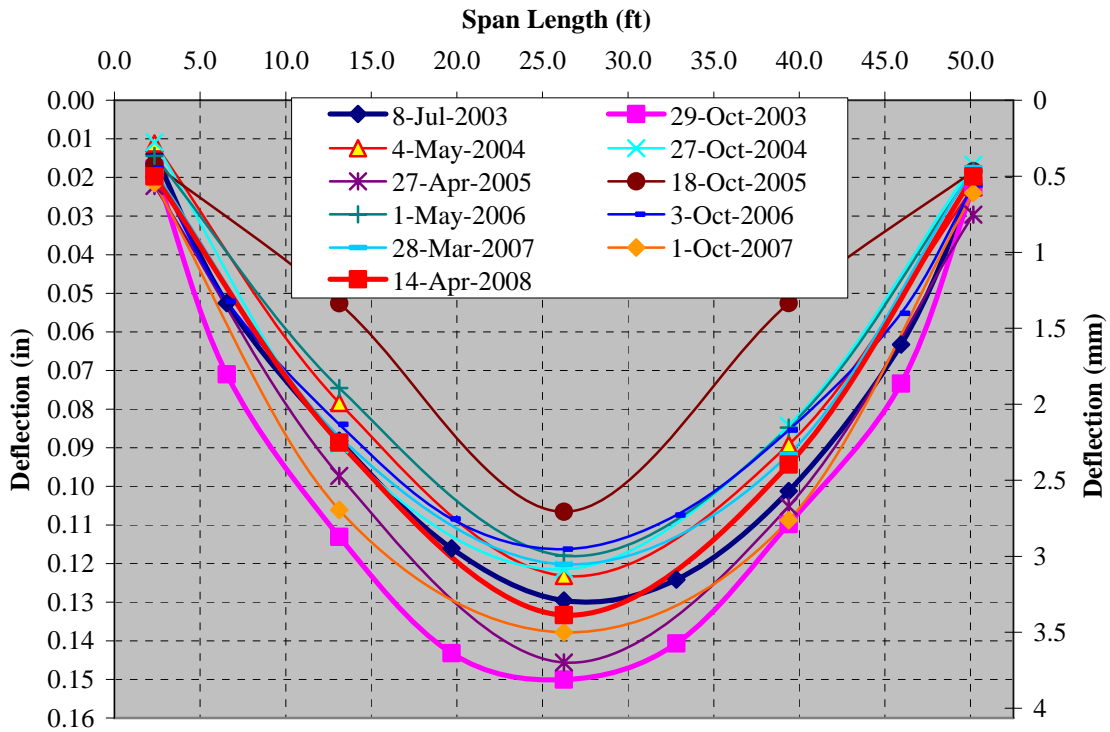


Figure A.15. Normalized Deflection Bridge X-495 - Stop 4, Exterior Girder

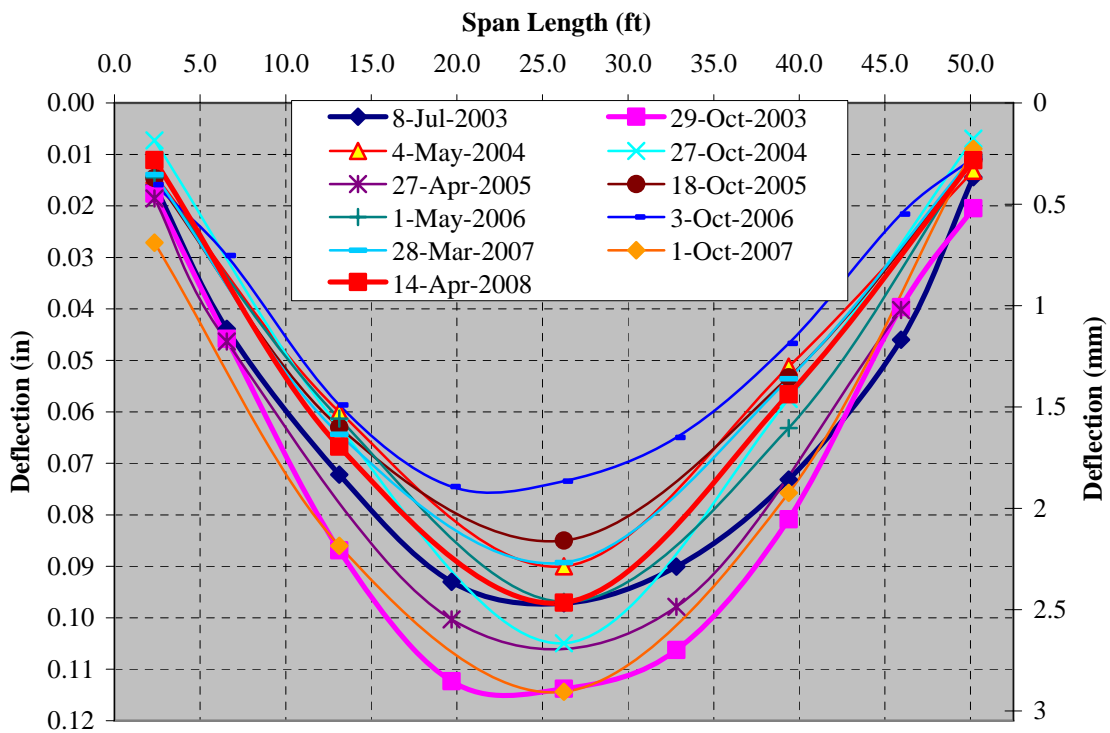


Figure A.16. Normalized Deflection Bridge X-495 - Stop 4, Interior Girder

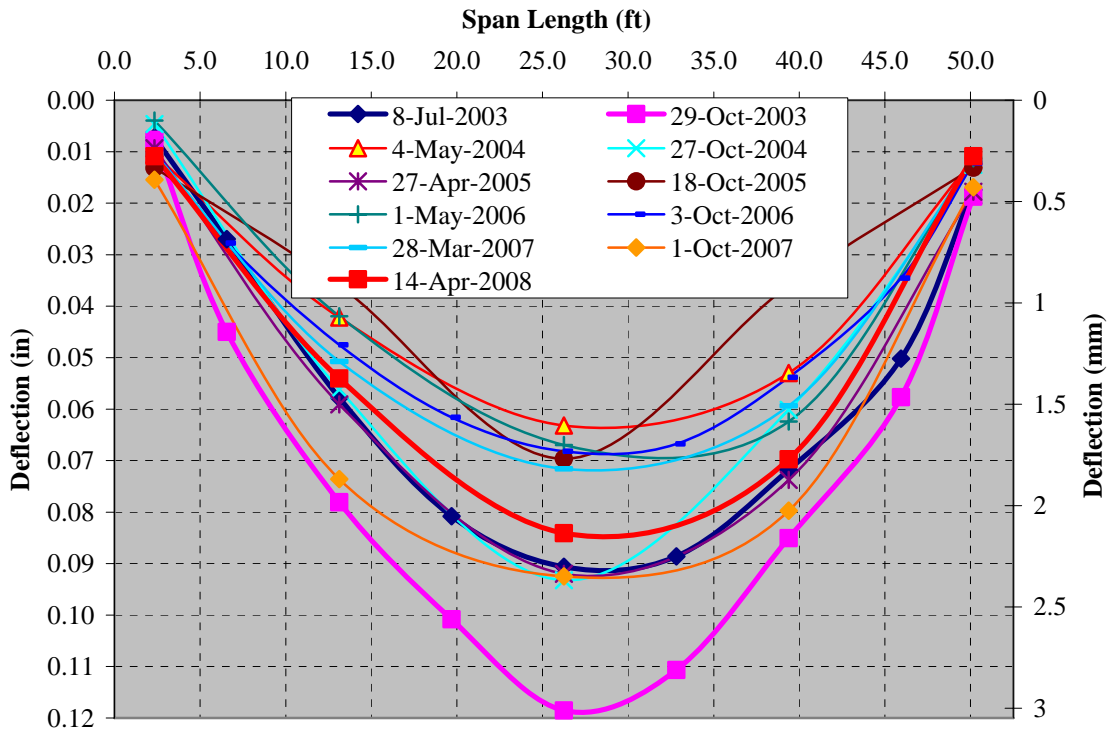


Figure A.17. Normalized Deflection Bridge X-495 - Stop 5, Exterior Girder

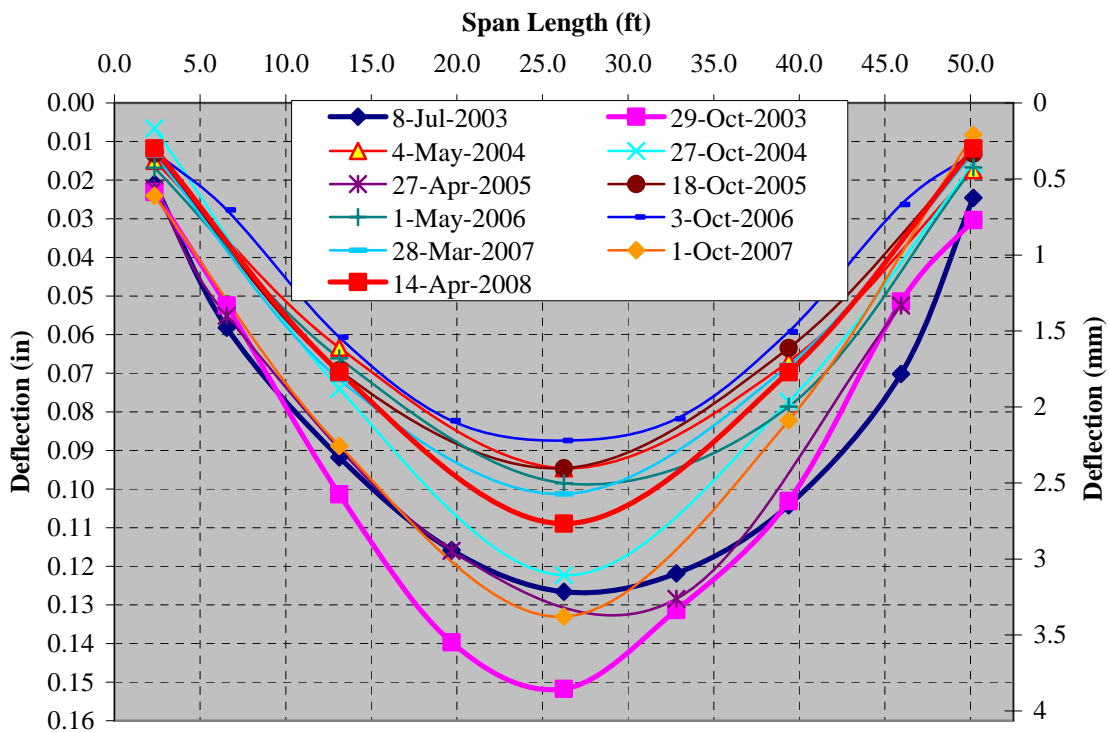


Figure A.18. Normalized Deflection Bridge X-495 - Stop 5, Interior Girder

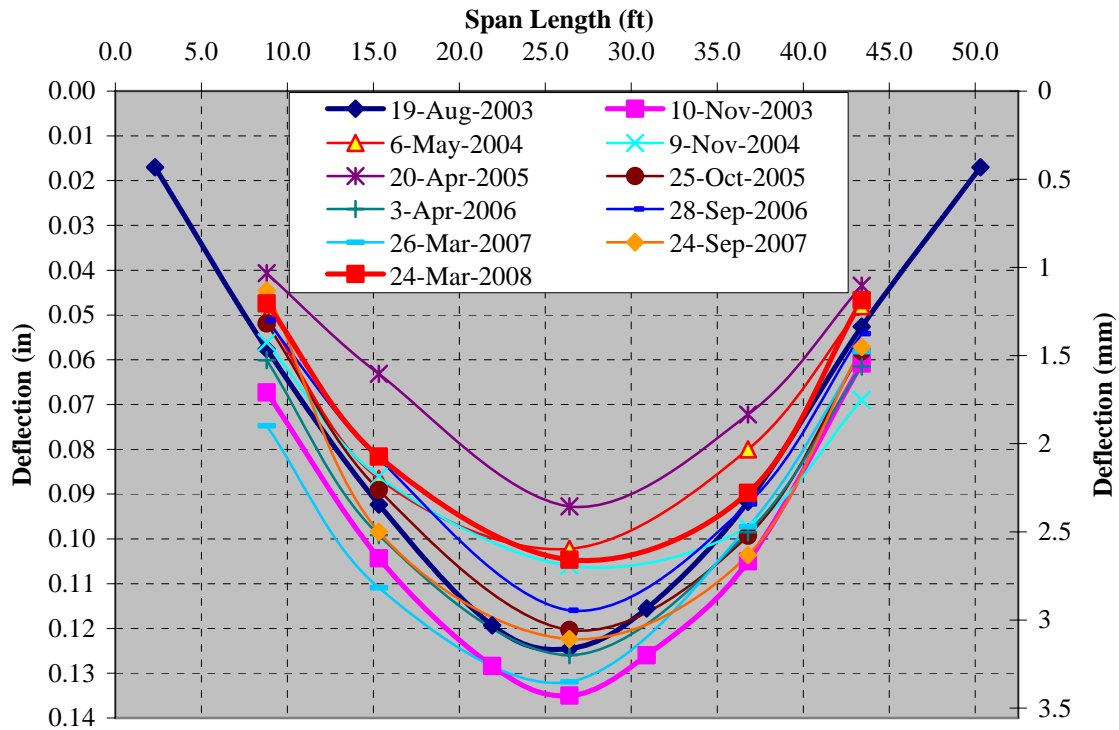


Figure A.19. Normalized Deflection Bridge X-596 - Stop 2, Exterior Girder

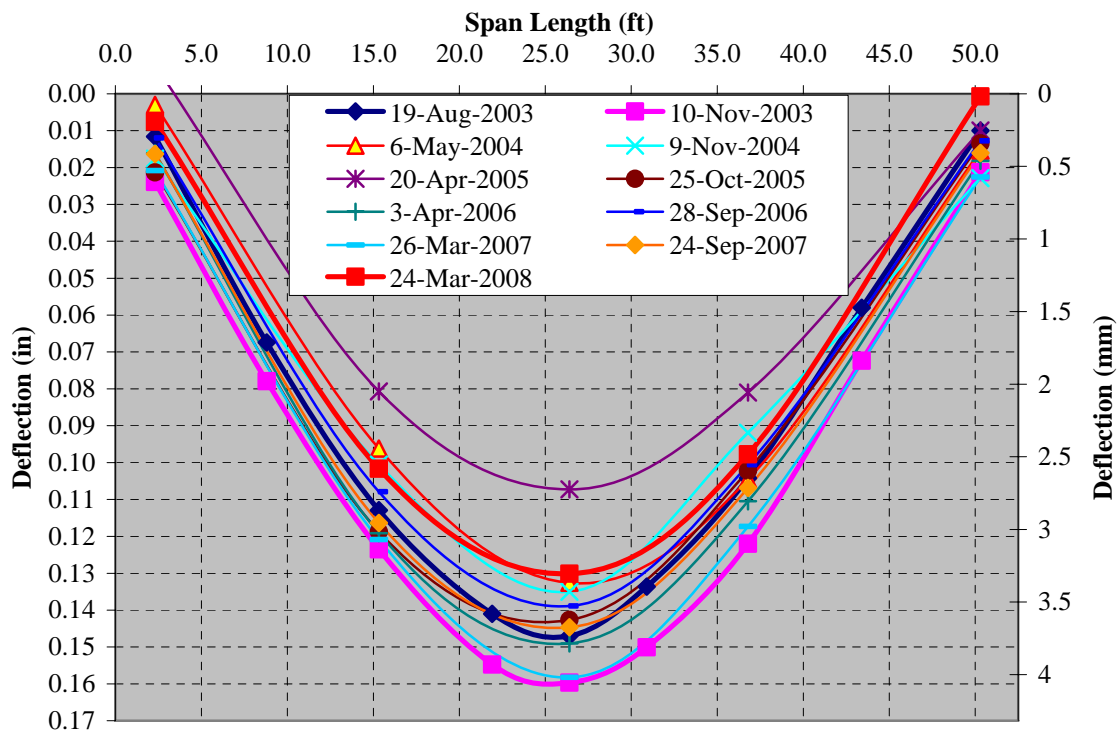


Figure A.20. Normalized Deflection Bridge X-596 - Stop 2, Interior Girder

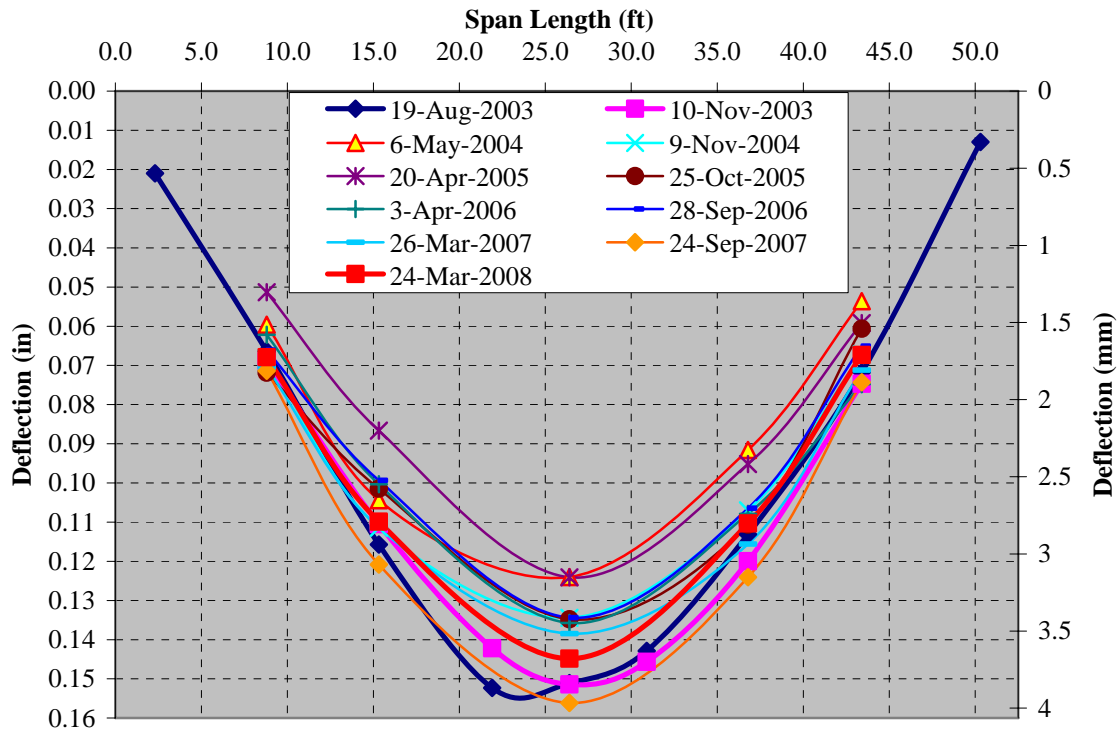


Figure A.21. Normalized Deflection Bridge X-596 - Stop 4, Exterior Girder

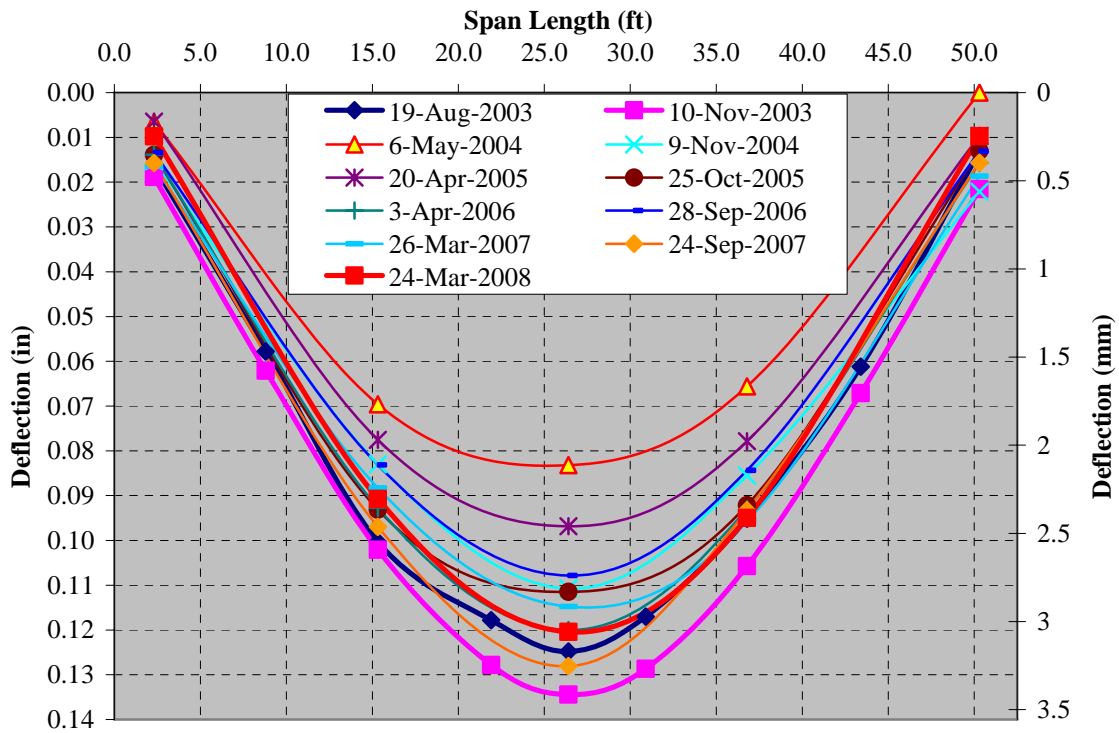


Figure A.22. Normalized Deflection Bridge X-596 - Stop 4, Interior Girder

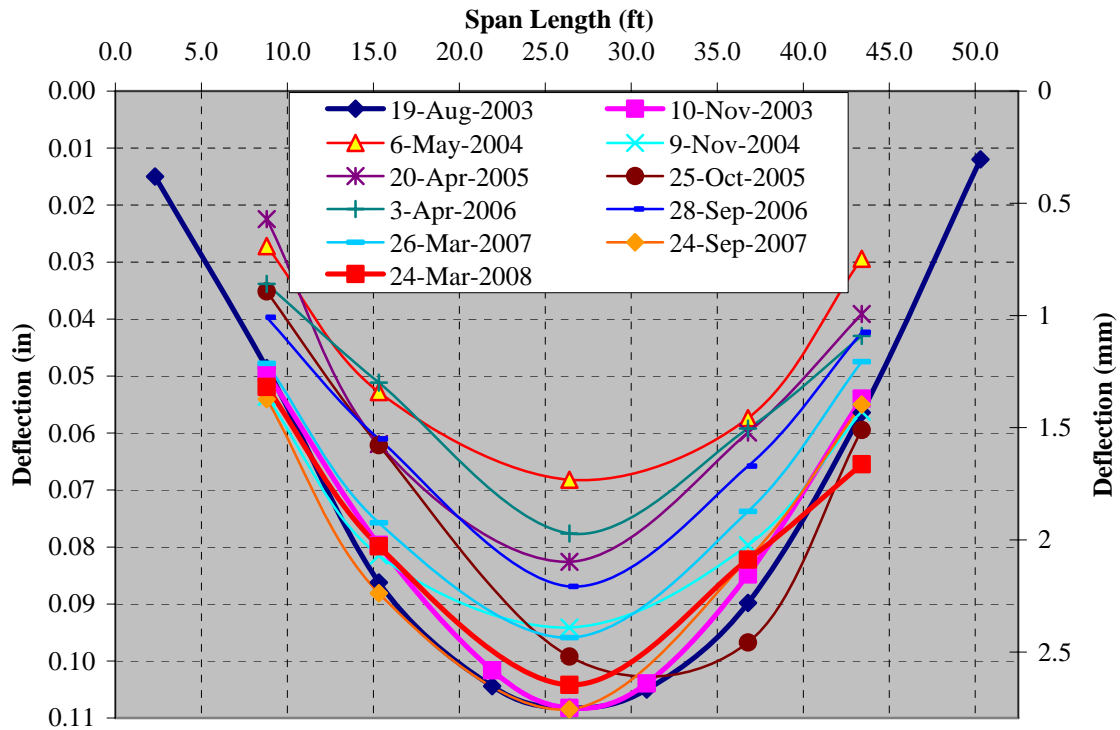


Figure A.23. Normalized Deflection Bridge X-596 - Stop 5 Exterior Girder

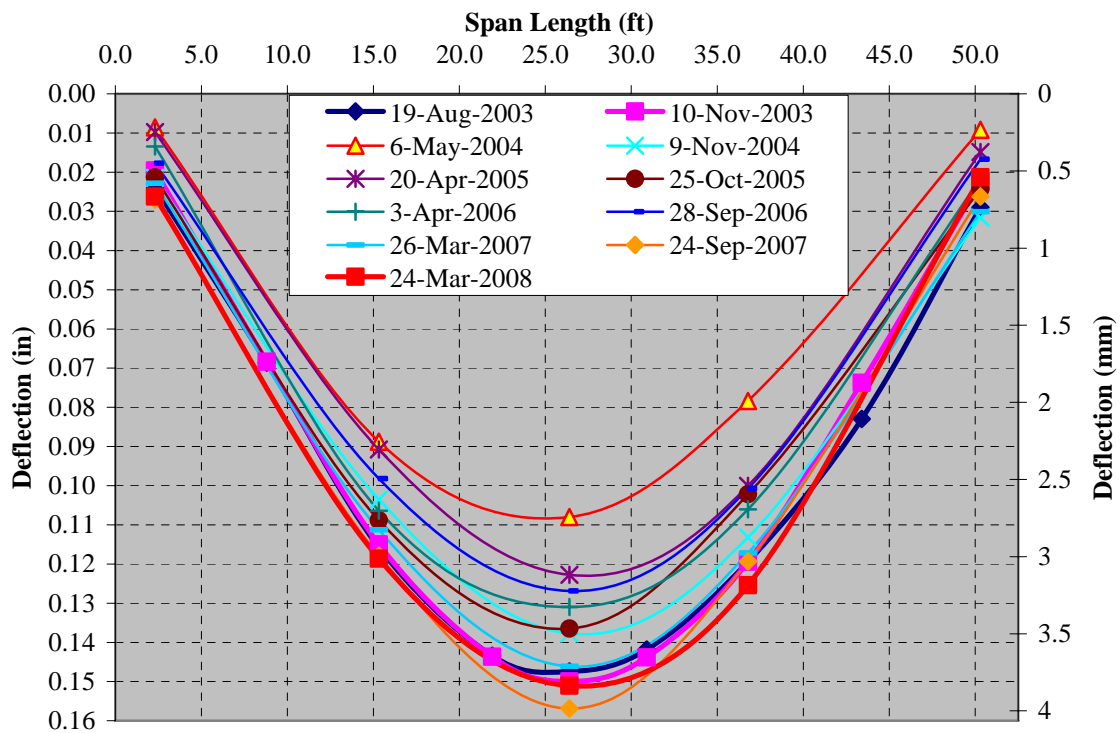
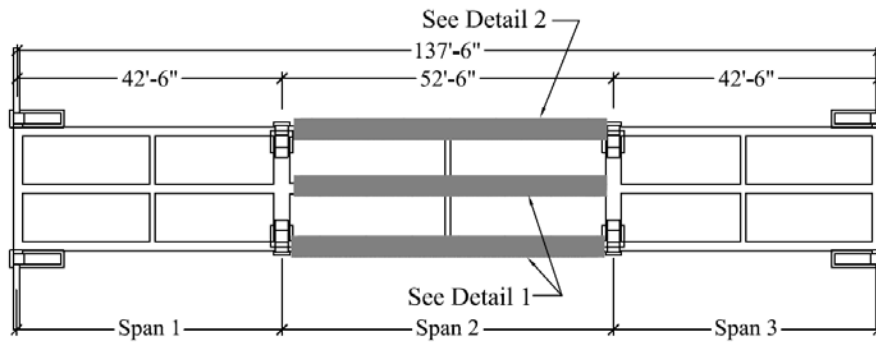
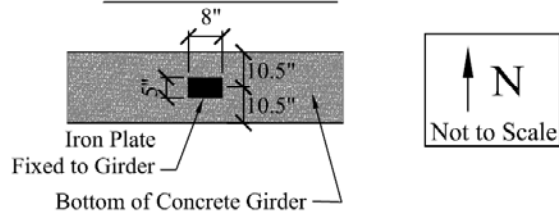


Figure A.24. Normalized Deflection Bridge X-596 - Stop 5 Interior Girder

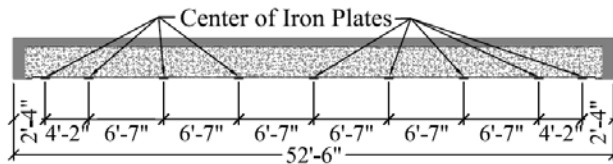
APPENDIX B.
LOAD TESTING DIAGRAMS



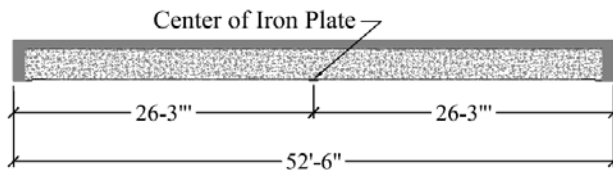
Detail of Iron Plate



Detail 1 - 9 Plates per Girder

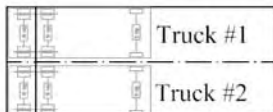
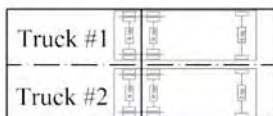
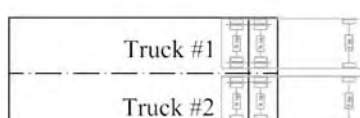
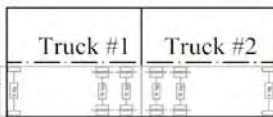
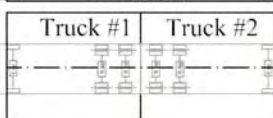


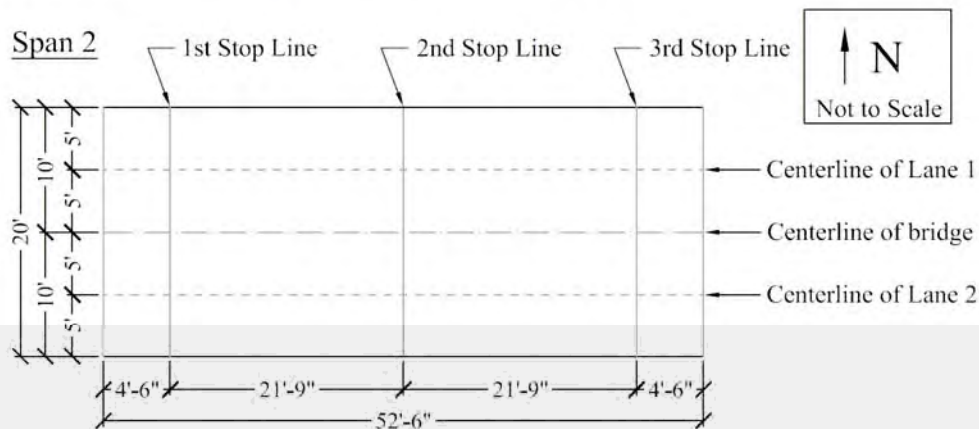
Detail 2 - 1 Plate at Mid-Span



Conversion Units: 1 in = 25.4 mm; 1 ft = 0.3048 m

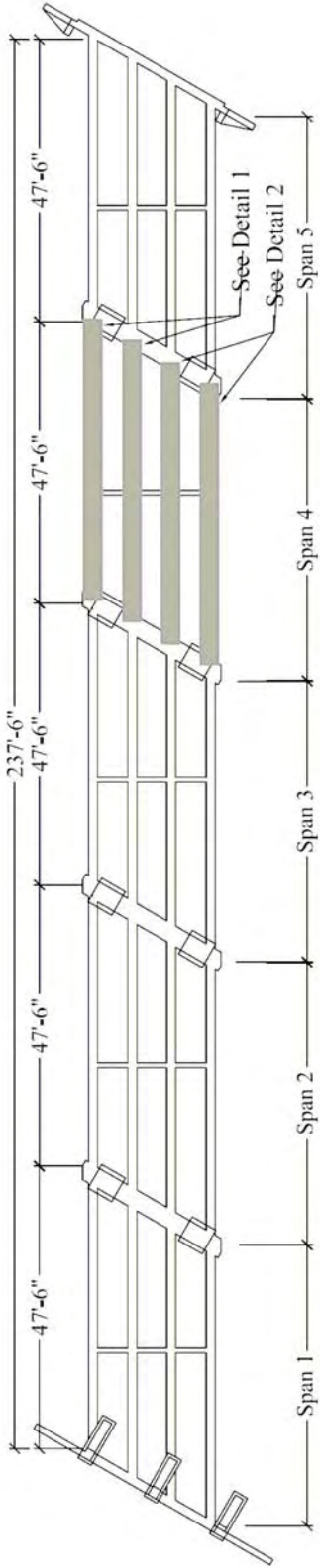
Figure B.1. Iron Plate / Prism Installation - Bridge X-596

| | | |
|------------------------------------|---|--|
| Test 1 Maximum Shear |  | Truck #1 is centered in Lane 1 facing East with the centroid of its rear axles over the first stop line; Truck #2 is centered in Lane 2 facing East with the centroid of its rear axles over the first stop line |
| Test 2 Maximum Moment |  | Truck #1 is centered in Lane 1 facing East with the centroid of its rear axles over the second stop line; Truck #2 is centered in Lane 2 facing East with the centroid of its rear axles over the second stop line |
| Test 3 Maximum Shear |  | Truck #1 is centered in Lane 1 facing East with the centroid of its rear axles over the third stop line; Truck #2 is centered in Lane 2 facing East with the centroid of its rear axles over the third stop line |
| Test 4 Overload Exterior Girder |  | Trucks #1&2 are centered in Lane 1 back-to-back at the second stop line (Midspan) |
| Test 5 Overload Interior Girder |  | Trucks #1&2 are centered about the bridge (roadway) centerline back-to-back at the second stop line (Midspan) |

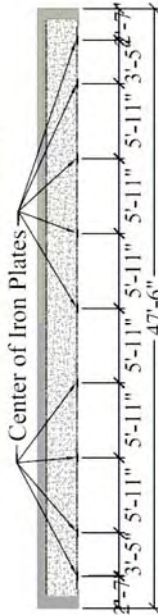


Conversion Units: 1 in = 25.4 mm; 1 ft = 0.3048 m

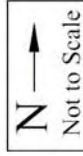
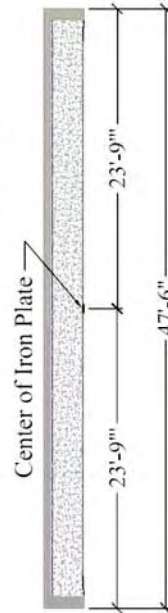
Figure B.2. Truck Stops - Bridge X-596



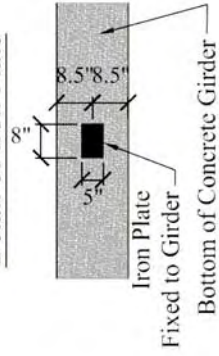
Detail 1 - 9 Plates per Girder



Detail 2 - 1 Plate at Mid-Span

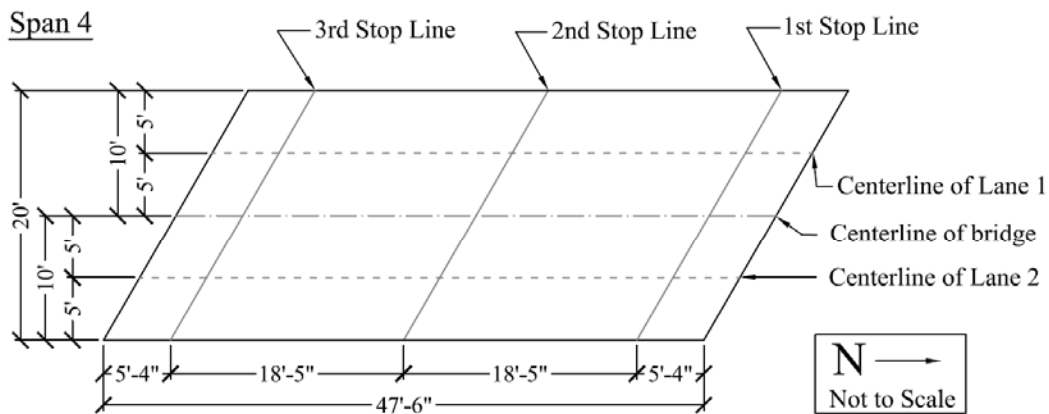
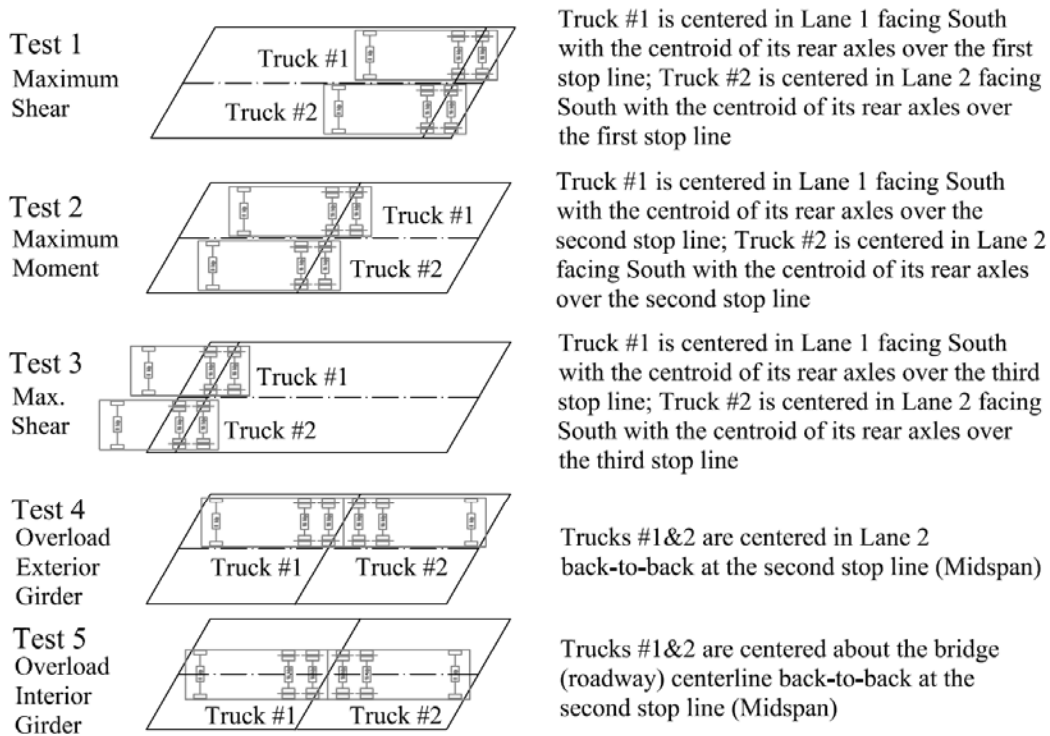


Detail of Iron Plate



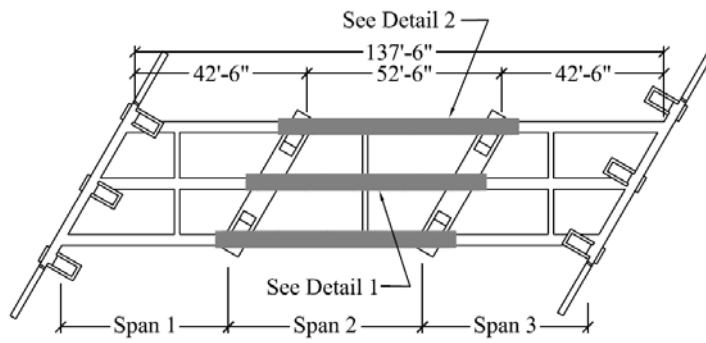
Conversion Units: 1 in = 25.4 mm; 1 ft = 0.3048 m

Figure B.3. Iron Plate / Prism Installation - Bridge T-530

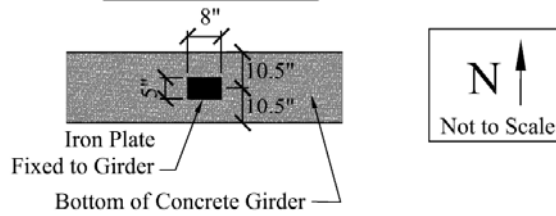


Conversion Units: 1 in = 25.4 mm; 1 ft = 0.3048 m

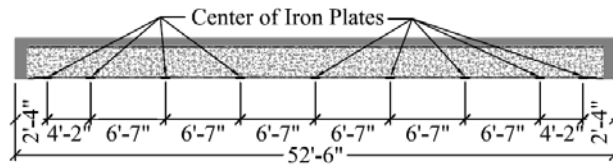
Figure B.4. Truck Stops - Bridge T-530



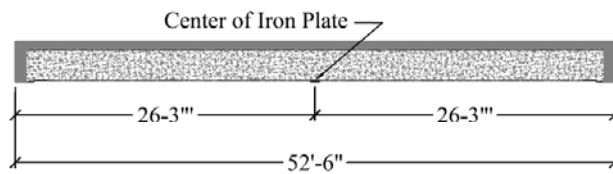
Detail of Iron Plate



Detail 1 - 9 Plates per Girder

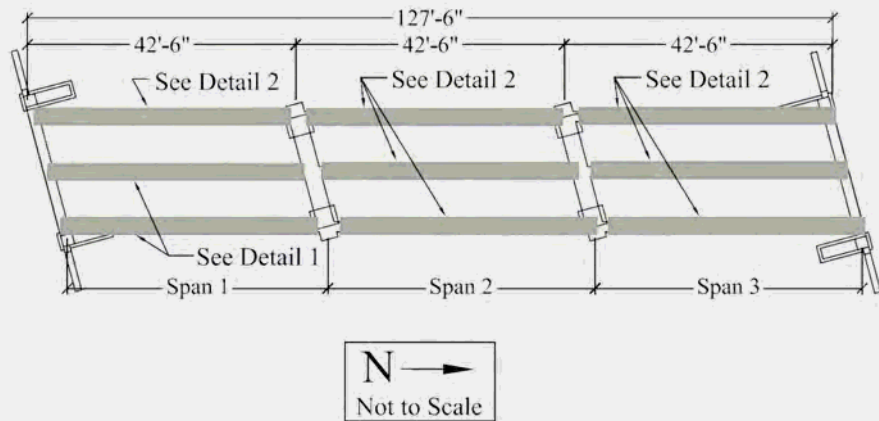


Detail 2 - 1 Plate at Mid-Span

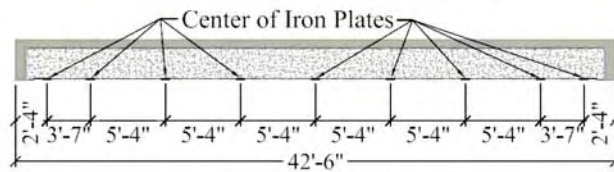


Conversion Units: 1 in = 25.4 mm; 1 ft = 0.3048 m

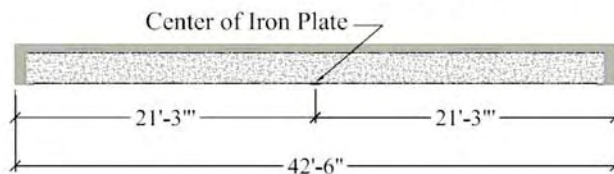
Figure B.5. Iron Plate / Prism Installation - Bridge X-495



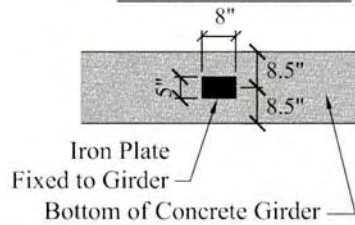
Detail 1 - 9 Plates per Girder



Detail 2 - 1 Plate at Mid-Span

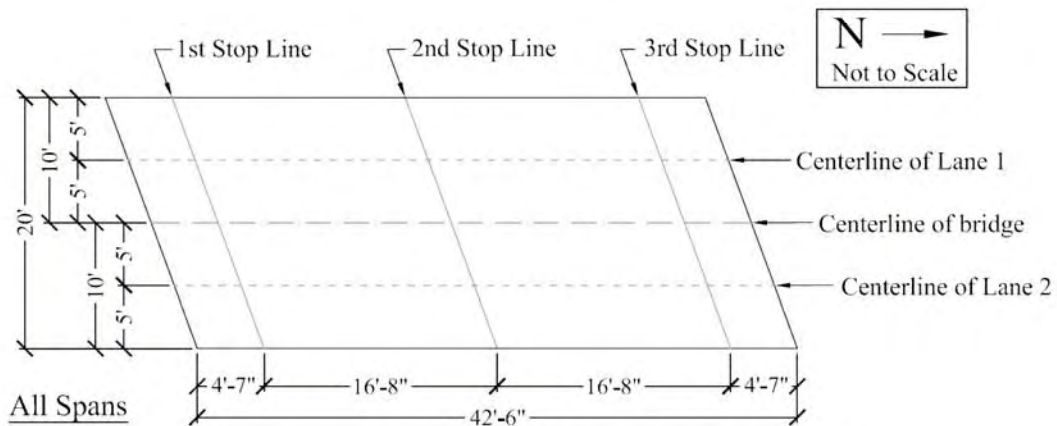
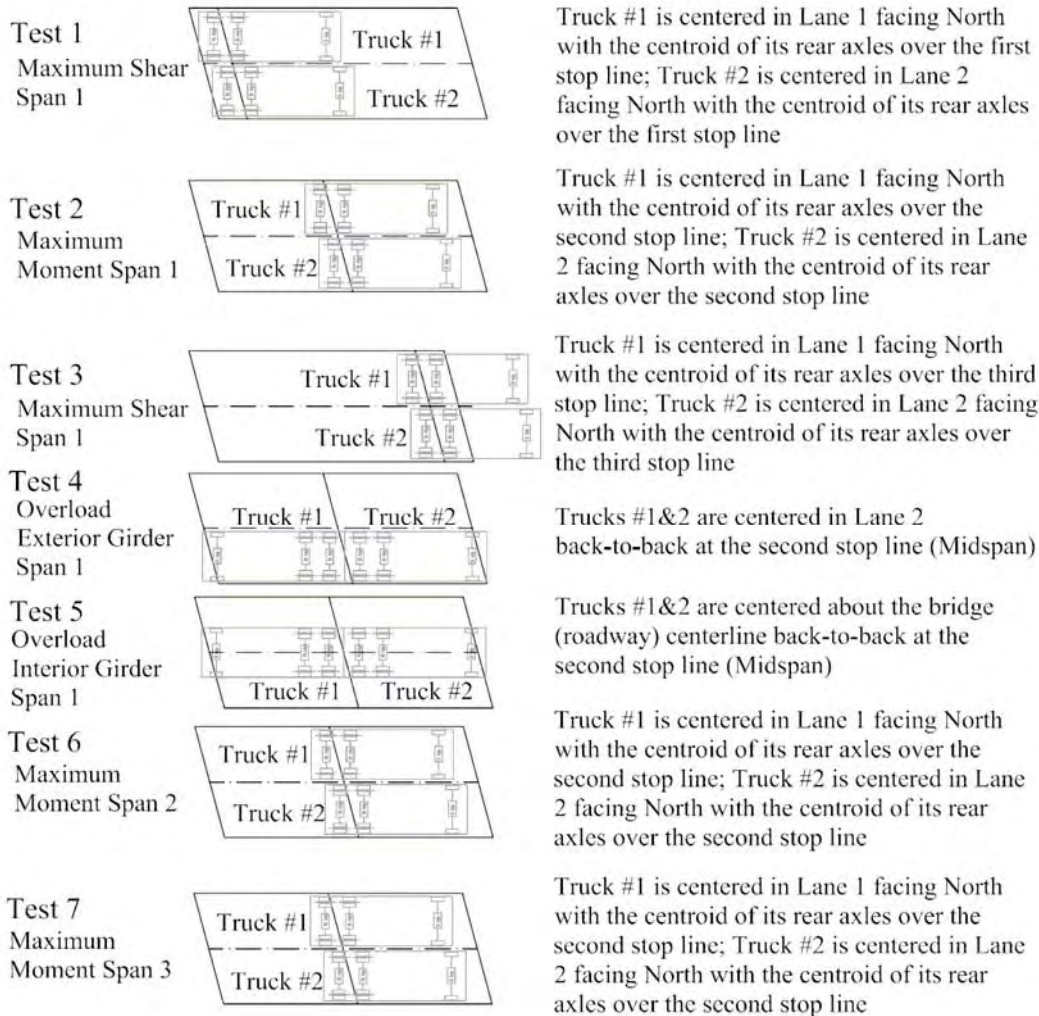


Detail of Iron Plate



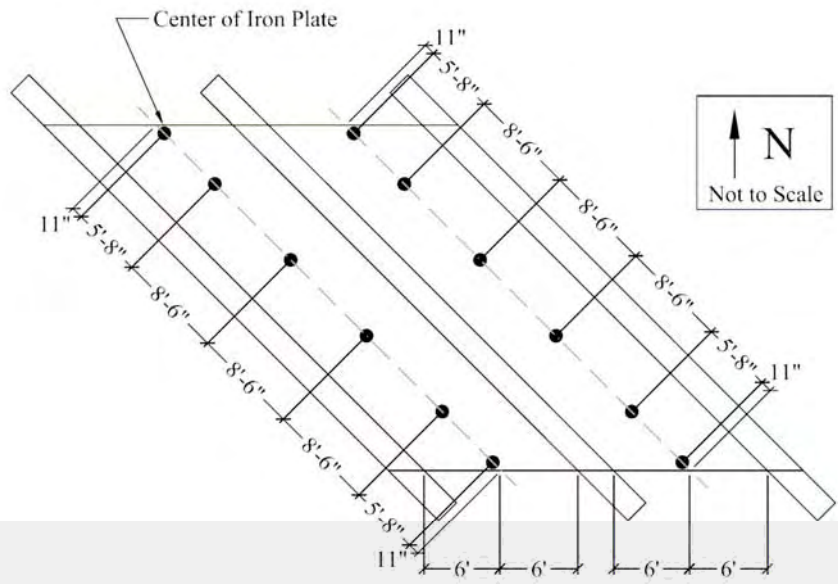
Conversion Units: 1 in = 25.4 mm; 1 ft = 0.3048 m

Figure B.7. Iron Plate / Prism Installation - Bridge P-962



Conversion Units: 1 in = 25.4 mm; 1 ft = 0.3048 m

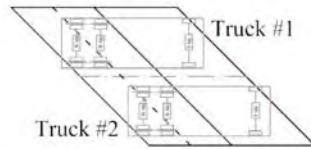
Figure B.8. Truck Stops - Bridge P-962



Conversion Units: 1 in = 25.4 mm; 1 ft = 0.3048 m

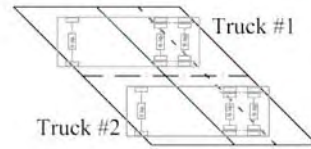
Figure B.9. Iron Plate / Prism Installation - Bridge Y-298

Test 1
Maximum
Moment
Span 1

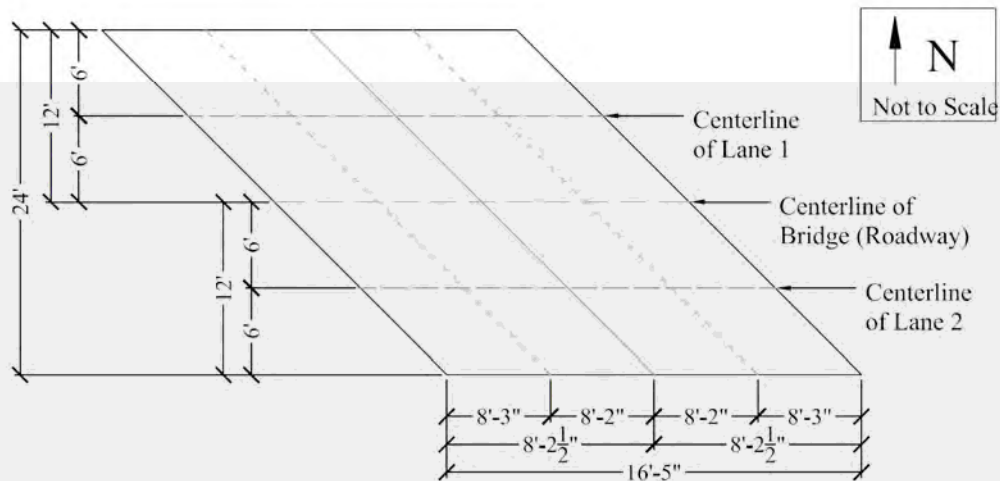


Truck #1 is centered in Lane 1 facing East with the centroid of its rear axles over the first stop line
Truck #2 is centered in Lane 2 facing East with the centroid of its rear axles over the first stop line

Test 2
Maximum
Moment
Span 2



Truck #1 is centered in Lane 1 facing West with the centroid of its rear axles over the second stop line
Truck #2 is centered in Lane 2 facing West with the centroid of its rear axles over the second stop line



Conversion Units: 1 in = 25.4 mm; 1 ft = 0.3048 m

Figure B.10. Truck Stops - Bridge Y-298

APPENDIX C
LOAD TESTING FIELD PROCEDURES

This appendix outlines the final detailed procedure used to load test project bridges. The details of testing herein include: preparation, setup, testing, and teardown.

1. Test Preparation. Many steps were taken to ensure a smooth day of testing. Before the test day, iron plates for mounting the prisms were properly installed. The location of the plates was pre-determined and the plates were mounted along the bottom centerline of the girders. See Appendix D for plate installation details.

Next, the data cards for the Total Station were checked for free space. Each data card holds twelve files. Using the Total Station or computer, each card was accessed. Old files were deleted only after it was certain that the data was either backed up or not valuable. See the Leica software package or the Leica Help Binder for more information (Leica 2003). The batteries were given twenty-four hours to fully charge. Once ready, one data card and one battery were kept on the Total Station while the other two were placed in the Leica Total Station case. On the day before testing, all personnel involved were contacted for a last reminder about the load test place and time. Lastly, all equipment was gathered and checked to be in working order.

2. Test Setup. With three people assisting, the test setup took no longer than sixty minutes at any project bridge. Upon arrival at the site, all vehicles were parked in a visible location clear of traffic. All personnel wore orange safety vests and hard hats when necessary; also, everyone was reminded to always watch for traffic and to keep all personnel and equipment on one side of the road when possible.

Visiting the site prior testing was necessary for developing a plan on how to set up the site. Unpacking all equipment was the first step; all equipment must be kept together, clean, dry, out of sunlight, and far away from traffic. Next, the tested span was clearly marked with

marking/spray paint for the truck stop locations following a pre-drawn plan (see Appendix D). The roadway was marked only where necessary to keep the testing as simple as possible.

The rest of the site setup took place underneath the structure. The Total Station was placed approximately 50 to 100 feet away from and nearly perpendicular to the tested span, in a shady location, and with an unobstructed view of the tested span. A position in clear sight of all prisms was chosen to maximize the angle between the prism targets on the bridge.. The soil under the Total Station had to be firm and stable. The tripod was first set up: first, the legs were unfastened, released to a desired length, and tightened. The bases of the tripod legs should be approximately equidistant from each other and about three feet apart. Each leg base was then stepped on with enough weight to drive the leg firmly into the soil. The Total Station (instrument) was taken out of its case and secured to the tripod (see Figure C.1). The instrument case was closed to keep it clean and dry. The base of each leg was firmly stood on again. At this point, the legs should not be able to move much in the soil. If movement occurred, the soil would not be considered stable enough and the Total Station would be moved. While looking at the leveling bubble on the instrument, each leg was released, adjusted, and tightened to balance the bubble in the center ring. Next, the “ON” button was pressed followed by the electronic level button to display the fine-adjustments needed to perfectly level the instrument. Using the finger screws at the base of the instrument, the instrument was leveled so that each tilt direction measured 0°00’00”. “CONT” was pressed to return to the main menu.



Figure C.1. Total Station and Tripod

From then on, no personnel would be allowed near the Total Station unless absolutely necessary. The operator of the Total Station was not to stand within two feet of any of the tripod's legs at any time. The operator should only apply the minimum necessary force to work the instrument. Also, this person needed to take slow, gentle footsteps when moving within ten feet of the instrument: any vibration would compromise the instrument's accuracy.

The reference points were set up next. A location within about 25 feet of the straight-line distance from the Total Station to the tested span was chosen for each reference point, ensuring that each reference point was also at least 50 feet away from the others. Reference points must also be on stable soil, in the shade, and in clear site of the Total Station. A tripod was set up in the same manor as for the Total Station. The cap was removed from the prism and the prism-tribarch assembly was securely fastened to the tripod. The reference point did not need to be level; however, the prism must directly face the Total Station. The base of each leg was firmly

stood on again. At this point, the legs should not be able to move into the soil much; otherwise, the soil would not be considered stable enough and the reference point would be moved. The prism was turned to face the Total Station. This process was repeated for the remaining reference points.

Lastly, the prism-magnet mount assemblies were installed on the bridge. Standing behind the Total Station, it was noted which prisms would appear near each other (see Figure C.2). The short and long magnet mounts were used to resolve this issue; for example, the short mounts (Figure C.3) were used on the prisms nearest to the Total Station and the long magnet mounts (Figure C.4) were used for the prisms further away. The appropriate magnet mount was firmly screwed onto the prism; the prism cap was removed and set in the carrying case. The prisms are very delicate and absolutely must be kept clean and scratch free to avoid compromising readings.

Sections of range poles were tightly screwed together so as to easily reach the plates on the girders above. The prism-magnet mount assembly was screwed about two turns onto the end of the range pole(s). Using the range pole(s), the assembly was raised up to the appropriate plate, being careful not to damage the equipment. The face of the prism was lined up to directly view the Total Station and the assembly was then gently set onto the plate. That the assembly was securely attached to the bridge girder was confirmed. If a plate was not secure, a spare iron plate and quick-set epoxy was used for replacement. The range pole was then smoothly unscrewed from the assembly. This process was repeated for every prism position. Figures C.5, C.6, and C.7 illustrate this process.



Figure C.2. Site Setup



Figure C.3. Short Magnet Mount and Prism



Figure C.4. Long Magnet Mount and Prism



Figure C.5. Screw Range Pole onto Prism



Figure C.6. Pull Down the Prism



Figure C.7. Range Pole Assembly

Before getting started, traffic control was reviewed. Traffic control was very important to keep the traveling public and everyone on the site safe. The MoDOT crew was briefed on the test procedure; the flagmen were instructed to explain the situation to stopped traffic. Correct signing, flagging, and other traffic control devices were placed, as required by official MoDOT guidelines. Four MoDOT personnel were on site; two truck drivers and one flagman at each end (see Figure C.8).

Keeping good field notes for future reference was extremely important. A new page was used in the Field Book (see Figure C.9). On the left side, a sketch was drawn of the layout of the span, Total Station, reference points, and prisms, including all point numbers and a north arrow. On the right side, notes were taken including bridge location, load test number, weather conditions, date, names of Missouri S&T personnel on site, and any problems that occurred. The truck weight tickets were collected; the tickets included the truck's gross weight and either the front axle or rear axle weight.



Figure C.8. Traffic Control During Testing

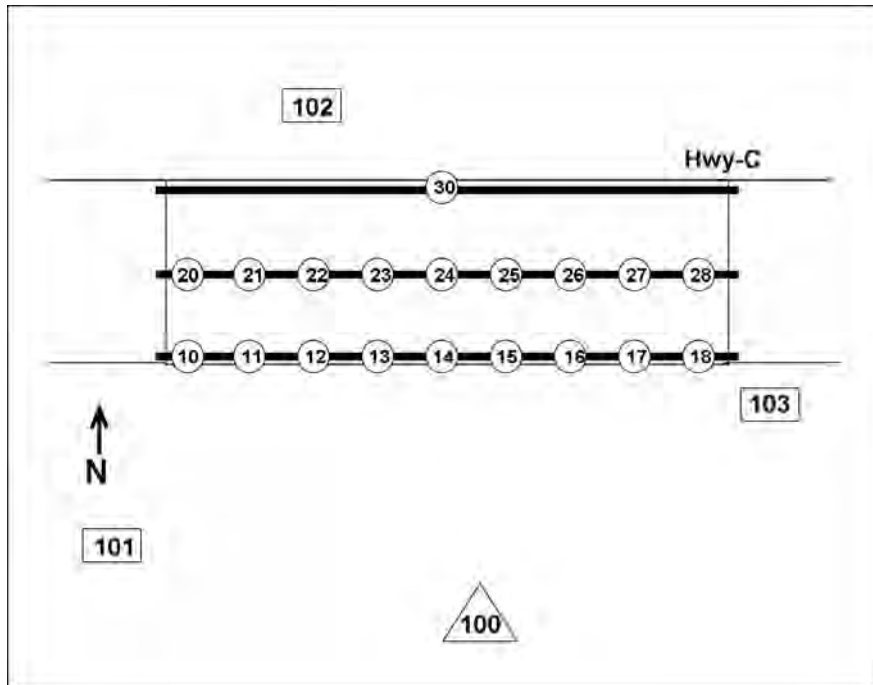


Figure C.9. Field Book Diagram of the Load Test (Not to Scale)

If the trucks differed significantly in weight, individual trucks and where each stopped during each load test run was documented. When scheduling the load test, trucks of the same weight and size as the previous load tests should be requested. Truck dimensions should also be checked on site.

With all equipment in place and ready for testing, the Total Station was set up. Set up began from the Main Menu. The right side of the screen must display the correct time, ample battery power, the auto-target icon, and the memory card icon. The “SETUP” menu was entered. User template must be set to “User 5,” which held the following values: format GSI 16, distance in inches, angle in degrees-minutes-seconds, temperature in degrees celsius, pressure in millibars, coordinates in northings-eastings, angles measured clockwise as positive, Face I as V-drive left. Other settings were entered: stability check on, compensator on, horizontal correction

on, EDM measuring program as precise measurement, and ATR on. See the Leica Help Binder for more details.

In the Setup Menu, the recording device was set to “Memory Card”; the measure file was set to a file that was free, indicated by a check mark. From the Setup Menu, “STN” was entered. The following values were entered: station number 100, instrument height zero, northing 10,000, easting 5,000, and elevation zero. The instrument was turned to the point furthest left (this should be a reference point); the instrument must be held gently yet firmly while turning. With the prism in the line of sight, “HZ0” was entered and the instrument locked onto the target and set the azimuth to zero. The instrument must not be touched while turning, locking, or shooting. “REC” was entered and the data was stored. In the Setup Menu, the same file number as the measure file was selected for the data file, and “CONT” was hit twice to return to the Main Menu.

Next, the Total Station must learn the location of each point. From the Main Menu, “MEAS” was entered to put the Total Station into measure mode and the instrument was again turned to the reference point furthest left. Point number was entered as 101 and “DIST” was entered. After the reading was taken, the Total Station displayed the point number, horizontal angle, vertical angle, distance, and height difference; “REC” was entered to record the data. The point number automatically turned to 102 as the display was cleared. The instrument was turned to the second reference point and the process was repeated. Next, the instrument was turned to the first point on the bridge. The instrument was directed to each point in the order listed on the field book. The point to the instrument was turned to must have the same point number as in the field book. After every point was recorded, the last reference point was located. When the last point was recorded, “ESC” was entered to return to the Main Menu.

Lastly, the Monitoring Program must be set up to automatically measure every point. From the Main Menu, the Monitoring Program was entered. Next “Point Selection” was chosen. Under “Control,” the file with the saved measurement and data information was selected. “Measure Method” must be set to “>” for a single forward-face reading; “Repetitions” was set to three. “SELCT” was chosen to each point to confirm that it matched the Field Book; “DONE” was entered to return to the Monitoring Program Menu.

3. Testing. With everything set up, testing proceeded smoothly. During testing, it was very important that no personnel go near the Total Station or reference points. Any vibrations near the base of the tripods risked compromising the accuracy of the readings; the Total Station especially must remain undisturbed throughout testing.

Testing began with a no-load control run. MoDOT personnel stopped traffic before the Total Station was set to start. All traffic was kept off of the bridge during testing; any vibration on the bridge could have compromised the accuracy of the readings. The instrument was activated by entering the “Monitoring” program at the Main Menu, then entering “Point Measurement,” and the Total Station began reading. Once the program was activated, everyone on site had to stand out of the way so as not to obstruct the instrument’s line of site. The time was read from the Total Station and entered into the Field Book with the test run number.

When the Total Station finished reading all prisms on the bridge, the next test run began. First, the flagmen were instructed to allow waiting traffic to pass. Afterwards, the road was again blocked. The trucks were directed into position following the lines painted on the road. Once stopped, the drivers were instructed to set their parking brakes and shut off engines to eliminate vibration. The instrument’s battery level was checked; if the battery level was determined to be too low, the battery was replaced. The instrument was activated; time and test run number were

again documented in the Field Book. This process was repeated for each test run (truck stop). Each test run took approximately 20 to 25 minutes.

The test finished with a final no-load control run. As before, the bridge was allowed to settle with traffic stopped for five minutes. After five minutes, the instrument was activated, and time and test run number were documented in the Field Book. Once the instrument completed its final run, the MoDOT personnel were instructed to release traffic and remove all traffic control.

4. Measuring Thermal Effects. To analyze thermal effects to temperature gradients in the structure, the temperature of the bridge was taken in several locations on the top and bottom surfaces in order to acquire an average temperature gradient. The plan for these measurements was determined before testing and a clear diagram was drawn to show the horizontal locations where measurements were to be taken. The locations were marked in order to take the temperature in the same location at every reading. Shade, inconsistent surfaces, clouds, and wind can affect the surface temperature in isolated locations of the span. The readings were taken at the start of testing, at halfway, and at the end of testing, every 90 minutes on average. Thermal corrections to the load testing data are discussed in Section 6.2.

Temperature readings were taken with a Raytek MT-4 thermal gun (Raytek Corporation 2004). The thermal gun is pointed at the surface (within several feet of the actual surface) and the trigger is pulled. The reading was then recorded in degrees Fahrenheit. The bottom surface temperature was taken at the bottom of the girder at a region of consistent surface: lane marking paint, potholes, and surface cracks were avoided.

5. Tear Down. With all testing completed, the equipment was to be taken down and transported back to Missouri S&T. Total Station shut-down was first: after escaping to the Main Menu, the “OFF” button was pressed twice to turn the instrument off. The Total Station was

released from the tripod and placed securely into its case. The case must be clean and dry and the instrument must always fit snugly in its case.

Next, the reference points were taken apart. The prism-tribrach assemblies were unscrewed from their tripods, the caps were placed on each prism face, and the assemblies were securely placed into the storage case. The protective caps were securely fastened to all four tripods. Each tripod's legs were released, shortened, tightened, and then fastened together.

All prism-magnet mount assemblies were taken down next. The range pole(s) were screwed tightly together just as they were during setup. The pole assembly was held up in line with the prism, screwed two turns onto the prism, and gently pried from the iron plate. If a prism or a plate was loose, it was documented in the Field Book. When lowering the prism-magnet mount assembly, the person holding the pole must pay close attention to whether or not the prism is securely screwed onto the end of the pole. The assembly was unscrewed, the cap was placed on the prism face, and the assembly was placed in the storage case. The process was repeated for each prism. The storage case must be kept clean and dry.

6. Troubleshooting. While the Total Station was easy to operate, some problems were presented during testing. During testing, the instrument occasionally posted errors when attempting to take a reading. Due to programming, if the instrument cannot take an accurate measurement it voids the reading. The error displayed again in Data Processing (Section 6). The error was caused by one of several factors: heat shimmer, people or wildlife in the instrument's line of site, target prisms not directly facing the instrument, or measuring over water. The risk of error was minimized during test set up: minimize measuring over water and aim the target prisms properly. Choosing a cooler, less humid day and time to test was also beneficial.

During testing, the battery may run dead. Before each test run, the battery level was checked. If the battery must be replaced, first the Main Menu was escaped to and the instrument was turned off. The instrument must be handled gently. After changing the battery, the instrument was turned back on. Next, the electronic level was checked: the instrument should not have moved while the battery was changed. If the instrument was out of level, it displayed an error message. Next, the instrument was turned to the first reference point and the azimuth was set to zero; if the azimuth at this point was near zero, it was okay to proceed.

During testing, the instrument may become out of level. This would be caused by several set up factors: the instrument was on unstable soil, the tripod legs were not properly driven into the soil, the tripod legs or instrument were not securely fastened, the instrument was not properly handled, the tripod legs were bumped, or vibrations were induced near the instrument. This problem was corrected by first pressing the electronic level button to display the fine-adjustment needed to perfectly level the instrument. Using the finger screws at the base of the instrument, the instrument was leveled so that each tilt direction measured $0^{\circ}00'00''$. "CONT" was pressed to return to the Main Menu. The instrument was turned to the first reference point where the azimuth had been set to zero during set up; the target should still be in the instrument's line of site. The azimuth was set to zero. Testing was restarted with a no-load run, and then a load test was attempted.

During testing, the instrument may freeze or lock up, similarly to when a personal computer crashes. If the instrument stopped and would not respond to any command, escaping was attempted to cancel the operation, otherwise the instrument was turned off. If the instrument still did not respond, the battery was removed to shut it off and then the battery was reinstalled the instrument turned back on and the monitoring program re-entered. The test was either

restarted; or “Point Selection” was entered and the points that had already been measured were turned off and the test was continued. One or two points that were recently measured should be re-measured for comparison when analyzing the data. Instrument lock up was a rare occurrence. If it happened more than once, or if the instrument failed to recover, the sales representatives should be contacted immediately.

7. Data Transfer and Processing. To begin processing the data, the Leica software package was installed on the desired computer. The instrument was plugged into the computer using the Leica Serial Cable. The instrument was turned on; “EXTRA” was selected, next “On-line Mode” was entered from the Extra Functions Menu. The instrument was now in on-line mode. The software instructions were followed to download the needed data from the instrument’s data card. Following data transfer, the instrument was turned off, unplugged, and placed back in its storage case.

The data file was opened in Microsoft Notepad (Microsoft Corporation 2004). Each row of data represented a specific measurement; all of the measurements were listed in the exact order that they were taken. Microsoft Excel was used to break the file into rows and columns in spreadsheet format (Microsoft Corporation 2004). Everything in the data file was copied to the clipboard and pasted into Excel. The data file was then closed and the Excel file was saved. All rows in the first column were selected and Text to Columns was chosen from the Data Menu. Fixed width was selected. A break was manually placed before the plus or minus sign in each series of numbers, as well as after that series (ended by a space). This was done for each number set; next “finish” was selected and the data was broken into columns. Some columns contained useless information and were deleted: these columns had numbers with decimal points, or contained the same number in every row. The first column was also deleted as it contained the

point numbers used during testing. Eleven total columns remained. For the load testing results, the only relevant columns were the first column (point numbers) and the fifth column (elevation in feet multiplied by 10,000).

Before proceeding, all files, including the originals, were backed up in multiple places. The first set of measurements was the result of the manual turning. The following rows contained three sets of numbers per point number, with the point numbers listed in the order they were measured during testing; the series then repeated for every test (truck stop) in the order that it was performed. The data for each test was separated. On every set of three readings (measurements), any reading that differed by more than 0.005 inches was removed (or the value of the internal error of the instrument for this test, which was a function of the slope distance from the instrument to the bridge span, and the angle measuring accuracy of the instrument), and the other two were averaged. If all three varied by the same amount, all three were simply averaged. Where the instrument failed to take a measurement, no elevation was recorded; this was never an issue because two other good readings were taken at this point. In most cases, all three readings differed by less than the instrument's internal error.

REFERENCES

- AASHTO. (2003). *Manual for condition evaluation and load resistance factor rating of highway bridges*. (2nd ed.).(2002). *Standard specification for highway bridges*. (17th ed.). Washington, D.C.: American Association of State Highway and Transportation Officials.
- ACI Committee 318-02. (2002). *Building code requirements for structural concrete and commentary (ACI 318R-02)*. Farmington Hills, MI: American Concrete Institute..
- ACI 437R-03. (2002). *Strength evaluation of existing concrete buildings*. Farmington Hills, MI: American Concrete Institute.
- ACI Committee 440. (2002). *Guide for the design and construction of externally bonded FRP systems for strengthening concrete structures (440.2R-02)*. Farmington Hills, MI: American Concrete Institute.
- ANSYS. (2004). *Finite Element Modeling Software, University Advanced Version 7.1* [computer software]. Canonsburg, PA: ANYSY, Inc.
- Benmokrane, B. Masmoudi, R. Chekired, M. Rahman, H. Debbache, Z. and Tadros, G. (1999). Design, construction, and monitoring of fiber reinforced polymer reinforced concrete bridge deck. *ACI Special Publication, 188*.
- Galati, N., Casadei, P., and Nanni, A. (2003). *Strengthening of martin springs outer road bridge*. (Center for Infrastructure Engineering Studies Publication No. 04-47). Rolla, MO: University of Missouri - Rolla.
- Koenigsfeld, D., and Myers, J. J. (2003). *Secondary reinforcement for fiber reinforced polymers reinforced concrete panels*. (Center for Infrastructure Engineering Studies Publication No. 03-45). Rolla, MO: University of Missouri - Rolla.

- Leica Geosystems. (2004). Leica TCA 2003 Total Station, www.leica-geosystems.com, May 20, 2004.
- Nawy, E.G. (2000). *Reinforced concrete: A fundamental approach*. (4th ed.). Upper Saddle River, NJ: Prentice Hall.
- FHWA. (2007). *National bridge inventory*. Washington, D.C.: U.S. Department of Transportation, Federal Highway Administration .
- Oh, B.H., Kim, K.S. and Lew, Y. (2002). Ultimate load behavior of post-tensioned prestressed concrete girder bridge through in-place failure test. *ACI Structural Journal*, 99(2).
- Pfeil, W. (1981). Twelve years monitoring of a long span prestressed concrete bridge. *ACI Concrete International*, 3(8).
- Stallings J., Tedesco J., El-Mihilmy M., and H. McCauley. (2000). Field performance of FRP bridge repairs. *ASCE Journal of Bridge Engineering*, 5(2), pp. 107-113.
- Stone D. (2002). *Investigation of FRP materials for bridge construction* (Doctoral Dissertation, Department of Civil Engineering, University of Missouri-Rolla, 2002).
- Vurpillot, S., Krueger, G., Benouaich, D., Clement, D. and Inaudi, D. (1998). Vertical deflection of a pre-stressed concrete bridge obtained using deformation sensors and inclinometer measurements. *ACI Structural Journal*, 95(5).
- Yang, Y. and Myers, J.J. (2003). Live load test results of Missouri's first high performance concrete superstructure bridge. *Proceedings from the Transportation Research Board 82nd Annual Meeting*. Washington, D.C., Transportation Research Board.



Missouri Department of Transportation
Organizational Results
P. O. Box 270
Jefferson City, MO 65102

573.526.4335
1 888 ASK MODOT
innovation@modot.mo.gov